

**THE FUNCTION OF EXONUCLEASE I IN
MEIOTIC RECOMBINATION:
A GENETIC AND PHYSICAL ANALYSIS**

A thesis submitted for the degree of
Doctor of Philosophy

by

Rebecca Emily Keelagher BSc (Hons)

Department of Genetics
University of Leicester
September 2010

The Function of Exonuclease I in Meiotic Recombination: A Genetic and Physical Analysis

Rebecca Emily Keelagher

Department of Genetics, University of Leicester
Thesis submitted for the degree of Doctor of Philosophy, September 2010

ABSTRACT

Exo1 is a member of the Rad2 protein family and possesses both 5'-3' exonuclease and 5' flap endonuclease activities. In addition to performing a variety of functions during mitotic growth, Exo1 is also important for the production of crossovers during meiosis. However, its precise molecular role has remained ambiguous and several models have been proposed to account for the crossover deficit observed in its absence. Here, physical evidence that the nuclease activity of Exo1 is essential for normal 5'-3' resection at the Spo11-dependent *HIS4* hotspot in otherwise wild-type cells is presented. This same activity was also required for normal levels of gene conversion at the locus. Nevertheless, gene conversions were frequently observed at a distance beyond that at which resection was readily detectable arguing that it is not the extent of the initial DNA end resection that limits heteroduplex formation. In addition to these nuclease-dependent functions, nuclease-deficient *exo1* mutants were found to be capable of maintaining crossing-over at wild-type levels in a number of genetic intervals, suggesting that Exo1 also plays a nuclease-independent role in crossover promotion. Furthermore, the results of both physical and genetic analyses imply that Sgs1 does not contribute significantly to resection during meiosis in *exo1* Δ cells, indicating that the mitotic and meiotic resection machinery differs. In light of these new insights, a model describing the formation of heteroduplex DNA and crossovers during meiosis is proposed.

ACKNOWLEDGEMENTS

There are many people without whom this thesis would not exist. Firstly, my supervisor, Rhona: thank you for being so supportive over the last four years, for your patience, optimism and enthusiasm (and your wonderfully quick chapter turnaround rate!). I can honestly say that I would not have reached this stage had it not been for your encouragement and kind words.

Thank you also to Vicky for always being my first port of call with any question, for being a positive, smiling face and a fantastic source of help and support; Amit for your kindness in making me feel welcome as a new arrival, helping with student supervisions and passing on your insider lab knowledge; Maryam for sharing so much of this experience with me and always making me smile; Rob for being an endless source of knowledge and my adopted post-doc for all matters radioactive; Alastair, Slava and Adam for help with DNA extractions and providing a lot of helpful information and Eva, Phil, Louise and Andy for giving up your time to help me and teaching me so much. To Gary, Rally, Trish, Kees, Alex C, Mathura, Flav, Jannine, Nicky, Raff, Chris, Dan, Shanow, Alex W, Kayoko, Ed, Mariaelena, Reshma and all other members of the lab and department, past and present: thank you for all your help and for making this such a lovely place to work - I'll miss you all.

Last but by no means least, to my parents and the rest of my family and friends: thank you so much for reminding me what really matters and for all your patience, support and love. I couldn't have finished this without you.

ABBREVIATIONS

5'-FOA	- 5'-fluoroorotic acid
bp	- base pairs
BSA	- bovine serum albumin
cM	- centi-Morgan
CO	- crossover
Cp	- crossing-point
DAPI	- 4-6-diamidino-2-phenylindole
dHJ	- double Holliday junction
DNA	- deoxyribonucleic acid
dNTP	- deoxynucleoside triphosphate
DSB	- double-strand break
dsDNA	- double-stranded deoxyribonucleic acid
EDTA	- ethylenediaminetetraacetic acid
hDNA	- heteroduplex deoxyribonucleic acid
HEPES	- 4-(2-hydroxyethyl)-1-piperazineethanesulfonic acid
HJ	- Holliday junction
kb	- kilobases
LB	- Luria-Bertani medium
MI	- the first meiotic division
MII	- the second meiotic division
MMR	- mismatch repair
MMS	- methyl methanesulphonate
NCO	- non-crossover
NMS	- non-Mendelian segregation
NPD	- non-parental ditype
OD	- optical density
ORF	- open reading frame
PCR	- polymerase chain reaction
PD	- parental ditype
PMS	- post-meiotic segregation
PRM	- poorly-repaired mismatch
qPCR	- quantitative polymerase chain reaction
rDNA	- ribosomal deoxyribonucleic acid
RPA	- replication protein A
SC	- synaptonemal complex
SDS	- sodium dodecyl sulphate
SDSA	- synthesis-dependent strand annealing
SEI	- single-end invasion
SPS	- supplemented pre-sporulation medium
SSC	- 150 mM sodium chloride, 15 mM sodium citrate; pH7.0
ssDNA	- single-stranded deoxyribonucleic acid
SSPE	- 150 mM sodium chloride, 10 mM sodium phosphate, 1 mM EDTA; pH7.4
TBE	- 90 mM Tris, 90 mM Boric acid, 2 mM EDTA
TE	- 10 mM Tris-HCl, 1 mM EDTA; pH8.0
TT	- tetratype
WRM	- well-repaired mismatch
YEPD	- yeast extract, peptone, dextrose medium
YEPEG	- yeast extract, peptone, ethanol, glycerol medium

LIST OF CONTENTS

INTRODUCTION	1
1.1 MEIOSIS: AN OVERVIEW	1
1.2 INITIATING RECOMBINATION	6
1.2.1 DISTRIBUTING DOUBLE-STRAND BREAKS	6
1.2.2 CATALYSING BREAK FORMATION.....	7
1.2.3 DNA END RESECTION	8
1.2.3.1 <i>The process of resection</i>	8
1.2.3.2 <i>The regulation of resection</i>	12
1.3 PATHWAYS TO REPAIR.....	14
1.3.1 THE DOUBLE-STRAND BREAK REPAIR MODEL	14
1.3.2 THE CROSSOVER PATHWAY	16
1.3.3 SYNTHESIS-DEPENDENT STRAND ANNEALING	19
1.3.4 AN ALTERNATIVE CROSSOVER PATHWAY	19
1.4 CROSSOVER CONTROL: OBLIGATION, INTERFERENCE AND HOMEOSTASIS	21
1.5 MISMATCH REPAIR IN MEIOSIS	24
1.5.1 THE MISMATCH REPAIR PROCESS	24
1.5.2 THE ROLE OF MISMATCH REPAIR DURING MEIOSIS	26
1.5.2.1 <i>Gene conversion gradients</i>	26
1.5.2.2 <i>Mismatch repair proteins in crossover promotion</i>	33
1.6 AIMS AND OBJECTIVES	37
MATERIALS AND METHODS	39
2.1 MATERIALS.....	39
2.1.1 YEAST STRAINS	39
2.1.2 PLASMIDS.....	39
2.1.3 OLIGONUCLEOTIDES	39
2.1.4 MEDIA.....	39
2.1.5 DNA MOLECULAR WEIGHT MARKERS	48
2.2 METHODS.....	48
2.2.1 AGAROSE GEL ELECTROPHORESIS	48
2.2.2 PREPARATION OF YEAST GENOMIC DNA.....	48
2.2.2.1 <i>Genomic DNA extraction by phenol/chloroform</i>	48
2.2.2.2 <i>Genomic DNA extraction by CTAB</i>	49
2.2.3 PLASMID DNA PREPARATION	50
2.2.4 RESTRICTION DIGESTION	50
2.2.5 QUANTIFICATION OF DNA	50
2.2.6 END-POINT POLYMERASE CHAIN REACTION.....	51
2.2.6.1 <i>PCR using Taq polymerase</i>	51
2.2.6.2 <i>Proofreading PCR</i>	51
2.2.6.3 <i>Colony PCR</i>	51

2.2.7 QUANTITATIVE PCR	51
2.2.8 ETHANOL PRECIPITATION	52
2.2.9 DNA PURIFICATION	52
2.2.10 MUTAGENESIS METHODS	53
2.2.10.1 PCR-based gene disruption	53
2.2.10.2 PCR-based allele replacement.....	53
2.2.10.3 Two-step gene replacement	53
2.2.11 DNA SEQUENCING	53
2.2.12 YEAST TRANSFORMATION	54
2.2.13 SYNCHRONOUS LIQUID SPORULATION	54
2.2.13.1 Monitoring meiotic progression by fluorescence microscopy.....	55
2.2.13.2 Monitoring meiotic progression by DNA analysis	55
2.2.14 SOUTHERN BLOTTING	55
2.2.14.1 Preparation of DNA and electrophoresis	55
2.2.14.2 Southern transfer and cross-linking	56
2.2.14.3 Radioactive labelling of probes.....	56
2.2.14.4 Hybridisation and stringency washes	57
2.2.14.5 Detection and quantification	57
2.2.15 GENETIC PROCEDURES	58
2.2.15.1 Mating and sporulation	58
2.2.15.2 Diploid selection	58
2.2.15.3 Sporulation protocol for recombination analysis.....	58
2.2.15.4 Tetrad dissection.....	59
2.2.15.5 Mating type testing	59
2.2.15.6 Spore viability analysis	59
2.2.15.7 Recombination analysis by tetrad dissection	59
2.2.15.8 Random Spore Analysis.....	60
2.2.16 STATISTICAL ANALYSIS.....	61

ANALYSING RESECTION AND GENE CONVERSION AT THE <i>HIS4</i> HOTSPOT.....	62
3.1 INTRODUCTION	62
3.2 MATERIALS AND METHODS.....	64
3.2.1 STRAIN CONSTRUCTION	64
3.2.2 RECONSTRUCTION EXPERIMENTS FOR QPCR ASSAY VALIDATION	65
3.2.3 LOSS OF RESTRICTION SITE ANALYSIS BY QPCR	65
3.2.4 QUANTITATIVE SOUTHERN BLOT ANALYSIS.....	67
3.2.5 MEASUREMENTS OF GENE CONVERSION	67
3.3 RESULTS.....	68
3.3.1 VERIFYING THE SUITABILITY OF THE <i>HIS4</i> HOTSPOT FOR RESECTION ANALYSIS.....	68
3.3.2 SELECTION OF <i>HIS4</i> RESTRICTION SITES AND ASSAY VALIDATION	68
3.3.3 ANALYSIS OF MEIOTIC DSB RESECTION AT <i>HIS4</i>	70
3.3.4 GENE CONVERSION AT <i>HIS4</i> REQUIRES EXO1	77
3.3.5 THE FUNCTIONS OF EXO1 IN DNA RESECTION AND hDNA FORMATION ARE NUCLEASE-DEPENDENT	80
3.3.6 THE <i>POL3-CT</i> ALLELE CONFERS A SEVERE MITOTIC GROWTH DEFECT IN THE SK1 BACKGROUND	80
3.4 DISCUSSION	81

3.4.1 A NEW METHOD WITH WHICH TO STUDY RESECTION AT SPO11-DEPENDENT DSBs	81
3.4.2 EXO1 IS REQUIRED FOR FULL-LENGTH RESECTION OF MEIOTIC DSBs	82
3.4.3 EXO1 AND DNA SYNTHESIS MAY COLLABORATE IN THE FORMATION OF HETERODUPLEX DNA	82
3.4.4 COULD A REDUCTION IN DNA END RESECTION SIMULTANEOUSLY ACCOUNT FOR THE REDUCTION IN GENE CONVERSION AND CROSSING-OVER OBSERVED IN <i>EXO1Δ</i> ?	84
THE ROLE OF EXONUCLEASE I IN CROSSOVER PROMOTION.....	85
4.1 INTRODUCTION	85
4.2 MATERIALS AND METHODS.....	88
4.2.1 STRAIN CONSTRUCTION	88
4.2.2 TETRAD ANALYSIS.....	88
4.2.3 RANDOM SPORE ANALYSIS.....	89
4.3 RESULTS.....	92
4.3.1 NEITHER THE EXONUCLEASE NOR ENDONUCLEASE ACTIVITIES OF EXO1 ARE ESSENTIAL FOR CROSSING-OVER.....	92
4.3.2 CROSSOVER INTERFERENCE IN <i>EXO1Δ</i>	92
4.3.3 INCREASED RANDOM SPORE DEATH OCCURS IN THE PRESENCE OF NUCLEASE-DEFICIENT <i>EXO1</i>	99
4.3.4 WILD-TYPE LEVELS OF NON-MENDELIAN SEGREGATION AT <i>HIS4</i> ARE DEPENDENT UPON THE EXONUCLEOLYTIC ACTIVITY OF <i>EXO1</i>	102
4.3.5 CROSSING-OVER AT THE <i>HIS4</i> HOTSPOT MIRRORS OTHER INTERVALS ON CHROMOSOME III	105
4.3.6 THE NUCLEASE-INDEPENDENT FUNCTION OF EXO1 INCREASES THE ASSOCIATION OF SHORT hDNA TRACTS WITH CROSSING-OVER	107
4.3.7 LONGER hDNA TRACTS ARE PREFERENTIALLY ASSOCIATED WITH CROSSOVERS	111
4.4 DISCUSSION	112
4.4.1 RESECTION MAY INFLUENCE CROSSING-OVER IN A LOCUS-DEPENDENT MANNER.....	112
4.4.2 A STRUCTURAL ROLE FOR EXO1 IN CROSSOVER PROMOTION	113
4.4.3 THE <i>EXO1-D173A</i> AND <i>EXO1-E150D</i> ALLELES ARE NOT EQUIVALENT	114
4.4.4 THE NATURE OF THE SPORE DEATH IN THE SEPARATION-OF-FUNCTION MUTANTS.....	114
ANALYSIS OF PUTATIVE DNA REPAIR MUTANTS IN MEIOSIS	116
5.1 INTRODUCTION	116
5.2 MATERIALS AND METHODS.....	117
5.2.1 STRAIN CONSTRUCTION	117
5.3 RESULTS.....	119
5.3.1 TRM2 DOES NOT FUNCTION IN MEIOTIC RECOMBINATION	119
5.3.2 SPORE VIABILITY DISTRIBUTIONS IN THE ABSENCE OF <i>SGS1</i> AND <i>EXO1</i> ..	119
5.3.3 CROSSING-OVER IS NOT RESTORED IN <i>SGS1-MN EXO1Δ</i> AT 23°C	124
5.3.4 GENE CONVERSION IS NOT SIGNIFICANTLY REDUCED IN <i>SGS1-MN EXO1Δ</i> ..	124

5.3.5 A DIFFERENTIAL REQUIREMENT FOR <i>SGS1</i> IN <i>EXO1Δ</i> CELLS AT 23°C AND 33°C.....	125
5.3.6 INCREASING TEMPERATURE PROMOTES CHROMOSOME DISJUNCTION IN <i>EXO1Δ</i> STRAINS.....	127
5.4 DISCUSSION	130
5.4.1 NEITHER <i>SGS1</i> NOT <i>TRM2</i> CONTRIBUTE TO MEIOTIC DSB PROCESSING	130
5.4.2 THE NATURE OF THE CROSSOVER DEFICIT IN <i>EXO1Δ</i> AND THE EFFECT OF TEMPERATURE	131
 DISCUSSION & FUTURE DIRECTIONS.....	134
6.1 MULTIPLE FUNCTIONS FOR EXONUCLEASE I IN MEIOTIC RECOMBINATION.....	134
6.1.1 MEIOTIC DSB END RESECTION	134
6.1.2 THE INFLUENCE OF RESECTION UPON RECOMBINATION	139
6.1.3 COORDINATING THE MULTIPLE ROLES OF <i>EXO1</i>	140
6.2 CONCLUSIONS	141
REFERENCES	142

CHAPTER 1

INTRODUCTION

1.1 Meiosis: an overview

Meiosis is an essential process in all sexually reproducing eukaryotes. It results in a halving of the chromosome complement of the cell: reducing the genome from diploid (containing two copies of each chromosome) to haploid (containing a single copy of each chromosome). Thus, at fertilisation, nuclear fusion of two haploid meiotic products restores the diploid chromosome number. In order to accomplish this halving, meiosis proceeds via a single round of DNA replication followed by two successive nuclear divisions termed meiosis I and meiosis II (MI/MII). The first meiotic division, in contrast to nuclear divisions that take place during mitotic growth, separates homologous chromosome pairs to opposite poles and hence is referred to as reductional. Subsequently, sister chromatids separate during MII in an equational division similar to that observed during mitosis (see Figure 1.1).

Prior to the first division, programmed DNA double-strand breaks (DSBs) are produced (Sun *et al.*, 1989). The repair of these DSBs is carried out during prophase of meiosis I in a tightly-coordinated process which links DNA repair, alterations in chromosome structure and the polymerisation of the proteinaceous synaptonemal complex between paired homologues (Alani *et al.*, 1990; Padmore *et al.*, 1991). A unique feature of meiosis is the bias towards using the DNA of a non-sister chromatid as a template for repair rather than a sister chromatid. In the majority of organisms, the resulting inter-homologue interactions promote homologue pairing and crossover production (the reciprocal exchange of DNA between homologues). In addition to promoting genetic diversity within populations, crossovers (visualised cytologically as chiasmata) are essential for ensuring homologue disjunction at MI by promoting the successful bi-orientation of homologues on the meiotic spindle. A crossover deficit can thus lead to non-disjunction and the production of aneuploid gametes (see Figure 1.2). Although a small degree of aneuploidy can be tolerated in some organisms, non-disjunction is a major contributor to infertility. In humans for example, very few cases of aneuploidy produce viable foetuses, and

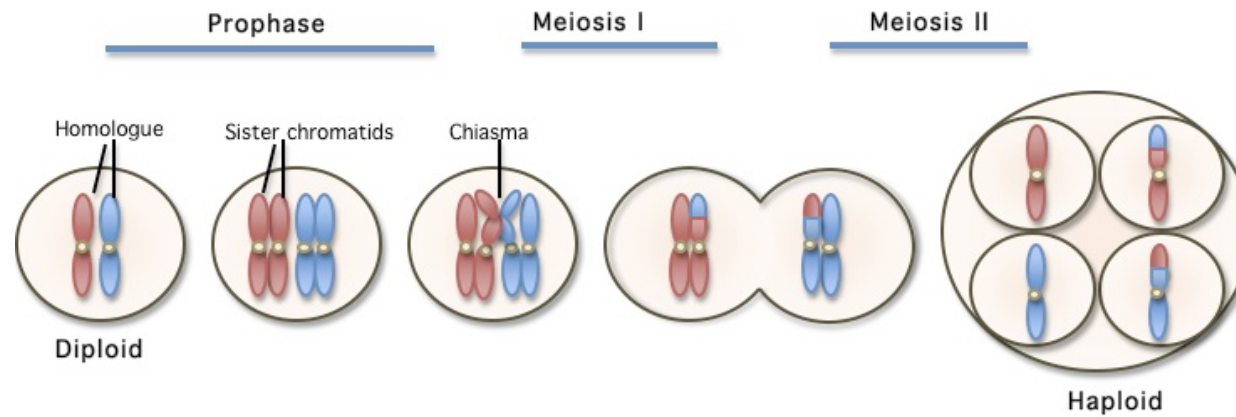
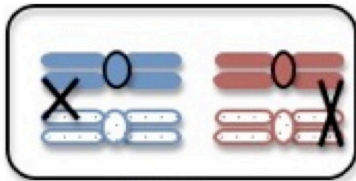


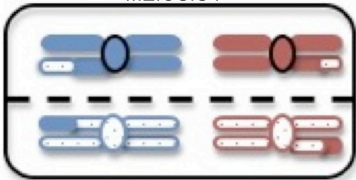
Figure 1.1: Meiosis proceeds via two sequential divisions.

Following DNA replication, homologous chromosomes pair and undergo recombination. The presence of chiasmata at sites of inter-homologue crossing-over acts to mediate the bipolar attachment of bivalent chromosomes on the meiotic spindle and ensures their segregation to opposite poles at MI. Sister chromatids then separate during MII following the removal of centromeric sister chromatid cohesin complexes, resulting in four non-identical haploid products from each diploid cell. In yeast, these four products are contained within an ascus and are called tetrads.

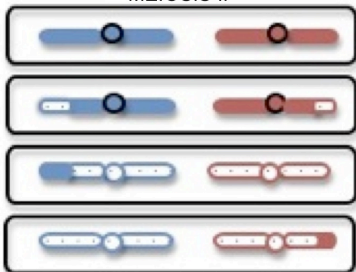
A. NORMAL SEGREGATION



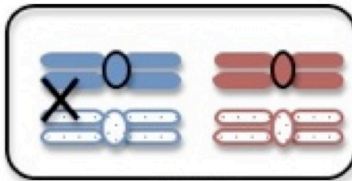
MEIOSIS I



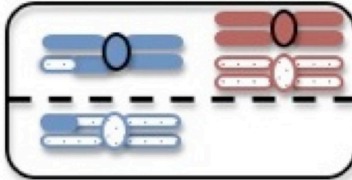
MEIOSIS II



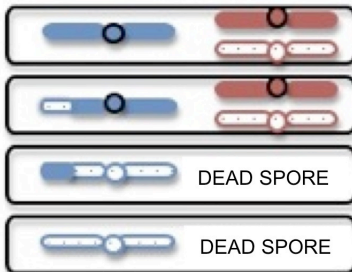
B. MEIOSIS I NON-DISJUNCTION



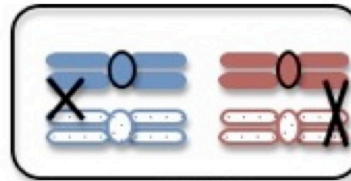
MEIOSIS I



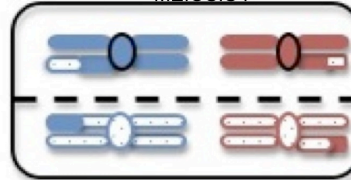
MEIOSIS II



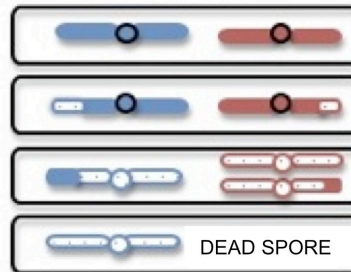
C. MEIOSIS II NON-DISJUNCTION



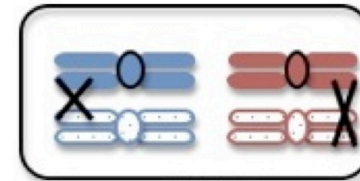
MEIOSIS I



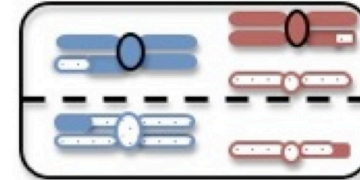
MEIOSIS II



D. PRECOCIOUS SEPARATION OF SISTER CHROMATIDS



MEIOSIS I



MEIOSIS II

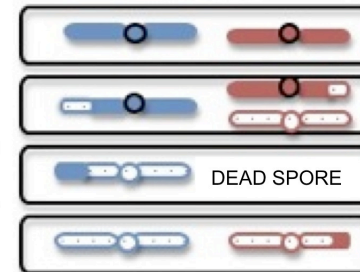


Figure 1.2: Spore viability patterns indicative of chromosome segregation defects.

Two pairs of homologous chromosomes are shown (red and blue). Chromosomes of the same colour and pattern represent sister chromatids, while chromosomes of the same colour but different pattern (filled and dotted) represent homologues (redrawn from Chaix, 2007). **(A)** Normal segregation: both homologous pairs undergo crossing-over, ensuring their accurate disjunction at meiosis I. This results in 4 spores, each containing one copy of each chromosome. **(B)** Meiosis I non-disjunction: when one homologous pair fails to recombine, non-disjunction at the first meiotic division can occur, resulting in two disomic spores containing both chromosomes originating from the same parent and two inviable nullisomic spores. If it is chromosome III that non-disjoins, the disomic spores will also be unable to mate as they will express both a and α mating types. Centromeric markers can demonstrate that spores containing the disomes are sisters. **(C)** Meiosis II non-disjunction: the failure of sister chromatids to segregate at meiosis II results in one homozygous disomic spore and one inviable nullisomic spore. The two remaining spores will be sisters. **(D)** Precocious separation of sister chromatids (PSSC): if sister chromatids separate from each other before meiosis I, an inviable, nullisomic spore and a heterozygous disomic spore will be produced. If the disomic spore results from the precocious separation of chromosome III sister chromatids, it will be non-mating. The two remaining spores will be non-sisters.

those that do are associated with congenital birth defects and developmental abnormalities. The most common viable aneuploidy is trisomy of chromosome 21, which results in Down Syndrome (Hassold and Hunt, 2001).

Much of our current understanding of the recombination process has been gained through the study of yeast and other fungi in which the products of meiosis are contained within an ascus (reviewed by Orr-Weaver and Szostak, 1985). As these species are capable of proliferation as haploid eukaryotes, the four meiotic products originating from each diploid cell can be recovered and analysed using a variety of methods. Spore viability patterns alone can be informative; for instance, meiosis I non-disjunction of a single homologue pair results in two disomic spores and two nullisomic spores (Figure 1.2). In the budding yeast *Saccharomyces cerevisiae*, the disomic spores are usually viable and can be identified as containing sister chromatids by analysis of centromeric markers. Non-disjunction of more than one homologue can lead to the death of all four spores and therefore, in strains defective in crossover formation, decreased viability is characteristically associated with the production of asci (known as tetrads in yeast) containing either four, two or zero viable spores. Meiosis II non-disjunction and spore death resulting from the precocious separation of sister chromatids (PSSC) can be similarly inferred (Figure 1.2). Moreover, a great deal of insight into the molecular mechanisms involved in meiotic recombination has been gained from the genetic analysis of marker segregation following tetrad dissection (for examples see Gilbertson and Stahl, 1996; Merker *et al.*, 2003; Hoffmann and Borts, 2005; Hoffmann *et al.*, 2005; Jessop *et al.*, 2005).

In addition to genetic analyses, physical studies in *Saccharomyces cerevisiae* are also possible (examples include Borts *et al.*, 1986; Schwacha and Kleckner, 1995; Hunter and Kleckner, 2001). These commonly employ the SK1 strain background (Kane and Roth, 1974) in which cells progress through meiosis relatively rapidly and synchronously, thereby enabling detectable levels of transient intermediates to be achieved. In combination, genetic and physical analyses can be powerful tools in unravelling the molecular basis of the recombination process (for an example, see de los Santos *et al.*, 2003). Whilst differences between species have emerged, studies in higher eukaryotes such as mice have provided support for a number of features

originally revealed in yeast (discussed in Svetlanov and Cohen, 2004). Therefore, *Saccharomyces cerevisiae* provides an excellent model organism in which to study the molecular components and processes involved in recombination. The remainder of this dissertation will focus mainly upon research carried out in this organism.

1.2 Initiating recombination

1.2.1 Distributing double-strand breaks

The initiating event of meiotic recombination is the formation of DNA double-strand breaks. This takes place following DNA replication (Borde *et al.*, 2000; Murakami *et al.*, 2003). DSBs are not distributed at random but occur at higher frequencies in certain regions of the genome, which are referred to as recombination hotspots (Baudat and Nicolas, 1997; Gerton *et al.*, 2000; Mieczkowski *et al.*, 2006; Blitzblau *et al.*, 2007; Buhler *et al.*, 2007). While hotspots have been classified into various subtypes, they are characteristically found in regions associated with an open chromatin conformation and hence exhibit DNase-I and MNase hypersensitivity (Ohta *et al.*, 1994; Wu and Lichten, 1994). These are generally intergenic regions of DNA and are rich in guanine and cytosine bases (Gerton *et al.*, 2000). The significance of chromatin status in determining break sites has been further highlighted by evidence demonstrating that histone modifications can dramatically affect the frequency of DSB formation (reviewed in Borde *et al.*, 2009; Kniewel and Keeney, 2009).

Activity at α -hotspots is dependent upon the action of transcription factors, the binding of which is likely to increase the accessibility of the DNA to the recombination machinery. However, the requirement for transcription factor binding at these sites does not extend to a requirement for transcription *per se* as deletion of a TATAA sequence at *HIS4* was shown to drastically reduce transcription without decreasing DSB formation (White *et al.*, 1992). An alternative explanation proposed for the requisite binding is that transcription factors act to tether or recruit the recombination-initiating proteins to the DSB site (Fan and Petes, 1996). Conversely, β -hotspots achieve an open chromatin conformation by harbouring particular DNA sequences that result in the exclusion of nucleosomes from that region (Kirkpatrick *et al.*, 1999).

Break formation can be further modulated by various environmental influences including nutritional status (Abdullah and Borts, 2001), temperature (Fan *et al.*, 1995; Cotton *et al.*, 2009) and sporulation medium composition (Cotton, 2007). Although these factors have been best studied at the *HIS4* hotspot, they are likely to impact upon other hotspots also, making a sizeable contribution to recombination that is often not fully considered. For example, the transcription factor Gcn4 affects the transcription of over 500 genes (Natarajan *et al.*, 2001) and is known to influence recombination frequencies in a locus-specific manner, presumably by its action at α -hotspots (Abdullah and Borts, 2001). Importantly, cellular levels of Gcn4 are controlled in response to a wide range of signals including amino acid starvation and stress (Hinnebusch and Natarajan, 2002), demonstrating one potential mechanism whereby cellular and environmental factors could have significant effects upon break frequency and meiotic recombination.

1.2.2 Catalysing break formation

The enzyme responsible for meiotic DSB catalysis was initially discovered as a protein-DNA complex present at the 5' termini of DSB sites in mutants prevented from undergoing repair (Keeney and Kleckner, 1995; Liu *et al.*, 1995). Subsequently, this factor was identified as Spo11, a topoisomerase II-like protein that is thought to function as a homo-dimer to catalyse break formation via a transesterification reaction (Keeney *et al.*, 1997). In addition, at least nine accessory proteins have been identified which are absolutely required for DSB formation (see Hunter, 2006; Keeney and Neale, 2006 for reviews). Of particular note are Mre11, Rad50 and Xrs2, which together form the highly conserved MRX complex (Johzuka and Ogawa, 1995; Trujillo *et al.*, 2003). In addition to playing a central role during meiosis, the MRX complex (and its mammalian homologue MRN [for Mre11, Rad50 and Nbs1]) also performs a wide range of cellular functions during vegetative growth and is a critical component in several DNA damage response pathways (reviewed in Borde and Cobb, 2009).

Once DSB formation has been achieved, Spo11 must be removed from the DNA ends in order for repair to commence. Removal takes place via endonucleolytic cleavage of the DNA to release Spo11-oligonucleotide complexes in a process thought to require the nuclease activity of Mre11 (Neale *et al.*, 2005). This

dependence upon Mre11 is supported by the demonstration that separation-of-function alleles of MRX components (such as the *rad50S* point mutation) and nuclease-deficient alleles of Mre11 allow break formation to take place but prevent further processing, leaving Spo11 covalently attached to the DNA (Alani *et al.*, 1990; Nairz and Klein, 1997; Furuse *et al.*, 1998; Tsubouchi and Ogawa, 1998; Moreau *et al.*, 1999). An additional accessory protein required at this stage is Sae2 and *sae2Δ* mutants exhibit the same phenotype as the above-described MRX alleles (McKee and Kleckner, 1997; Prinz *et al.*, 1997). Sae2 does not possess any recognisable functional motifs but Sae2-like enzymes have been identified in a number of organisms ranging from humans to worms (Penkner *et al.*, 2007; Sartori *et al.*, 2007; Uanschou *et al.*, 2007). Although no direct protein-protein interactions takes place in the absence of a DNA substrate, Sae2 appears able to stimulate the nuclease activity of MRX (Lengsfeld *et al.*, 2007; Kim *et al.*, 2008). Indeed, evidence suggests that the *rad50S* phenotype results from an inability of MRX and Sae2 to interact (Clerici *et al.*, 2005). However, Sae2 itself has also been shown to possess endonuclease activity independent of MRX *in vitro* and the nuclease activities of both MRX and Sae2 are thought likely to cooperate in the cleavage of DNA hairpin structures (Lengsfeld *et al.*, 2007). It is unclear therefore whether Sae2 merely stimulates MRX or plays a direct catalytic role itself in the removal of Spo11.

1.2.3 DNA end resection

1.2.3.1 The process of resection

The 5' to 3' resection of the DNA ends following DSB formation is a step common to all models of double-strand break repair. Resection rapidly follows the release of Spo11-oligonucleotide complexes from the break site and results in 3' overhanging strands that are initially bound by the high-affinity single-strand binding replication protein A (RPA). With the aid of mediator factors, Rad51 and Dmc1 then displace RPA to form the recombinogenic nucleoprotein filaments required to catalyse strand-invasion (Gasior *et al.*, 2001). Initial evidence for the presence of this single-stranded DNA (ssDNA) came from experiments demonstrating that the ends of DNA fragments formed by meiotic breaks at the *ARG4* hotspot were sensitive to digestion by the ssDNA-specific S1 nuclease (Sun *et al.*, 1989). Further investigation employing non-denaturing Southern blotting and strand-specific RNA probes revealed the polarity of resection. Finally, using a loss-of-restriction-site approach

(see Section 3.1 for further information), Sun *et al.* (1991) were able to estimate that these ssDNA tails extended up to 800 bp in length.

The identity of the protein or proteins responsible for this resection remains uncertain but likely candidates include Mre11 and Exo1. Mre11 possesses both exonuclease and endonuclease activities and (as mentioned previously) is likely to play an active role in the removal of Spo11 from break sites, in concert with Sae2. The nuclease functions of Mre11 have been shown to be highly structure-specific *in vitro* (Paull and Gellert, 1998; Trujillo and Sung, 2001). As an exonuclease, Mre11 acts upon double-stranded DNA (dsDNA) ends in a 3' to 5' direction. Although this is the reverse of the polarity required to catalyse the formation of 3' single-stranded tails, it has been proposed that Mre11 could be involved via its endonuclease activity that preferentially cleaves at DNA hairpin-ends and ssDNA to dsDNA transitions. This model requires that Mre11 acts in conjunction with a helicase to first unwind the DNA, allowing subsequent cleavage to take place at transiently formed secondary structures (reviewed in Hoffmann and Borts, 2004; Krogh and Symington, 2004). However, due to the requirement for Mre11 in Spo11 removal (without which no resection can occur), it is difficult to provide experimental evidence supporting a later resection role for the nuclease at Spo11-dependent DSBs.

A protein possessing a double-stranded exonuclease function with the expected 5' to 3' polarity is Exo1 (Exonuclease I) (Fiorentini *et al.*, 1997), which was originally isolated in *Schizosaccharomyces pombe* as a transcript whose expression was up-regulated during meiosis (Szankasi and Smith, 1995). The *Saccharomyces cerevisiae* Exo1 homologue is similarly up-regulated (Chu *et al.*, 1998; Tsubouchi and Ogawa, 2000) and *EXO1* deletion has been shown to result in increased levels of MI non-disjunction due to reduced crossing-over (Khazanehdari and Borts, 2000; Kirkpatrick *et al.*, 2000; Tsubouchi and Ogawa, 2000). Furthermore, *exo1Δ* mutants have been implicated in reducing the amount of heteroduplex DNA (hDNA) formed during meiosis at certain loci (Khazanehdari and Borts, 2000) although a significant reduction is not observed at all loci or in all studies (discussed further in Section 1.5). Additionally, the ability of *exo1Δ* diploids to produce spores and the relatively high viability of those spores suggests that whilst Exo1 appears to be the strongest

candidate identified to date, it cannot be the sole factor contributing to resection of meiotic DSBs (Khazanehdari and Borts, 2000; Kirkpatrick *et al.*, 2000; Tsubouchi and Ogawa, 2000).

The lack of physical evidence supporting a requirement for Exo1 in meiotic resection is a further impediment to reliably assigning a role in resection. To date, attempts to provide this evidence have relied upon use of the *dmc1* Δ mutation to ensure visualisation of the resection intermediates. In the absence of Dmc1, recombination is blocked at the strand invasion stage resulting in cell-cycle arrest and the production of extra-long resection tracts (Bishop *et al.*, 1992). In the first such experiment, Tsubouchi *et al.* (2000) studied DSB formation at the artificial *HIS4LEU2* hotspot. In this investigation, DSBs were shown to appear as normal in *exo1* Δ but their disappearance was delayed by 1-2 hours compared to wild-type. Passage through MI was similarly delayed. A comparison between *dmc1* Δ (in which the hyper-resection is visible as highly smeared DSB bands following Southern blotting) and *dmc1* Δ *exo1* Δ showed that whilst resection was still occurring in the double mutant, the bands appeared more discrete. More recently, Manfrini *et al.* (2010), confirmed the requirement for Exo1 in the production of hyper-resected intermediates during meiosis using a denaturing Southern blot approach and furthermore identified a role for both Sgs1 and Dna2 in catalysing the majority of the remaining resection. This is reminiscent of the dual resection pathways in operation during the repair of accidental DSBs formed during mitotic growth (see below). However, it remains unclear as to what extent *dmc1* Δ hyper-resection is reflective of wild-type resection and it has been argued that Exo1 may be playing a later role in the meiotic recombination process distinct from the initial resection taking place at break sites (discussed at greater length in Section 1.5). Thus, the factors mediating the resection of Spo11-catalysed DSBs in the presence of Dmc1 have not been unequivocally demonstrated.

The recent discovery that Sgs1 and Dna2 are involved in the resection of DSBs inflicted during vegetative growth (Mimitou and Symington, 2008; Zhu *et al.*, 2008) represents a significant advance in our understanding of the DNA repair process. While Sgs1 is a member of the highly-conserved RecQ family of helicases (named after the *Escherichia coli* *recQ*⁺ gene), members of which play many crucial roles in

maintaining genome stability (Chu and Hickson, 2009), Dna2 is an essential enzyme involved in DNA replication and possesses ATPase, DNA helicase and 5' to 3' single-stranded endonuclease activities (Bae and Seo, 2000). Using the conditional expression of site-specific endonucleases to generate breaks at either the *MAT* locus or between directly repeated regions of homology, Zhu *et al.*, (2008) and Mimitou and Symington (2008) were able to estimate the extent and rate of resection either directly (by physical analysis: probing the single-stranded regions uncovered) or indirectly (by measuring the amount of product formed by single-strand annealing [SSA] when resection reached far enough to uncover the homologous flanking regions) in a series of yeast mutants. This demonstrated the existence of two independent pathways by which resection can proceed. The first of these pathways is dependent upon the action of Exo1 alone while the second 'two-step' pathway relies upon the helicase activity of Sgs1 to unwind the DNA helix, thereby providing a substrate upon which the single-stranded endonuclease Dna2 can act. Similar 'two-step' strategies have been observed in human cells (Gravel *et al.*, 2008), *Xenopus laevis* (Liao *et al.*, 2008) and archaea (Hopkins and Paull, 2008). This work revealed that the role of MRX is largely confined to an Sae2-dependent initial processing step, producing approximately 100 bp of ssDNA. Subsequent to this, processive resection is rapidly carried out by one or both of the pathways described above. In *sgs1Δ exo1Δ* double mutants, the intermediates of the initial cleavage step accumulate and are then subject to slow, limited resection mediated by MRX/Sae2.

Although the above-described studies go a long way towards accounting for the previously unexplained redundancy displayed by mutants defective in the resection of mitotic DSBs, it is not known how the various factors are coordinated. In addition, it is questionable as to what extent the resection observed is representative of normal resection as the assays were mostly carried out in cells prevented from undergoing strand invasion. This meant that breaks were required to undergo extensive resection before repair was possible. For example, the SSA assays required around 7 kb (Mimitou and Symington, 2008) or 25 kb (Zhu *et al.*, 2008) of resection in order to uncover repeat sequences, both of which are considerably longer than required for strand invasion and furthermore, are far in excess of the lengths estimated to occur during meiotic repair (approximately 500-800 bp; Sun *et al.*, 1991; Bishop *et al.*, 1992). Significantly, when gene conversion was assessed in an *sgs1Δ exo1Δ* mutant proficient

for homologous recombination (HR), an appreciable amount of conversion was detected at the *MAT* locus, albeit at less than wild-type levels (Mimitou and Symington, 2008; Zhu *et al.*, 2008). This supports previous experiments demonstrating that extensive tracts of homology are not necessary to generate substrates proficient for strand invasion (Jinks-Robertson *et al.*, 1993; Ira and Haber, 2002).

Prior to these publications, the tRNA methyltransferase Trm2 was considered to be an alternative nuclease candidate. Trm2 catalyses the methylation of the uridine molecule present in tRNAs at position 54, a modification that is found in most bacterial and eukaryotic elongator tRNAs (Nordlund *et al.*, 2000). However, the function of this modification is not clear as no apparent phenotypic changes result from its absence. In addition to a methyltransferase role, Trm2 has also been shown to possess a nuclease activity that acts to promote HR in vegetative cells (Asefa *et al.*, 1998; Choudhury *et al.*, 2007a; Choudhury *et al.*, 2007b). Notably, a synergistic relationship between Trm2 and Exo1 was observed, resulting in dramatically increased sensitivity to both MMS and prolonged expression of the HO-endonuclease in the *trm2Δ exo1Δ* double mutant compared to either single mutant (Choudhury *et al.*, 2007a). If a similar synergism were active during meiotic repair, this could go some way towards explaining the seemingly mild *exo1Δ* phenotype. In contrast, experiments from a separate research group failed to detect any nuclease activity associated with Trm2 during mitotic growth and consequently reported wild-type spore viability in a *trm2Δ* homozygous diploid (Nordlund *et al.*, 2000). The effect of deleting both Trm2 and Exo1 during meiosis is unknown.

1.2.3.2 The regulation of resection

In addition to regulating the commitment to resection, the cell must also control the extent of resection in order to prevent the production of excessive lengths of ssDNA that may otherwise lead to genomic instability. This regulation almost certainly involves Tel1 and Mec1, the *Saccharomyces cerevisiae* homologues of the highly conserved PI3K-family protein kinases known as ATM (ataxia telangiectasia mutated) and ATR (ataxia telangiectasia and RAD3-related) in vertebrates. These checkpoint kinases are crucial mediators involved in the sensing and response to a wide range of DNA damage including DSBs (for a review see Harrison and Haber,

2006). While Tel1 is activated following the sensing of DSBs by MRX, Mec1 is activated by the presence of RPA-coated ssDNA (Zou and Elledge, 2003). One function of Mec1-dependent signalling may thus be to down-regulate nuclease function, restricting ssDNA production in a negative feedback loop. The mechanisms by which this takes place are not clear; however, phosphorylation of Exo1 in yeast has been demonstrated to occur in response to a variety of DNA damage and this modification may indeed act to limit the accumulation of ssDNA (Smolka *et al.*, 2007; Morin *et al.*, 2008). Similarly, in humans, hExo1 is phosphorylated in response to DSB formation and following the stalling of replication forks in an ATR-dependent fashion (El-Shemerly *et al.*, 2005; El-Shemerly *et al.*, 2008; Bolderson *et al.*, 2009). This suggests that the down-regulation of Exo1 may represent one of the processes important in controlling the length of resected intermediates produced in response to accidental DSBs.

In meiosis, processing by MRX/Sae2 is obligatory to detach Spo11 following break formation and in mutants defective in Spo11 removal, the unprocessed DSBs activate a Tel1-dependent checkpoint (Usui *et al.*, 2001). In addition, full nucleolytic processing of meiotic breaks requires the phosphorylation of Sae2 in a Tel1 and Mec1-dependent fashion (Cartagena-Lirola *et al.*, 2006; Terasawa *et al.*, 2008; Manfrini *et al.*, 2010). In this manner, an initial requirement for MRX/Sae2 may be analogous to the situation observed at endonuclease-induced mitotic breaks. Beyond this stage however, it is not clear how further ssDNA tracts are generated and it remains possible that distinct regulatory controls govern the resection of Spo11-dependent breaks. The cellular responses to programmed Spo11-dependent DSBs and accidental meiotic DSBs are significantly different (Cartagena-Lirola *et al.*, 2008) and this differential response is likely to be critical in establishing the altered repair outcome required at Spo11-catalysed breaks. A primary aim of meiotic repair is to promote crossing-over in order to ensure homologue non-disjunction at the first meiotic division. In contrast, when DSBs are formed during other stages of the cell cycle, crossing-over is largely repressed (Ira *et al.*, 2003), most likely to counteract the potentially deleterious consequences associated with un-regulated crossing-over such as loss of heterozygosity, chromosomal rearrangements and chromosome missegregation (Richardson *et al.*, 2004). What is more, mitotic HR preferentially utilises a sister chromatid template for repair, while a barrier to this is imposed

during meiosis by meiosis-specific mediators, leading to a strong inter-homologue bias (Carballo *et al.*, 2008).

In conclusion, it is clear that our understanding of resection (and in particular the resection of programmed Spo11-dependent DSBs in meiosis) is lacking in several key areas. Consequently, a current challenge facing the field involves the delineation of the control pathways that mediate resection of both meiotic and mitotic DSBs. The unambiguous identification of the proteins involved and the development of methods for accurately measuring resection are likely to be crucial steps in this process.

1.3 Pathways to repair

1.3.1 The double-strand break repair model

In 1983, Szostak *et al.* described a model to account for the recombinant products detected in segregation analysis based upon the hypothesis that recombination is initiated by DSBs. This double-strand break repair (DSBR) model posits that breaks are subsequently processed to 3' overhanging strands, one of which invades the homologue to form a small D-loop. DNA synthesis is then primed from this 3' end, extending the D-loop until the other 3' end is able to anneal to complementary DNA sequence. Synthesis also proceeds from this second 3' end, with branch migration leading to the formation of a double Holliday junction. Finally, cleavage of this double Holliday Junction in alternative orientations was suggested to result in either crossover or non-crossover products (see Figure 1.3; Szostak *et al.*, 1983).

However, subsequent genetic experiments cast doubt on certain aspects of this model and indeed whether a single pathway could be responsible for creating both crossovers and non-crossovers. For example, the Szostak model predicts that non-crossovers should exhibit heteroduplex DNA (hDNA) on both DNA molecules on opposite sides of the DSB (see Figure 1.3F). This is contradicted by numerous genetic studies, which demonstrate that the formation of hDNA in non-crossovers occurs primarily on one side of the DSB, consistent with hDNA being produced only on the broken DNA strand (Porter *et al.*, 1993; Gilbertson and Stahl, 1996; Merker *et al.*, 2003; Hoffmann and Borts, 2005; Hoffmann *et al.*, 2005; Jessop *et al.*, 2005). Such analyses also revealed the existence of a particular class of recombinant

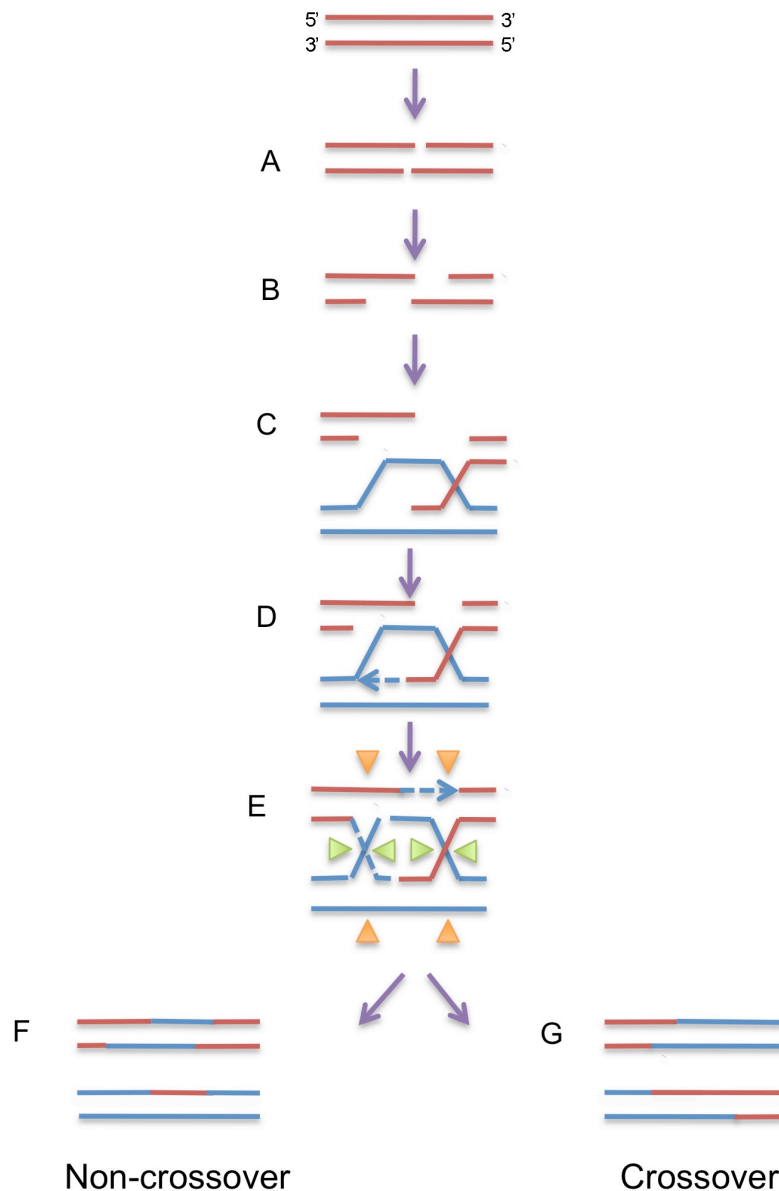


Figure 1.3: The double-strand break repair model

Following double-strand break formation (**A**), the DNA is resected in a 5' to 3' direction (**B**) leaving 3' overhanging strands that invade a homologous chromosome (**C**). DNA synthesis then extends from the 3' terminus of the invading strand (**D**). Second end capture and DNA synthesis results in the formation of a double Holliday junction (**E**), which is then cleaved in either the same orientation (eg: both pairs of green triangles or both orange triangles) or alternate orientations at each junction to yield either a non-crossover (**F**) or a crossover (**G**), respectively. Adapted from Szostak *et al.*, (1983).

tetrads featuring hDNA in a ‘trans’ configuration (for details see Porter *et al.*, 1993), yet the DSBR model is inconsistent with this type of event. Furthermore, physical studies have yielded evidence to suggest that more than one pathway is responsible for generating hDNA during the recombination process (Schwacha and Kleckner, 1995; Allers and Lichten, 2001) and mutations that block the formation of the major class of crossovers also block the formation of single-end invasion (SEI) and double Holliday junction (dHJ) intermediates while allowing non-crossovers to form as normal (see below; Borner *et al.*, 2004). Therefore, separate pathways generate crossovers and non-crossovers during meiosis with single-end invasion and double Holliday junction intermediates belonging to the pathway that generates crossover products exclusively.

1.3.2 The crossover pathway

The stabilisation of a nascent D-loop to form a SEI is the first molecularly distinct event in the major crossover pathway (Figure 1.4). These intermediates can be physically detected by two-dimensional gel electrophoresis at hotspot sites modified by the addition of restriction site polymorphisms that allow the parental origin of the each DNA duplex to be determined (Hunter and Kleckner, 2001). These SEIs form within patches of developing synaptonemal complex (SC) and rely upon the ‘ZMM’ group of meiosis-specific proteins consisting of Zip1, Zip2, Zip3, Zip4, Msh4, Msh5, Mer3 and the more recently identified Spo16 (Borner *et al.*, 2004; Shinohara *et al.*, 2008). Although slight differences between individual mutants are apparent, deletion of any *ZMM* confers a similar phenotype that can be dramatically affected by changes in sporulation temperature (Borner *et al.*, 2004). In the SK1 strain background at 33°C, the *zmm* crossover pathway is defective at the DSB to SEI transition, leading to a drastic reduction in crossovers and the arrest of sporulation prior to the first meiotic division. However, non-crossovers form as normal, providing further support for the theory that crossover control is imposed at (or prior to) the point of strand invasion. Contrastingly, at 23°C, a significant amount of spore formation takes place and DSBs fated to become crossovers seemingly lose this designation, progressing randomly to both crossovers and non-crossovers. The checkpoint monitoring crossover-specific intermediates thus appears to be more robust at higher temperature. At both temperatures, aberrant SC formation is

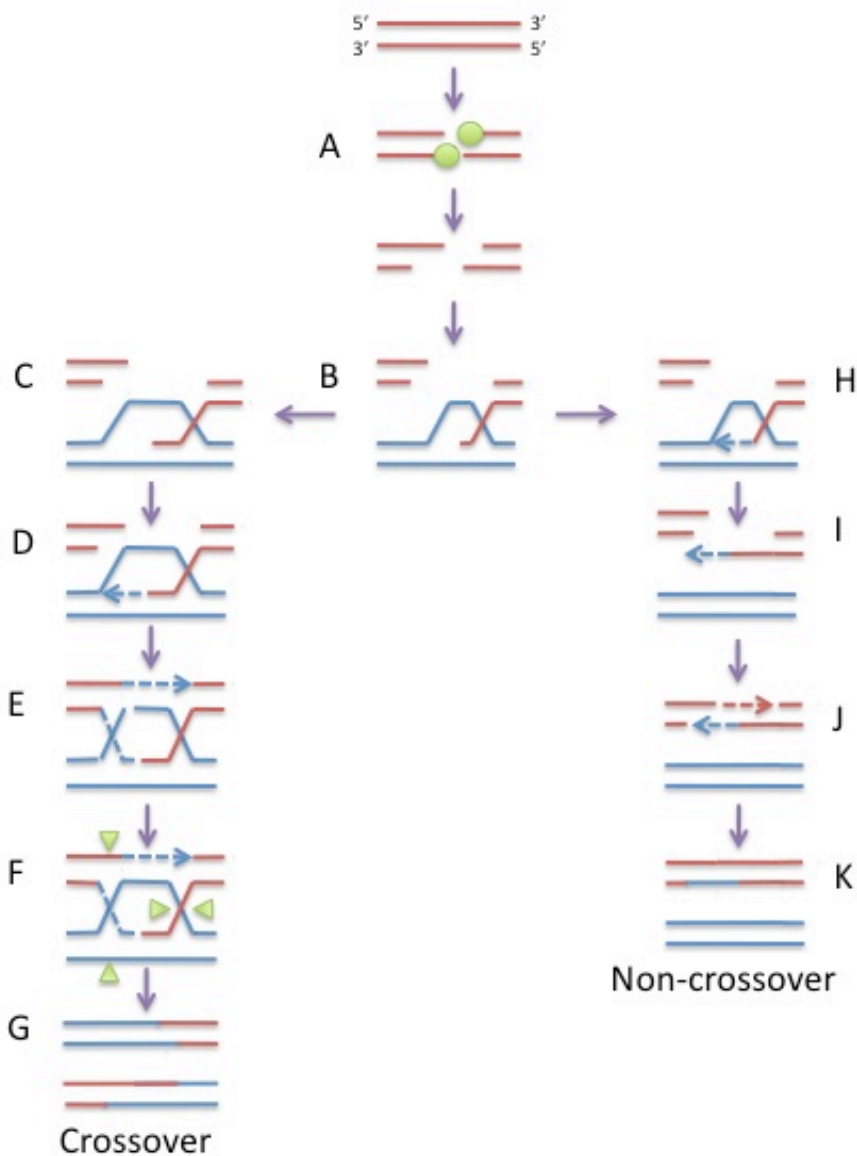


Figure 1.4: Model for recombinant molecule production in meiosis.

Following DSB formation (A) and removal of Spo11p (Spo11 is represented by green circles), DNA end resection occurs to produce 3' overhangs that can invade a homologous chromosome (B). The distinguishing event of the crossover pathway is the formation of a stable single-end invasion (SEI) intermediate (C). Following extension (D), second-end capture and double Holliday junction (dHJ) formation take place (E), cleavage of which (F; represented by green triangles) yields a crossover (G). If following synthesis (H) the initial invasion is displaced (I), synthesis-dependent strand annealing (J) may result in a non-crossover (K).

observed and there is a loss of genetically detectable crossover interference (see Section 1.4; reviewed in Lynn *et al.*, 2007).

Despite the collaborative nature of this group of proteins in crossover promotion, each ZMM (with the exception of the Msh4p/Msh5p heterodimer) plays a unique role in the process. The Zip proteins are essential components of the SC (Egydio de Carvalho and Colaiacovo, 2006), while Msh4, Msh5 and Mer3 are involved in DNA processing. The Msh4/Msh5 heterodimer is thought to encircle the D-loop produced by strand invasions, forming a sliding clamp that may stabilise the interaction (Snowden *et al.*, 2004), while Mer3 is a helicase that stimulates the extension of heteroduplex DNA during strand exchange in a 3' to 5' direction, an action that is again likely to increase the stability of the strand invasion intermediate (Nakagawa and Ogawa, 1999; Nakagawa and Kolodner, 2002; Mazina *et al.*, 2004). Although the biochemical function of Spo16 has not been determined, it has been implicated in extension of the SC (Shinohara *et al.*, 2008). In addition to the meiosis-specific ZMM group of proteins, several constitutively expressed enzymes are also required for normal crossover levels. These include Mlh1, Mlh3 and Exo1 (discussed in Section 1.5.2), and the Mus81/Mms4 complex (discussed in Section 1.3.4).

Following stabilisation of the invading strand to form a SEI, interaction with the second DNA end, recombination-associated DNA synthesis and ligation lead to the formation of a dHJ intermediate, cleavage of which yields a crossover (Figure 1.4). The identity of the nuclease responsible for this crucial final step has long remained elusive. Recently, using a screening-based approach to identify proteins capable of Holliday junction cleavage, Ip *et al.*, (2008) discovered that Yen1 (a member of the XPG family of endonucleases) possesses such activity. In parallel, hGen1 (the human orthologue of Yen1) was independently identified following biochemical analysis of nuclear fractions prepared from HeLa cells, suggesting that this enzyme may constitute the canonical resolvase in mitotic cells (Ip *et al.*, 2008). However, genetic evidence confirming these *in vitro* studies has not been produced and may be difficult to provide given the existence of other proteins that are potentially capable of resolving intact or nicked Holliday junctions. These alternative candidates include Sgs1 (Wu and Hickson, 2003), the Mus81/Mms4 complex (Hollingsworth and Brill,

2004; see Section 1.3.4), the Mlh1/Mlh3 heterodimer (Nishant *et al.*, 2008; discussed further in Section 1.5.2) and the Slx1/4 complex (Fricke and Brill, 2003). At present therefore, the identity of the meiotic Holliday junction resolvase(s) remains unknown.

1.3.3 Synthesis-dependent strand annealing

Not all DSBs are repaired to yield a crossover event. Whilst a lack of physically detectable intermediates render the molecular events occurring in the non-crossover pathway uncertain, it is thought likely to proceed via synthesis-dependent strand annealing (Paques and Haber, 1999). The initiating events in this pathway are similar to those in the crossover pathway; however, a stable SEI intermediate is not produced. Instead, the invading strand is displaced and anneals to the complementary sequence uncovered by resection on the opposite side of the break. DNA synthesis then acts to fill in the remaining gaps, followed by ligation of the DNA ends (see Figure 1.4). The results of a genetic assay designed to allow for the detection of recombinant molecules that can be specifically accounted for by synthesis-dependent strand annealing support a key role for this process in generating non-crossover products during meiosis (McMahill *et al.*, 2007).

1.3.4 An alternative crossover pathway

As studies of *zmm* mutants have demonstrated, the impairment of the *ZMM* pathway does not eliminate all crossovers. A large proportion of these remaining crossovers have been attributed to the action of the Mus81/Mms4 complex (Figure 1.5). Mus81 is a member of the XPG family of structure-specific endonucleases and functions in concert with the non-catalytic Mms4 (Eme1 in *Schizosaccharomyces pombe* and humans). Although the *in vivo* substrate of this complex remains somewhat controversial, it is capable of cleaving a variety of nicked joint molecule structures *in vitro* (reviewed in Hollingsworth and Brill, 2004). In *S. cerevisiae*, crossing-over decreases by approximately 25% in the absence of Mus81/Mms4, while sporulation and spore viability are reduced further still (de los Santos *et al.*, 2001). However, in contrast to those formed by the *ZMM* pathway, the crossovers produced by Mus81/Mms4 do not appear to exhibit interference (Section 1.4; de los Santos *et al.*, 2003; Argueso *et al.*, 2004).

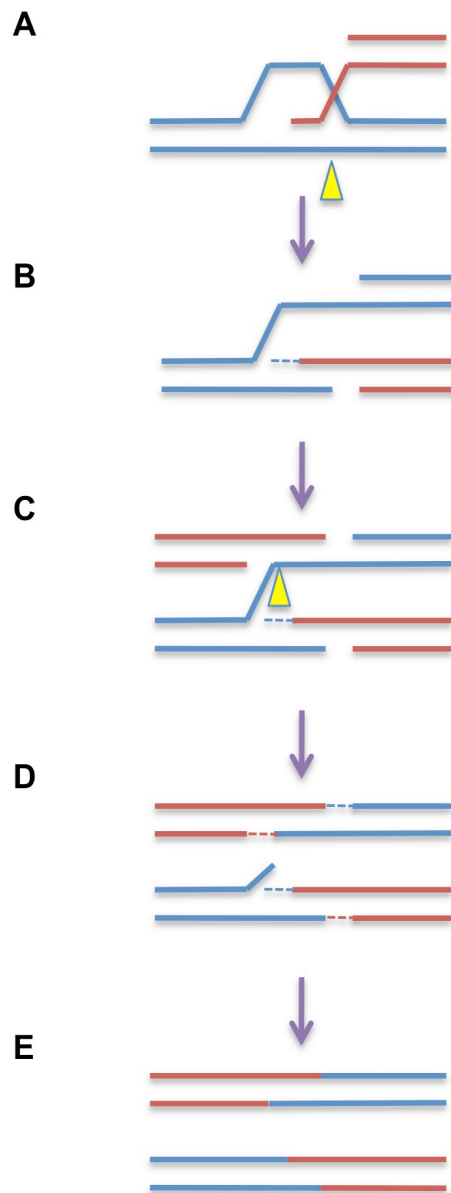


Figure 1.5: Model for the molecular function of Mus81/Mms4 in crossover production

The Mus81/Mms4 complex (represented by the yellow triangles) is proposed to act via sequential D-loop nicking to generate crossover products. Following cleavage of the four-way junction produced upon strand invasion (**A**, **B**), subsequent second-end capture and DNA synthesis lead to the formation of a nicked HJ structure. Cleavage of this intermediate (**C**), followed by flap removal and ligation (**D**), results in a crossover product (**E**). Adapted from Osman *et al.*, (2003).

It has recently been suggested that the primary function of Mus81/Mms4 is to resolve inappropriately formed joint molecules in partnership with the *RecQ* helicase Sgs1 (Jessop and Lichten, 2008; Oh *et al.*, 2008). In *sgs1 mus81/mms4* double mutants, unresolved joint molecules accumulate, preventing DNA segregation. However, single mutant studies suggest that this is the result of two distinct defects, leading the authors to propose a model whereby Sgs1 acts at an early stage to prevent the formation of aberrant joint molecules that would otherwise rely upon Mus81/Mms4 for their resolution. Mus81/Mms4 may thus act as a back-up system to the potent anti-recombinogenic activity of Sgs1. This supports earlier experiments showing that deletion of *SGS1* restores crossovers to *zmm* mutants (Jessop *et al.*, 2006; Oh *et al.*, 2007) and further demonstrates the complex interplay between pro- and anti-recombinogenic factors necessary to ensure that recombination proceeds correctly. The small number of aberrant joint molecules observable during wild-type meiosis may explain the requirement for Mus81/Mms4 in non-mutant cells (Jessop and Lichten, 2008; Oh *et al.*, 2008).

In summary, there are at least two pathways by which meiotic crossovers can be formed in *S. cerevisiae*: the major *ZMM* pathway that processes crossover-designated breaks, and the Mus81/Mms4 pathway that helps to resolve inappropriate/otherwise unresolvable recombination events. However, the extent to which these two pathways contribute differs between species. In the fission yeast *Schizosaccharomyces pombe*, crossovers appear to be entirely dependent upon Mus81/Eme1 and do not exhibit interference (Boddy *et al.*, 2001; see below for description of interference). Contrastingly, in the nematode worm *Caenorhabditis elegans*, all crossovers rely upon a *ZMM*-mediated pathway (Zalevsky *et al.*, 1999). Evidence from mice suggests that Mus81 is required to generate a subset of Mlh1/Mlh3-independent crossovers (Holloway *et al.*, 2008), implying that the situation in higher eukaryotes is similar to that in *S. cerevisiae*.

1.4 Crossover control: obligation, interference and homeostasis

Although crossovers do not occur at the same place in the genome in each meiosis, those processed via the *ZMM* pathway are not distributed at random. Instead, they exhibit a phenomenon termed crossover interference, which describes the observation that the presence of a crossover at one position along a chromosome

reduces the chance of another occurring nearby, leading to an evenly spaced crossover distribution. This trend has been confirmed in a wide-range of organisms and imparts several characteristics that may be of benefit to the cell (reviewed in Hillers, 2004). A further facet of crossover control is the maintenance of crossovers when DSBs are reduced. This was initially suggested when a series of Spo11 alleles of decreasing catalytic activity did not result in a corresponding linear decrease in Zip3 complexes (thought to mark the sites of future interfering crossovers) (Henderson and Keeney, 2004). Specifically, the defect in DSB formation was much more severe than the decrease in Zip3 foci. Martini *et al.*, (2006) then assessed recombination using the same Spo11 hypomorphs and found that crossover levels are indeed maintained at near wild-type levels at the expense of non-crossovers despite decreasing levels of DSBs. This so-called crossover homeostasis was accompanied by the maintenance of crossover interference. Furthermore, Chen *et al.*, (2008) observed a reduction in CO homeostasis in *zip2Δ* and *zip4Δ* strains in which interference is also reduced. Whilst this supports the supposition that interference and homeostasis are manifestations of the same mechanism, the reduction in homeostasis observed was less severe than the reduction in interference, indicating that there are additional complexities to these processes than are currently understood.

How the cell controls which breaks are resolved as crossovers and which become non-crossovers is the subject of current debate and several models have been put forward to account for the distribution pattern seen. Originally, it was suspected that the synaptonemal complex (SC) was involved in communicating an inhibitory signal along the chromosome from designated crossover sites (Egel, 1978). This proposal was made more convincing by evidence that the fission yeast *Schizosaccharomyces pombe* and the fungus *Aspergillus nidulans* lack both interference and synaptonemal complex (Olson, 1978; Snow, 1979; Egel-Mitani, 1982). Additionally, in non-null alleles of *ZIP1*, the amount of interference was shown to increase coordinately with the extent of synapsis (Tung and Roeder, 1998). Despite the convenience of this model however, observations argue that it cannot account for all aspects of interference. For example, although all *zmm* mutants lack interference when assessed genetically, cytological studies imply that interference remains intact. Synapsis initiation complexes (SICs; which include the proteins Zip2 and Zip3) are thought to

correspond to the sites of future interfering crossovers in wild-type cells. Staining of SIC foci demonstrated that their distribution displays interference in both wild-type, *msb4Δ* and *zip1Δ* backgrounds (Fung *et al.*, 2004). Thus it seems that the underlying mechanism controlling the distribution of crossovers is functional in these mutants but the pathway is defective at a later point. Additionally, in *zmm* mutants at high temperature, synapsis is defective but the crossover/non-crossover decision is still made successfully (Borner *et al.*, 2004). These results argue that the synaptonemal complex does not mediate the transmission of interference.

An alternative proposal is the “counting model” which puts forward the idea that crossovers are separated from each other by a fixed number of non-crossovers (Foss *et al.*, 1993). Whilst mathematical modelling of linkage data from *Drosophila melanogaster* and *Neurospora crassa* provided support for this concept (Foss *et al.*, 1993), studies in *Saccharomyces cerevisiae* were unable to satisfy fundamental predictions of the model (Foss and Stahl, 1995). Additionally, the demonstration that yeast cells are able to vary crossover/non-crossover ratios in response to DSB levels appears to be a direct contradiction of this theory (Martini *et al.*, 2006). A second model, the “mechanical stress model”, portrays crossovers to be the consequence of a build-up of stress within the chromatin fibre. This stress is said to result from the constriction of chromatin expansion within the cell, causing a conformational change (such as buckling or twisting) and consequent crossover designation at certain sites. This designation would then lead to a local relief of stress along the chromosome axis, reducing the chance of another crossover forming nearby (Kleckner *et al.*, 2004). In addition to predicting the existence of crossover homeostasis, this model may also offer an explanation as to why temperature influences the ability of certain mutants to form crossovers, as temperature could affect the physical state of the chromatin (Borner *et al.*, 2004). If this is an accurate interpretation of the basis of crossover control, it suggests that mutations in proteins involved in constraining chromatin such as histone modifiers or remodelling factors would act to reduce or eliminate interference, yet with the potential exceptions of Ndj1 and Csm4 (proteins required for the clustering of homologues into an arrangement known as the bouquet during meiosis), without which a partial disruption in interference is observed (Chua and Roeder, 1997; Wanat *et al.*, 2008), no components fitting this description have been discovered.

1.5 Mismatch repair in meiosis

1.5.1 The mismatch repair process

The mismatch repair (MMR) machinery is essential for maintaining genomic stability and acts to correct DNA mismatches formed during replication and recombination. The initial characterisation of MMR was carried out in the prokaryote *Escherichia coli*. In this organism, repair is initiated by the binding of a MutS ATPase homodimer to a mismatch such as a base-base mismatch or a small insertion or deletion. A second ATPase homodimeric protein, MutL, is then recruited and functions to coordinate mismatch recognition and repair. Interaction between MutS and MutL serves to activate the latent endonuclease activity of MutH, which nicks the newly synthesised (and transiently unmethylated) DNA strand at the nearest d(GATC) hemimethylated site. This allows for the loading of UrvD (DNA helicase II), leading to the unwinding of the DNA and the creation of a length of ssDNA that is bound by single-strand binding protein. Removal of this ssDNA (including the mismatch) is then performed by one of four redundant exonucleases: the 3' to 5' ExoI and ExoX and the 5' to 3' ExoVII and RecJ. In this way, the ssDNA can be degraded regardless of the position of the initiating nick relative to the mismatch. Finally, the high-fidelity DNA polymerase III acts to resynthesise the missing DNA and the remaining nick is sealed by DNA ligase (reviewed in Kunkel and Erie, 2005; Jiricny, 2006).

In eukaryotes, the basic mechanics of the prokaryotic system are maintained but made more complex by an increased specialisation for different types of mismatch. This specialisation is possible due to the increased number of MMR components expressed. For example, eukaryotic MMR requires three MutS homologues: Msh2, Msh3 and Msh6. Three further MutS homologues also exist but do not function in mismatch repair: Msh4 and Msh5 are expressed during meiosis exclusively (see section 1.3.2) while Msh1 is involved in the repair of mitochondrial DNA (Reenan and Kolodner, 1992). Although Msh2 is required for the recognition of all types of mismatch, it forms a heterodimer with either Msh6 (to form MutS α) or Msh3 (to form MutS β) depending upon the type of mismatch present (Marsischky *et al.*, 1996). Similarly, yeast expresses four MutL homologues: Mlh1, Mlh2, Mlh3 and Pms1 (Pms2 in humans). Although Mlh1 forms distinct heterodimers with all three remaining MutL homologues, the Mlh1/Pms1 (MutL α) heterodimer appears to be

the most important in terms of MMR (Habraken *et al.*, 1997), with the Mlh1/Mlh2 (MutL β) and Mlh1/Mlh3 (MutL γ) complexes playing lesser, more specialised roles (Flores-Rozas and Kolodner, 1998; Wang *et al.*, 1999; Harfe *et al.*, 2000). In addition to the MutS and MutL heterodimers, MMR requires several factors involved in DNA replication (proliferating cell nuclear antigen [PCNA], replication factor C [RFC] and DNA polymerase δ), the single-strand binding replication protein A (RPA) and the 5' to 3' exonuclease, Exo1 (Constantin *et al.*, 2005).

In the absence of a MutH homologue, the mechanisms underlying eukaryotic strand discrimination and mismatch excision are less well understood than the equivalent systems in *E. coli*. It is possible that existing nicks such as the 3' terminus of the leading strand or the gaps between Okazaki fragments on the lagging strand direct the post-replicative MMR machinery to the discontinuous strand (Jiricny, 2006). *In vitro* assays have demonstrated that Exo1 is required for efficient repair of mismatches located both 5' and 3' to DNA nicks, despite the fact that Exo1 is only able to function in a 5' to 3' direction (Dzantiev *et al.*, 2004; Constantin *et al.*, 2005). An explanation for this surprising finding came with the discovery that the MutL α heterodimer possesses a latent endonuclease activity capable of introducing single-strand breaks in the vicinity of a mismatch (Kadyrov *et al.*, 2006; Kadyrov *et al.*, 2007). This incision is strongly biased towards the strand featuring a pre-existing nick and requires a DQHA(X)₂E(X)₄E metal-binding motif found in the Pms1 subunit. In this manner, MutL-mediated incision on the distal side of a mismatch located 3' to a DNA nick can provide an entry point for Exo1 to catalyse mismatch excision. Nevertheless, the MMR defect seen in *exo1* Δ cells is considerably less severe than that observed in the absence of Msh2, suggesting that some MMR may occur in an Exo1-independent fashion (Tishkoff *et al.*, 1997). This residual activity is also seen in *in vitro* assays carried out in Exo1^{-/-} mouse embryonic fibroblasts (Wei *et al.*, 2003) and can be reconstituted in cell-free preparations that lack Exo1 but contain purified recombinant human proteins of other MMR components (Kadyrov *et al.*, 2009). In these systems, a gapped excision intermediate is not detected, leading to the suggestion that the mismatch is instead removed by synthesis-driven strand displacement of the DNA spanning the region (Kadyrov *et al.*, 2009).

1.5.2 The role of mismatch repair during meiosis

In meiosis, in addition to replication errors, the mismatches produced in hDNA during recombination provide substrates for the MMR machinery. Indeed, recognition of these mismatches is important for the prevention of inappropriate recombination between diverged sequences (Chambers *et al.*, 1996). In situations where sequences are sufficiently similar to allow recombination to proceed, the resolution of meiotic mismatches may result in a gene conversion: the non-reciprocal transfer of genetic information between DNA homologues. These events can be identified in *S. cerevisiae* by non-Mendelian segregation of the two alleles in a tetrad. For example, if two alleles *A* and *a* are present at a given locus and a DSB on an *A* chromatid is repaired by strand invasion of an *a* chromatid, an *A/a* mismatch may be formed. This would be detected as a conversion if the *A* allele were excised and the *a* used as a template for DNA synthesis. Alternately, if the mismatch were repaired to the genotype of the *A* allele, Mendelian segregation would be restored. These two outcomes are known as conversion-type and restoration-type repair respectively. If mismatches remain unrepaired, the alleles will segregate from each other during the first mitotic division following spore germination, resulting in a sectorized colony. This is termed post-meiotic segregation (PMS). Both gene conversions and PMS events result in non-Mendelian segregation (NMS) patterns in tetrad analysis. These events are referred to using nomenclature derived from fungi that undergo a mitotic division following meiosis to give eight haploid products (Figure 1.6).

1.5.2.1. Gene conversion gradients

Linear variations in the gene conversion frequency at different positions along the gene have been observed at several yeast loci including *ARG4* (Nicolas *et al.*, 1989), *HIS4* (Detloff *et al.*, 1992), *HIS2* (Malone *et al.*, 1992) and *CYS3* (Vedel and Nicolas, 1999). This phenomenon has been termed a polarity gradient. Typically, the polarity is determined by the location of the initiating DSB hotspot, consistent with gene conversions resulting from the repair of mismatches formed in the hDNA that extends outwards from the break site during the repair process. However, several findings suggest that the extent of gene conversion observed for a given allele cannot be solely accounted for by the frequency with which it is incorporated into hDNA and argue that the action of the MMR complex upon the mismatch formed is also important in gradient formation. It is known that the MMR machinery does not

function equally well on all types of mismatch. Certain alleles such as C/C mismatches (Detloff *et al.*, 1991) and palindromes (Nag *et al.*, 1989) yield high numbers of PMS events, suggesting that they are poorly recognised and/or repaired. Therefore, one approach to investigate the role of MMR in gradient formation has been to analyse the segregation of these poorly repairable mismatches (PRMs). In such a study at the *HIS4* locus in the AS4/13 strain background, Detloff *et al.* (1992) observed that unlike well-repairable mismatches (WRMs), the conversion rates of PRMs situated at differing distances from the *HIS4* hotspot did not exhibit a steep gradient. This led to the suggestion that polarity gradients are (at least partially) a by-product of the action of the MMR machinery, a conclusion that is also supported by studies of MMR deficient mutants. For example, upon deletion of *MSH2*, polarity gradients at *HIS4* and *ARG4* are almost abolished (Reenan and Kolodner, 1992; Alani *et al.*, 1994).

To account for these observations, two models have been proposed. The first of these, the heteroduplex rejection model, posits that polarity gradients result from the recognition of mismatches in nascent hDNA by the MMR machinery and the subsequent disruption of hDNA extension prior to inclusion of the mismatch. Therefore, the extent and slope of the gradient is dependent upon both the number of mismatches present and the frequency with which they are detected (Reenan and Kolodner, 1992; Alani *et al.*, 1994). To test this hypothesis, Hillers and Stahl (1999) assessed the frequency of NMS exhibited by a PRM at the 3' (low) end of the *HIS4* gene in the presence and absence of an additional mismatch sited closer to the hotspot break site. This demonstrated that the downstream PRM was less likely to be incorporated into hDNA when the additional mismatch was present, supporting the heteroduplex rejection model.

Alternatively, the conversion/restoration model proposes that the gradient arises as a consequence of how the mismatches are repaired. Specifically, it suggests that alleles close to the break site are preferentially repaired to yield conversions whereas more distal mismatches are converted or restored at random (Detloff and Petes, 1992). Support for this hypothesis was provided by co-conversion studies in which a PRM placed at the 3' (low) end of the *HIS4* gradient was used in conjunction with a WRM

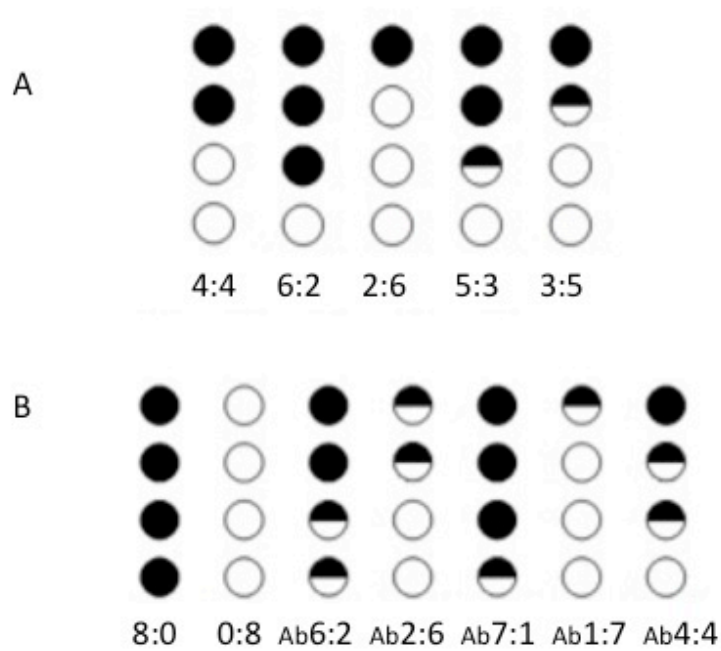


Figure 1.6: Non-Mendelian segregation in yeast

(A) In the absence of recombination, two alleles may be expected to segregate with a 4:4 distribution. However, if mismatches are produced between homologues during recombination, mismatch repair can lead to 6:2 or 2:6 tetrads being produced. In the absence of mismatch repair, these mismatches will segregate away from each other at the first mitotic event following germination, leading to 5:3 and 3:5 events. (B) More complex events(s) involving all four chromatids can result in the aberrant (Ab) segregation patterns shown above.

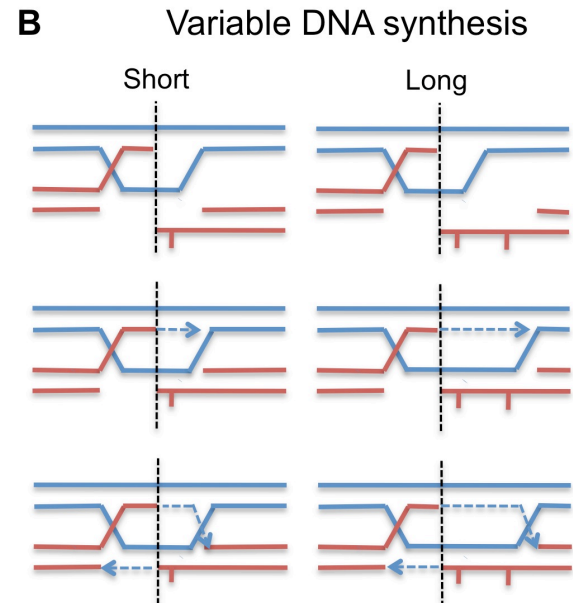
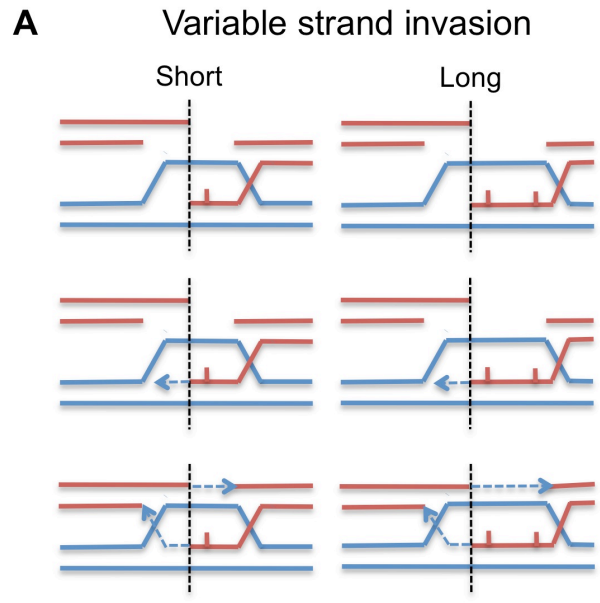
situated closer to the hDNA initiation site (Kirkpatrick *et al.*, 1998). Two WRMs were studied in separate crosses. These were situated at either +2 bp or +688 bp with respect to the *HIS4* ORF and resulted in the same single-base mismatch at both locations. When tetrads exhibiting PMS of the 3' allele (in which hDNA is thought to have extended the full length of *HIS4* and hence included the WRMs) were examined, a greater conversion frequency was observed for the +2 bp allele than for the +688 bp allele (50% and 28% aberrant segregation respectively). This argues that alleles closer to the hDNA initiation site are more likely to undergo conversion-type repair than more distant alleles as predicted by the conversion/restoration model.

While the conversion/restoration model suggests that hDNA extends the full length of a conversion gradient, a constant hDNA length cannot account for a greater than two-fold gradient (when 100% of alleles at the high end of the gradient are converted compared to 50% of alleles at the low end). While this fits with data from the *HIS4* hotspot in the AS4/13 strain background, experiments in other strain backgrounds (such as Y55 and SK1) reveal the existence of considerably steeper gradients (for examples see Reenan and Kolodner, 1992; Khazanehdari and Borts, 2000). Moreover, it has been demonstrated that a gradient still exists (albeit reduced) in mismatch defective *mlb1Δ* and *msb2Δ* strains in the same strain backgrounds (Reenan and Kolodner, 1992; Hunter and Borts, 1997; Hoffmann *et al.*, 2005). Therefore, regardless of the effect of the mismatch repair system and central to the ability of both models to account for polarity gradient formation is a requirement for variable heteroduplex tract lengths. Processes that may be expected to influence the length of hDNA include both strand resection and DNA synthesis. In particular, it has been suggested that the resection of meiotic breaks is one mechanism by which conversion gradients are initiated. If the lengths of the ssDNA tails produced following DSB formation are variable, a large number of molecules may undergo resection close to the DSB site, but fewer molecules would be resected as far as more distally located markers. This could thus lead to varying amounts of hDNA being formed either upon strand invasion or during recombination-associated DNA synthesis, contributing to the establishment of a polarity gradient (Figure 1.7; Borts *et al.*, 2000; Hoffmann and Borts, 2004). Such heterogeneity in resection length is supported by the fuzzy appearance of DSB bands on Southern blots (Bishop *et al.*, 1992), and Sun *et al.* (1991) and Vedel and Nicolas (1999) reported that the

distributions in the lengths of resected molecules produced at *ARG4* and *CYS3* parallel the conversion gradients observed at the same loci.

If the contribution of resection to gradient formation were significant, mutations that reduce resection tract lengths would be expected to reduce the frequency of NMS. When the most likely candidate for this role, Exo1, is considered, contradictory results regarding the effect of *EXO1* deletion have been produced. For example, no decrease in NMS was detected by monitoring prototroph formation between heteroalleles at both *HIS4LEU2* and *ARG4* in the SK1 strain background (Tsubouchi and Ogawa, 2000), while in the AS4/13 background, tetrad analysis demonstrated a significant decrease in the conversion frequency of markers at *ARG4* but not at *HIS4* (Kirkpatrick *et al.*, 2000). Khazanehdari & Borts (2000) on the other hand, observed a consistent decrease in conversion rate at all loci in *exo1Δ* Y55 strains, but this decrease was only statistically significant at *HIS4*. In this latter study, conversion frequencies at all points along the *HIS4* conversion gradient were reduced in *exo1Δ* by approximately half, leading to the suggestion that Exo1 is responsible either for the resection of approximately half of all breaks at *HIS4* or that in the absence of Exo1, all breaks are resected half as far as normal. However, these two scenarios could not be distinguished between further using the genetic data. Given these findings, two alternate but not mutually exclusive possibilities are suggested to account for the seemingly conflicting data produced by studies of *exo1Δ* mutants: firstly, the extent to which Exo1 is required for resection may vary depending upon the locus of interest and secondly, the contribution resection makes to conversion gradient formation may vary depending upon the locus studied. Locus-dependent contributions of the various mechanisms involved in gradient formation have also been suggested to account for apparently contradictory results concerning the role of MMR in the process (for further information, see Nicolas and Petes, 1994; Borts *et al.*, 2000).

The identification of a novel allele of *POL3* in which the last four amino acids of the protein are missing provided an interesting insight into the influence of recombination-related DNA synthesis on gene conversion (Maloisel *et al.*, 2004). The *POL3* gene encodes the catalytic subunit of DNA polymerase δ and whereas *POL3* deletion mutants are inviable, the *pol3-ct* allele appears to be specifically



C Uncoordinated resection and synthesis may result in flap production

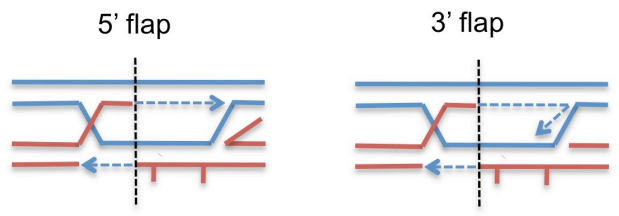


Figure 1.7: Models for the role of resection in heteroduplex tract formation and crossover formation

(A) Resection could influence the extent of hDNA formed by influencing the amount of DNA incorporated upon strand invasion. (B) Alternatively, if strand invasion is short, resection could act to determine the amount of DNA synthesis that occurs. In these examples, the short vertical lines represent potential mismatches situated at varying distances from the DSB. If synthesis and resection are not coordinated (C), DNA flaps may form. These flaps could potentially be either 5' or 3' flaps.

defective in various aspects of meiotic recombination but does not exhibit any defects in cell growth or the response to DNA damage (Maloisel *et al.*, 2004). Crucially, in the AS4/13 background, the *pol3-ct* mutant exhibited a distance-dependent effect on the gene conversion gradient at *HIS4* whereby alleles placed close to the initiating DSB (+2 bp into *HIS4*) showed wild-type conversion levels, yet conversion of alleles further away was significantly reduced. The fold decrease in non-Mendelian segregation observed in *pol3-ct* when compared to wild-type rose in a linear fashion with increasing distance from the DSB site, resulting in a steeper polarity gradient in the mutant than in wild-type. Alleles at *ARG4* and *TYR7* also exhibited significantly decreased NMS frequencies (Maloisel *et al.*, 2004). This phenotype led the authors to suggest that the processivity of recombination-related DNA synthesis was inhibited in *pol3-ct* strains and argues that while DNA synthesis is important in determining the extent to which hDNA is extended during recombination, it is not involved in the initiation of hDNA. The effect of the *pol3-ct* allele upon gene conversion in other strain backgrounds was not assessed.

1.5.2.2 Mismatch repair proteins in crossover promotion

Several MMR proteins have been demonstrated to play an additional mismatch-independent role in promoting crossing-over during meiosis (reviewed in Hoffmann and Borts, 2004). For example, deletion of *MLH1* reduces crossovers to a similar extent as deletion of *MSH4* or *MSH5*. Furthermore, analysis of an *mlb1Δ msb4Δ* double mutant suggests that the two genes operate in the same recombination pathway (Hunter and Borts, 1997). Mlh1 appears to function in concert with Mlh3 to perform this role and *mlb3Δ* mutants display a meiotic phenotype similar to that resulting from inactivation of *MLH1* (Wang *et al.*, 1999). The requirement for the Mlh1/Mlh3 heterodimer in crossover formation is highly conserved among higher eukaryotes and both *Mlh1^{-/-}* and *Mlh3^{-/-}* mice are infertile (Edelmann *et al.*, 1996; Lipkin *et al.*, 2002). However, synapsis occurs as normal in these mutants and temporal analysis of Mlh1 and Mlh3 in wild-type cells has shown that foci formation reaches a peak in early pachytene, arguing that the MutL heterodimer functions downstream of Msh4/Msh5 (Baker *et al.*, 1996). This later role is consistent with genetic studies in yeast (Hunter and Borts, 1997).

Despite the fundamental nature of these proteins in recombination, the precise molecular function of Mlh1/Mlh3 remains uncertain. Wild-type levels of crossing-over requires ATP binding by Mlh1 and Mlh3, suggesting that the conformational change resulting from such binding is crucial (Hoffmann *et al.*, 2003; Sacho *et al.*, 2008; Cotton *et al.*, 2010). Given that the Mlh1/Mlh3 complex is required around the time of dHJ resolution, it has been proposed that this conformational change may activate and/or direct a Holliday junction resolvase (Hoffmann and Borts, 2004). More recently, point mutations in the DQHA(X)₂E(X)₄E motif required for the ATPase-dependent endonuclease activity of Mlh3 have been shown to reduce crossing-over to the same extent as *mlh3*Δ, raising the possibility that Mlh1/Mlh3 may participate in dHJ resolution directly (Nishant *et al.*, 2008).

In contrast to *mlh1*Δ mutants, *exo1*Δ strains do not exhibit any increase in PMS events at small, well repairable mismatches (Khazanehdari and Borts, 2000) and only a slight increase when larger palindromic insertions were studied (Kirkpatrick *et al.*, 2000) demonstrating that Exo1 does not play a major role in meiotic MMR. However, crossing-over in the absence of Exo1 is reduced to a similar extent as in *msb4*Δ strains (Khazanehdari and Borts, 2000; Kirkpatrick *et al.*, 2000; Tsubouchi and Ogawa, 2000). As discussed in Section 1.2.3.1, Exo1 has been implicated in the resection of meiotic DSBs. However, the exact role of Exo1 during meiosis remains controversial and several models have been proposed to account for the *exo1*Δ crossover deficit (Hoffmann and Borts, 2004). As described above, measurements of gene conversion have shown that deletion of *EXO1* may reduce the amount of hDNA formed at *HIS4* (Khazanehdari and Borts, 2000) and *ARG4* (Kirkpatrick *et al.*, 2000). There is convincing evidence to suggest that crossovers are associated with longer tracts of heteroduplex DNA than those resulting in non-crossovers (Terasawa *et al.*, 2007; Chen *et al.*, 2008; Mancera *et al.*, 2008) and it is possible therefore that the decreased crossing-over observed in *exo1*Δ is a simply a consequence of the reduction in hDNA length.

As crossover control is imposed at or prior to the formation of any stable strand invasion intermediate (Bishop and Zickler, 2004), one theory is that shorter resection tracts following DSB formation may decrease the stability of strand invasion events, resulting in molecular interactions less likely to form a stable SEI and subsequently

be resolved as a crossover. In support of this, *exo1Δ msb4Δ* and *exo1Δ msb5Δ* strains do not exhibit a further reduction in crossing-over compared to either single mutant, suggesting that all three proteins operate in the same pathway (Khazanehdari and Borts, 2000; Kirkpatrick *et al.*, 2000; Tsubouchi and Ogawa, 2000). It may therefore be the case that Exo1 acts at an early stage to resect those breaks that will be targeted towards the ZMM crossover pathway. Consistent with this, the change in the *HIS4* gene conversion gradient in *exo1Δ* could be interpreted as being caused by a proportion of breaks being resected less (Khazanehdari and Borts, 2000). What is more, spore viability is significantly decreased in the *exo1Δ msb4Δ* double mutant compared to *msb4Δ* alone (Khazanehdari and Borts, 2000; Tsubouchi and Ogawa, 2000), arguing that there is some level of functional redundancy in operation between the two enzymes. Perhaps in the absence of Exo1, Msh4 is still able to stabilise some invasions sufficiently to enable repair. Similarly, without Msh4, Exo1 could further resect the DNA to make the intermediate more stable. In the absence of both proteins, a greater proportion of breaks may remain unrepaired, hence the reduction in spore viability. If Exo1-mediated resection does indeed target DSBs for the ZMM crossover pathway, it follows that *exo1Δ* strains may exhibit defects in crossover interference. However, while the numbers of *exo1Δ* tetrads studied in publications to date are not sufficient to assess whether or not this is the case, spore viability was shown to be significantly higher in *exo1Δ* than *msb4Δ* despite a similar reduction in crossing-over. To reconcile this disparity it was suggested that whereas the remaining crossovers in *msb4Δ* are distributed at random (later demonstrated in Novak *et al.*, 2001), crossovers in *exo1Δ* retain interference and are thus better positioned to promote homologue disjunction (Khazanehdari and Borts, 2000; Tsubouchi and Ogawa, 2000).

A variation on the above theme is the suggestion that Exo1 (rather than being required for resection prior to strand invasion) acts to carry out continuous resection as recombination-related DNA synthesis proceeds (Figure 1.7; Hoffmann and Borts, 2004). If this resection is prevented, two consequences can be envisaged that could reduce crossing-over. In the first instance, DNA synthesis may be curtailed, leading to displacement of the invading strand. This would prevent the formation of a dHJ and subsequently a crossover, causing the repair process to resemble that of SDSA. Alternatively, synthesis could proceed unimpeded, which in the absence of

continuous resection could lead to the formation of DNA flaps that may hinder dHJ formation. Both of these scenarios necessitate that the processes of DNA resection and synthesis are normally coupled, implying that in situations where synthesis is reduced, resection would be similarly decreased and thus synthesis-defective mutants and resection-deficient mutants should display similar phenotypes. As described above, the *pol3-ct* allele is thought to exhibit reduced processivity during recombination-related DNA synthesis, leading to decreased hDNA production and fewer crossovers (Maloisel *et al.*, 2004). Although no assessment of resection was made in these strains, they do not appear to be deficient in ZMM-mediated crossovers, as crossover interference remains intact. In fact, interference is slightly strengthened when compared to the wild-type, arguing that the missing crossovers may represent those dependent on Mus81/Mms4. While this appears to be at odds with the *exo1Δ msb4Δ* phenotype, which suggests that *exo1Δ* mutants lack ZMM-mediated crossovers, it may be that interference remains intact in *pol3-ct* because the synthesis defect occurs after crossover designation has occurred. Therefore, without direct measurements of resection, the coordination of synthesis and resection is difficult to assess.

Finally, it has been suggested that replication and resection are not generally coordinated, potentially leading to the production of 5' or 3' flaps following second-end capture (Figure 1.7). A 3' flap would provide a substrate for the Mus81/Mms4 complex as shown in Figure 1.7, while 5' flaps could be removed by Exo1 using either the exonuclease or endonuclease activities of Exo1 (Abdullah *et al.*, 2004; Hoffmann and Borts, 2004; Hunter, 2006). Exo1 may thus play a later 'trimming' role to facilitate the formation of ligatable DNA ends in order to create a dHJ structure. A role for Mus81/Mms4 in resolving the flaps produced by replication beyond the end of resection is in good agreement with the suggestion that *pol3-ct* strains are deficient in this class of crossover (Maloisel *et al.*, 2004). A later role is also consistent with the effect of the *Exo1^{-/-}* mutation in mice, which renders both males and females infertile (Wei *et al.*, 2003). In a study of meiotic progression in mice *Exo1^{-/-}* oocytes, reduced localisation of Mlh1 and Mlh3 was observed followed by a severe reduction in chiasmata (albeit less severe than in *Mlh1^{-/-}* and *Mlh3^{-/-}*) immediately prior to the first meiotic division, leading to the suggestion that Exo1 acts to promote crossover formation via stabilisation of the Mlh1/Mlh3 heterodimer

(Kan *et al.*, 2008). It is difficult however to reconcile this stabilising role with the reduction in heteroduplex tract length seen in yeast. Therefore, no single model proposed to date is able to reconcile all aspects of the *exo1Δ* phenotype satisfactorily and the molecular role of Exo1 in the recombination process remains unclear.

1.6 Aims and objectives

The 5' to 3' resection of DNA ends following meiotic DSB formation is a common feature of all homologous recombination models and the stretches of ssDNA produced are key substrates required for the initiation of DNA repair. However, despite the importance of this process, many of the underlying molecular aspects governing both the formation and function of this ssDNA remain unclear. A key potential nuclease that may be involved is Exo1, without which crossing-over is significantly reduced, leading to errors in chromosome segregation. At several alleles, non-Mendelian segregation is also reduced in *exo1Δ* cells, raising the possibility that resection tracts can influence the length of hDNA produced during DNA repair. As crossovers are associated with longer tracts of hDNA than non-crossovers, it has been hypothesised that the shorter tracts observed in *exo1Δ* could also be responsible for the crossover defect observed.

In this work, we aimed to test this hypothesis by assessing the extent to which resection influences recombination and by examining the role of Exo1 in this process. In order to do this we sought to employ both genetic and physical methods of analysis, focussing upon the well-characterised Spo11-dependent *HIS4* hotspot where Exo1 has been implicated in break processing (Khazanehdari and Borts, 2000). Specifically, we aimed to devise an assay that would allow us to accurately measure the amount of ssDNA produced varying distances downstream of the *HIS4* break site. It was envisaged that this would permit us to demonstrate which proteins are involved in the resection process and to investigate both the influence of resection on non-Mendelian segregation and the extent to which resection and DNA synthesis are coordinated. We further aimed to study defined point mutations in *EXO1* known to differentially affect the exonuclease and endonuclease functions of the protein (Tran *et al.*, 2002) in order to determine the various catalytic and/or structural contributions made by Exo1 towards promoting inter-homologue

crossing-over. Other proteins implicated in mitotic DNA end resection were also assessed in an attempt to explore the degree of functional redundancy in operation.

It was hoped that this research would be beneficial in furthering our understanding of the factors that act to promote the accurate segregation of chromosomes during meiosis, a crucial eukaryotic process in which defects can have serious consequences including miscarriage, infertility and genetic abnormalities.

CHAPTER 2

MATERIALS AND METHODS

2.1 Materials

2.1.1 Yeast strains

All strains are derivatives of the *Saccharomyces cerevisiae* SK1 isolate (Kane and Roth, 1974) unless otherwise stated. Genotypes of the strains used are listed in Table 2.1. Only the strains used in experimental analyses are described rather than the numerous strains produced during strain construction. Details of the methods by which particular alleles were introduced are given in the relevant chapters.

2.1.2 Plasmids

A brief description of the plasmids used is given in Table 2.2.

2.1.3 Oligonucleotides

Oligonucleotides were designed with the aid of the Primer3 web interface (Rozen and Skaletsky, 2000) to have a melting temperature between 58°C and 60°C and a GC content of 40 to 60%. All were purchased from Invitrogen. The DNA sequences of the oligonucleotides used are given in Tables 2.3 and 2.4.

2.1.4 Media

Saccharomyces cerevisiae cells were routinely grown in YEPD (Yeast Extract, Peptone, Dextrose) medium containing 1% (w/v) Bacto yeast extract, 2% (w/v) dextrose, 2% (w/v) Bacto peptone and 0.05% (w/v) adenine hemisulphate in 0.05 M hydrochloric acid. To select against petite mutations, cells were tested for their ability to grow on YEPEG (Yeast Extract, Peptone, Ethanol, Glycerol) medium containing 1% (w/v) succinic acid, 1% (w/v) Bacto yeast extract, 2% (w/v) Bacto peptone, 2% (v/v) glycerol and 0.5% (w/v) adenine hemisulphate in 0.05M hydrochloric acid. The pH was adjusted to 5.5. After autoclaving, 3% (v/v) 100% ethanol was added. Minimal medium consisted of 0.68% (w/v) Difco yeast nitrogen base without amino acids and 2% (w/v) dextrose. Synthetic complete medium was as minimal medium but

Table 2.1: Strain genotypes

Strain ²	Genotype ¹
RK358	<i>his4-XhoI MATα ade1-1 lys5-P cyh2-Z CEN8:URA3 arg4-Nsp</i>
RK359	<i>his4-XhoI MATα ade1-1 lys5-P cyh2-Z CEN8:URA3 arg4-Nsp exo1Δ::KanMX4</i>
RK366	<i>his4-XhoI MATα ade1-1 lys5-P cyh2-Z CEN8:URA3 arg4-Nsp exo1Δ::KanMX4 sgs1-mn: KanMX4</i>
RK368	<i>his4-XhoI MATα ade1-1 lys5-P cyh2-Z CEN8:URA3 arg4-Nsp sgs1-mn: KanMX4</i>
RK377	<i>his4-XhoI MATα ade1-1 lys5-P cyh2-Z CEN8:URA3 arg4-Nsp exo1Δ::KanMX4 trm2Δ::KanMX4</i>
RK379	<i>his4-XhoI MATα ade1-1 lys5-P cyh2-Z CEN8:URA3 arg4-Nsp trm2Δ::KanMX4</i>
RK385	<i>his4-BglII MATα ade1-1 lys5-p cyh2-z CEN8:URA3 arg4-Nsp</i>
RK387	<i>his4-BglII MATα ade1-1 lys5-p cyh2-z CEN8:URA3 arg4-Nsp exo1Δ::KanMX4</i>
RK392	<i>leu2-R MATα ade1-1 met13-B trp5-S</i>
RK394	<i>leu2-R MATα ade1-1 met13-B trp5-S exo1Δ::KanMX4</i>
RK399	<i>his4-XhoI MATα ade1-1 lys5-P cyh2-Z CEN8:URA3 arg4-Nsp exo1-D173A</i>
RK404	<i>leu2-R MATα ade1-1 met13-B trp5-S trm2Δ::KanMX4</i>
RK406	<i>leu2-R MATα ade1-1 met13-B trp5-S sgs1-mn: KanMX4</i>
RK409	<i>his4-XhoI MATα ade1-1 lys5-P cyh2-Z CEN8:URA3 arg4-Nsp exo1-E150D</i>
RK410	<i>leu2-R MATα ade1-1 met13-B trp5-S exo1Δ::KanMX4 trm2Δ::KanMX4</i>
RK417	<i>leu2-R MATα ade1-1 met13-B trp5-S exo1Δ::KanMX4 sgs1-mn: KanMX4</i>
RK418	<i>leu2-R MATα ade1-1 met13-B trp5-S exo1-E150D</i>
RK425	<i>leu2-R MATα ade1-1 met13-B trp5-S exo1-D173A</i>

Table 2.1 (continued)

Strain ²	Genotype ¹										
RKD51	<u>his4-XhoI</u>	LEU2	<u>MATα</u>	<u>ade1-1</u>	<u>lys5-P</u>	MET13	<u>cyh2-z</u>	TRP5	<u>CEN8:URA3</u>	<u>arg4-Nsp</u>	
	HIS4	len2-R	MATa	ade1-1	LYS5	met13-B	CYH2	trp5-S	CEN8	ARG4	
RKD52	<u>his4-XhoI</u>	LEU2	<u>MATα</u>	<u>ade1-1</u>	<u>lys5-P</u>	MET13	<u>cyh2-z</u>	TRP5	<u>CEN8:URA3</u>	<u>arg4-Nsp</u>	<u>exo1Δ::KanMX4</u>
	HIS4	len2-R	MATa	ade1-1	LYS5	met13-B	CYH2	trp5-S	CEN8	ARG4	<u>exo1Δ::KanMX4</u>
RKD55	<u>his4-XhoI</u>	LEU2	<u>MATα</u>	<u>ade1-1</u>	<u>lys5-P</u>	MET13	<u>cyh2-z</u>	TRP5	<u>CEN8:URA3</u>	<u>arg4-Nsp</u>	<u>exo1-D173A</u>
	HIS4	len2-R	MATa	ade1-1	LYS5	met13-B	CYH2	trp5-S	CEN8	ARG4	<u>exo1-D173A</u>
RKD71, 72, 73	<u>his4-XhoI</u>	LEU2	<u>MATα</u>	<u>ade1-1</u>	<u>lys5-P</u>	MET13	<u>cyh2-z</u>	TRP5	<u>arg4-</u>	<u>rad50S::URA3</u>	
	HIS4	len2-R	MATa	ade1-1	LYS5	met13-B	CYH2	trp5-	ARG4	rad50S::URA3	
RKD72, 73, 74	<u>his4-XhoI</u>	LEU2	<u>MATα</u>	<u>ade1-1</u>	<u>lys5-P</u>	MET13	<u>cyh2-z</u>	TRP5	<u>arg4-</u>	<u>rad50S::URA3</u>	<u>exo1Δ::KanMX4</u>
	HIS4	len2-R	MATa	ade1-1	LYS5	met13-B	CYH2	trp5-	ARG4	rad50S::URA3	<u>exo1Δ::KanMX4</u>
RKD75, 76, 77	<u>his4-XhoI</u>	LEU2	<u>MATα</u>	<u>ade1-1</u>	<u>lys5-P</u>	MET13	<u>cyh2-z</u>	TRP5	<u>arg4-</u>	<u>rad50S::URA3</u>	<u>exo1-D173A</u>
	HIS4	len2-R	MATa	ade1-1	LYS5	met13-B	CYH2	trp5-	ARG4	rad50S::URA3	<u>exo1-D173A</u>
RKD62, 63, 64	RRP7	<u>his4-XhoI</u>	<u>FUS1</u>	<u>MATα</u>	<u>ade1-1</u>	<u>CAN1</u>	<u>cyh2-z</u>				
	RRP7-NatMX4	his4-ClaI	FUS1-HphMX4	MATa	ade1-1	can1	CYH2				
RKD65, 66, 67	RRP7	<u>his4-XhoI</u>	<u>FUS1</u>	<u>MATα</u>	<u>ade1-1</u>	<u>CAN1</u>	<u>cyh2-z</u>			<u>exo1Δ::KanMX4</u>	
	RRP7-NatMX4	his4-ClaI	FUS1-HphMX4	MATa	ade1-1	can1	CYH2			<u>exo1Δ::KanMX4</u>	
RKD68, 69, 70	RRP7	<u>his4-XhoI</u>	<u>FUS1</u>	<u>MATα</u>	<u>ade1-1</u>	<u>CAN1</u>	<u>cyh2-z</u>			<u>exo1-D173A</u>	
	RRP7-NatMX4	his4-ClaI	FUS1-HphMX4	MATa	ade1-1	can1	CYH2			<u>exo1-D173A</u>	
RKD78, 79, 80	RRP7	<u>his4-BglII</u>	<u>FUS1</u>	<u>MATα</u>	<u>ade1-1</u>	<u>CAN1</u>	<u>cyh2-z</u>				
	RRP7-NatMX4	his4-ClaI	FUS1-HphMX4	MATa	ade1-1	can1	CYH2				
RKD81, 82, 83	RRP7	<u>his4-BglII</u>	<u>FUS1</u>	<u>MATα</u>	<u>ade1-1</u>	<u>CAN1</u>	<u>cyh2-z</u>			<u>exo1Δ::KanMX4</u>	
	RRP7-NatMX4	his4-ClaI	FUS1-HphMX4	MATa	ade1-1	ade1-1	can1	CYH2		<u>exo1Δ::KanMX4</u>	
RKD84, 85, 86	RRP7	<u>his4-BglII</u>	<u>FUS1</u>	<u>MATα</u>	<u>ade1-1</u>	<u>CAN1</u>	<u>cyh2-z</u>			<u>exo1-D173A</u>	
	RRP7-NatMX4	his4-ClaI	FUS1-HphMX4	MATa	ade1-1	ade1-1	can1	CYH2		<u>exo1-D173A</u>	

¹ All strains are also ho Δ ::LYS2 lys2 ura3.

² When multiple strain numbers refer to the same genotype, each originated from an independently isolated single colony.

Table 2.2: Plasmids

Plasmid	Description	Reference
pWJ716	<i>KJUR43</i>	Erdeniz <i>et al.</i> (1997)
pVC4	<i>HIS4</i> 3' probe	V. E. Cotton, unpublished
pEAM71	<i>exo1</i> -D173A	Sokolsky and Alani (2000)
pJM3	<i>exo1</i> -E150D	J. Meadows, unpublished
pFA6-KanMX4	KanMX4	Wach <i>et al.</i> (1994)
pAG25	NatMX4	Goldstein and McCusker (1999)
pAG32	HphMX4	Goldstein and McCusker (1999)
pFA6a-P _{CLB2} -3xHA-KanMX6	P _{CLB2} -3xHA-KanMX6	Lee and Amon (2003)
pRED322	<i>his4</i> - <i>Bgl</i> II	Khazanehdari and Borts (2000)
pRHB12	<i>his4</i> - <i>Cla</i> I	Borts and Haber (1989)
pNH229	<i>trp5</i> - <i>S</i>	Martini <i>et al.</i> (2006)
pNH217	<i>met13</i> - <i>B</i>	Martini <i>et al.</i> (2006)
pNH223	<i>lys5</i> - <i>P</i>	Martini <i>et al.</i> (2006)

Table 2.3: Oligonucleotide sequences used in quantitative PCR analysis

Approximate position	Sequence (5' to 3')
5' in rDNA	ATCAGCTTGCCTTGATTACG
3' in rDNA	GT*TGCCCCCTTCTCTAAGC
5' of <i>Acl</i> I site (200bp from DSB)	TTCGATATAGAAGGTAAGAAAAGGAT
3' of <i>Acl</i> I site (200bp from DSB)	CAGCGCAGTTGTGCTATGAT
5' of <i>Nhe</i> I site (500bp from DSB)	ATTGGTGGCTTTGTCCCTTGC
3' of <i>Nhe</i> I site (500bp from DSB)	CAAGTGTTCGGCTGTTTTAGC
5' of <i>Cla</i> I site (800bp from DSB)	GAGCGTTGTCTAGGGTTGGT
3' of <i>Cla</i> I site (800bp from DSB)	TCACCCCTTGATCCAGATTTC
5' of <i>Aat</i> II site (1250bp from DSB)	GGCTGCCGATTTGTTCTACT
3' of <i>Aat</i> II site (1250bp from DSB)	TGGCTTAGCATCACCTTTCC
5' of <i>Bgl</i> II site (2000bp from DSB)	CGCTTCCAAGATTGTTCTAGC
3' of <i>Bgl</i> II site (2000bp from DSB)	ACATACATTTTGCGGCAGT

Table 2.4: Oligonucleotide sequences used in strain construction

Name	Sequence (5' to 3')	Purpose
ADE1 A1	TCTCGACTTGAACACGTCCA	Verification of <i>ade1-1</i> allele
ADE1 A4	ACACCGTCCCTGAGTATTAC	Verification of <i>ade1-1</i> allele
ADE1 ADAPT A	AATTCCAGCTGACCACCATGATGTCAATTACGAAGACTGAACTG	Introduction of <i>ade1-1</i> allele
ADE1 ADAPT B	GATCCCCGGGAATTGCCATGTGAGGAGTTACACTGGCGACT	Introduction of <i>ade1-1</i> allele
CEN8 A1	AGGGTGTATCACCACCTCTCT	Introduction of <i>CEN8:URA3</i> allele
CEN8 A4	CTTGAGACTCCCCGACCA	Introduction of <i>CEN8:URA3</i> allele
CEN8 A0	TTTTTCAGCCCACACATTTT	Verification of <i>CEN8:URA3</i> allele
CEN8 A5	AAATTCGGAGCATAAGCTGTT	Verification of <i>CEN8:URA3</i> allele
CLB2 SEQ F1	TAAGGTGCCTTAGGGGGACT	Sequencing of <i>CLB2</i> promoter
CLB2 SEQ F2	CCTCTTTGGGGAAAAGAGAA	Sequencing of <i>CLB2</i> promoter
EXO1 A1	CAGGTATATCIATATGCTCTC	Verification of <i>EXO1</i> mutations
EXO1 A4	GCACATGCCCAGCGCGCTCG	Verification of <i>EXO1</i> mutations
EXO1 ADAPT A	AATTCCAGCTGACCACCATGCTGCAGTTTTCATAAAAAGATTTAGT	Introduction of <i>EXO1</i> point mutations
EXO1 ADAPT B	GATCCCCGGGAATTGCCATGAATTTCATGCGGTAATCAGG	Introduction of <i>EXO1</i> point mutations
EXO1MX F	ATTAAAATAAAAAGGAGCTCGAAAAAACTGAAAGGCGTAGAAAGGACGTA CGCTGCAGGTCGACGG	Replacement of <i>EXO1</i> ORF with MX4 cassette
EXO1MX R	ATTGAAAAATATACCTCCGATATGAAACGTGCAGTACTTAACTTGATCG ATGAATTCGAGCTCGT	Replacement of <i>EXO1</i> ORF with MX4 cassette
FUS1 A1	CGAAGTGACTAAGGCTATAG	Insertion of HphMX4 cassette adjacent to <i>FUS1</i>
FUS1 A4	CATTGCCGCTTACTCCAAAC	Insertion of HphMX4 cassette adjacent to <i>FUS1</i>
HIS4 -333 F	TGCGATACGATGGGTCATAA	Verification of <i>his4</i> alleles
HIS4 +2541 R	CCCACCTCTTGCTACTACCTCTCTT	Verification of <i>his4</i> alleles
HIS4 +523 F	GCAAAGGCCATCGATTTGGGTCG	Amplification of <i>HIS4</i> probe sequence

Table 2.4 (continued)

Name	Sequence (5' to 3')	Purpose
HIS4 +1524 R	GGTGGAGATGCAAACACAATCTCC	Amplification of <i>HIS4</i> probe sequence
K2	TTCAGAAACAACCTCTGGCGCA	Verification of KanMX4 insertion
K3	CATCCTATGGAACCTGCCTCGG	Verification of KanMX4 insertion
KLACTIS INT 3'	GAGCAATGAACCCAATAACGAAATC	Construction of strains using method of Erdeniz <i>et al.</i> , 1997
KLACTIS INT 5'	CTTGACGTTTCGTTGACTGATGAGC	Construction of strains using method of Erdeniz <i>et al.</i> , 1997
LYS5 A1	CCTTCCAACCTTGCTTTTTCG	Verification of <i>lys5-P</i> mutation
LYS5 A4	AGGGAGAACAAGTTCGCTGA	Verification of <i>lys5-P</i> mutation
MET13 A1	GGCCGTCGTTTAGTCATTCT	Verification of <i>met13-B</i> mutation
MET13 A4	TGAAGGAAGAGGGTGTGAA	Verification of <i>met13-B</i> mutation
N2	GATTCGTCGTCCGATTCGTC	Verification of NatMX4 insertion
N3	AGGTCACCAACGTCAACGCA	Verification of NatMX4 insertion
PCLB2-SGS1 F	GGAAAAAATACAGATTATTGTTGTATATATTTAAAAAATCATACACGTACA CACAAGGCG	Insertion of <i>CLB2</i> promoter at <i>SGS1</i>
PCLB2-SGS1 R	GTAAAGTCGCCGTTTCCTTTAACCATTGTGTGCTCCCTTCTTAAGTTATGTG ACGGCTTCG	Insertion of <i>CLB2</i> promoter at <i>SGS1</i>
POL3CT A1	AATGTTGGTGATCGTGTGGA	Verification of the <i>pol3-ct</i> allele
POL3CT A4	TCTTATGTAGCGCCCGAAGT	Verification of the <i>pol3-ct</i> allele
POL3CT INS F	TGACATTTTATATATGCGGGTTAAGGTTAAAAAAGAGCTGCAGGAGAAA GTAGAACAATAACAGCTGAAGCTTCGTACGC	Introduction of <i>pol3-ct</i> allele
POL3CT INS R	ATGCAAAAAGTTGTTAGCCTTCTTAATCCTAATATGATGTGCCACCCTAT CGTTTTTTACATAGGCCACTAGTGGATCTG	Introduction of <i>pol3-ct</i> allele
RRP7 A1	GTGGATGAGGATGGATTCAC	Verification of NatMX4 insertion at <i>RRP7</i>

Table 2.4 (continued)

Name	Sequence (5' to 3')	Purpose
RRP7MX INS F	TCCTATTCGTGTAAGTTTAGTATGATGATGTGCATGACAACGTACGCTGC AGGTCGAC	Introduction of NatMX4 cassette adjacent to <i>RRP7</i>
RRP7MX INS R	GATGAACGGAAGTGACAATGTCACCCCCGGTGGAAGACTCTATCGATGA ATTTCGAGCTCG	Introduction of NatMX4 cassette adjacent to <i>RRP7</i>
SGS1 INT R	TTGAAGGCGGATCACCTCTA	Verification of <i>CLB2</i> promoter insertion at <i>SGS1</i>
TRM2 A1	GCTCCCAGAGAGCCTACACA	Verification of <i>TRM2</i> mutation
TRM2 A4	TGGTGGTGGTGAGTGATGAT	Verification of <i>TRM2</i> mutation
TRM2MX F	TGACATAAAAAGTACAAATCTGTCATTTTATTTTAGAGGAATAGTTTAGGA CAAAGTCATTCAGCTGAAGCTTCGTACGC	Replacement of <i>TRM2</i> ORF with MX4 cassette
TRM2MX R	GTACAGGAAGACATTTACTCTAGAAAAGATATACATAGTGATAGATATTTT ATATGTGCAACATAGGCCACTAGTGGATCTG	Replacement of <i>TRM2</i> ORF with MX4 cassette
TRP5 F	GACCGTGGAAGAATGACTAA	Verification of <i>trp5-S</i> mutation
TRP5 R	AAATGTGGCTGTTCTGACCG	Verification of <i>trp5-S</i> mutation
U2	ACTGGTATATGATTTTGTGGAC	Verification of <i>K.lactis URA3</i> insertion
U3	GAAGCGTACCAAAAAGAGAATC	Verification of <i>K.lactis URA3</i> insertion

with the addition of 875 mg/l nutrient mixture (Table 2.5), 6.3 ml/l 1% (w/v) leucine solution and 3 ml/l 1% (w/v) lysine solution. For synthetic complete media lacking a defined nutrient, the nutrient was omitted from the mixture described in Table 2.5.

For cyclohexamide, geneticin, hygromycin B, methyl methanesulphonate and nourseothricin containing media, the appropriate amount of the respective drug (Table 2.6) was added to YEPD medium following autoclaving. In the same manner, canavanine was added to synthetic complete medium lacking arginine and 5'-fluoroorotic acid was added to synthetic complete medium lacking uracil but supplemented with 50 µg/ml uracil.

Pre-sporulation (SPS) medium consisted of 0.5% (w/v) Bacto yeast extract, 1% (w/v) Bacto peptone, 0.17% (w/v) Difco yeast nitrogen base lacking amino acids and ammonium sulphate, 1% (w/v) potassium acetate, 0.5% (w/v) ammonium sulphate and 0.05 M potassium biphthalate, pH adjusted to 5.5. SPS was supplemented with 6.4 ml/l of 0.5% (w/v) adenine hemisulphate in 0.05% hydrochloric acid. Sporulation medium for time course and recombination analysis consisted of 2% (w/v) potassium acetate, pH 7.0. Diploids produced during strain construction were sporulated on synthetic complete potassium acetate medium containing 2% (w/v) potassium acetate, 0.22% (w/v) Bacto yeast extract, 0.05% (w/v) dextrose, 875 mg/l complete amino acid mix (Table 2.3) and 2.5% (w/v) Bacto agar. The medium was adjusted to pH 7.0.

Escherichia coli cultures were grown in Luria-Bertani (LB) medium containing 0.5% (w/v) Bacto yeast extract, 1% (w/v) Bacto tryptone and 0.5% (w/v) sodium chloride. To maintain plasmids during propagation, LB was supplemented with ampicillin to a final concentration of 100 µg/ml. *Escherichia coli* strains were routinely grown at 37°C. Liquid cultures were shaken during incubation.

All media were made using deionised water and pH adjusted to 6.0-6.5 with either 1 M hydrochloric acid or 1 M sodium hydroxide as appropriate unless otherwise stated. To make agar plates, 2.5% (w/v) Bacto agar was added. Stocks of yeast and bacterial strains were stored in 15% glycerol (v/v) at -80°C.

Table 2.5: Nutrient mixture composition

Nutrient¹	Amount (mg)
Adenine hemisulphate salt	800
L-arginine	800
L-aspartic acid	4000
L-histidine	800
L-leucine	800
L-lysine monohydrochloride	1200
L-methionine	800
L-phenylalanine	2000
L-threonine	8000
L-tryptophan	800
L-tyrosine	1200
Uracil	800

¹ All nutrients were purchased from Sigma.

Table 2.6: Drugs

Drug	Concentration	Supplier
Ampicillin	100 µg/ml	Melford Laboratories
Canavanine	60 µg/ml	Sigma
Cyclohexamide	10 µg/ml	Sigma
5'-Fluoroorotic acid (FOA)	1 mg/ml	Apollo Scientific
Geneticin (G418)	200/400 ¹ µg/ml	Invitrogen
Hygromycin B	300 µg/ml	Invitrogen
Methyl methanesulphonate (MMS)	0.015% (v/v)	Fluka Chemicals
Nourseothricin	100 µg/ml	Werner Bioagents

¹ For the initial selection of G418 resistant colonies, a 400 µg/ml concentration was used. For subsequent selection steps, a 200 µg/ml concentration was sufficient.

2.1.5 DNA molecular weight markers

Bacteriophage λ DNA digested with either *BstEII* or *HindIII* (New England Biolabs) was used as a molecular weight standard during agarose gel electrophoresis. Routinely, 250 ng of marker DNA was loaded per gel apart from electrophoresis prior to Southern blotting when 125 ng *BstEII* digested DNA or 37.5 ng *HindIII* digested DNA was loaded.

2.2 Methods

2.2.1 Agarose gel electrophoresis

Prior to loading, DNA samples were mixed with 0.25x their volume of 5x loading dye containing 10% (w/v) Ficoll type 400, 0.1 M EDTA, 0.2% (v/v) bromophenol blue and 0.5% (w/v) SDS. DNA molecules were separated using the appropriate percentage agarose for the size discrimination required. Agarose was melted in 1x TBE buffer (90 mM Tris base, 90 mM boric acid, 2 mM EDTA pH 8.0), which was also used as the running buffer. With the exception of gels run for Southern analysis (see Section 2.2.14), supplementation with ethidium bromide (0.5 $\mu\text{g}/\text{ml}$) was carried out prior to agarose polymerisation. Appropriate DNA markers from those listed in section 2.1.5 were used to allow determination of the size of the DNA fragments. Following electrophoresis, DNA was visualised and photographed under ultraviolet (UV) light using a Syngene Gene Genius Bioimaging System and GeneSnap from Syngene software.

2.2.2 Preparation of yeast genomic DNA

2.2.2.1 Genomic DNA extraction by phenol/chloroform

When high-quality genomic DNA from vegetative cells was required (such as for analysis by sequencing), a modified version of the phenol/chloroform method described in Borts *et al.*, (1986) was used. A 5 ml YEPD cell culture was grown overnight at 30°C. Cell cultures were pelleted by centrifugation in a benchtop centrifuge at 1500 xg for 3 min before being resuspended in 0.5 ml solution A (1.2 M sorbitol, 0.2 M Tris-HCl pH 8.5, 0.02 M EDTA, 1% (v/v) β -mercaptoethanol) and transferred to a 1.5 ml tube. 50 μl of 10 mg/ml zymolyase 20T (Seikagaku Corporation) was added and the samples incubated at 37°C until spheroplasted (approximately 25 min). Spheroplasts were pelleted by centrifugation in a microcentrifuge at 13,000 rpm for 1 min and resuspended in 50 μl 1 M sorbitol and

0.5 ml solution B (50 mM Tris-HCl pH 7.5, 100 mM NaCl, 100 mM EDTA pH 8.0, 0.5% SDS) by flicking. 50 μ l solution C was then added (1 mg/ml RNase, 4 mg/ml proteinase K) and samples were incubated at 65°C for at least 2 hours (usually overnight) with occasional flicking of the tubes to encourage resuspension. Following incubation, the tubes were briefly chilled on ice and 0.5 ml phenol:chloroform:isoamyl alcohol (25:24:1) added before centrifugation at 13,000 rpm for 10 min in a microcentrifuge. The upper aqueous layer was then transferred to a new 1.5 ml tube and the phenol:chloroform:isoamyl alcohol extraction repeated. Following the addition of 1 ml 100% ice-cold ethanol, DNA was spooled by inversion and the resulting pellet was washed in 70% ethanol before allowing it to air-dry briefly. The DNA was resuspended in 200 μ l 1x TE (10 mM Tris-HCl pH 8.0, 1 mM EDTA pH 8.0) and incubated at 65°C for 30 min to encourage resuspension. DNA was stored at -20°C.

2.2.2.2 Genomic DNA extraction by CTAB

DNA from cell samples taken during meiotic time-courses for analysis by Southern blotting or qPCR was extracted using a modified version of the CTAB method (Allers and Lichten, 2000) to preserve single-stranded intermediates. Following thawing of the cell samples on ice, cells were washed in 1 ml cold spheroplasting buffer (1 M sorbitol, 50 mM KPO₄ pH 7.5, 10 mM EDTA) and transferred to a 1.5 ml microcentrifuge tube. Cells were pelleted at 13,000 rpm for 1 min in a microcentrifuge before pouring off the supernatant. Cell pellets were then resuspended completely in 100 μ l spheroplasting buffer, 12.5 mg/ml zymolyase 20T and 5% (v/v) β -mercaptoethanol and incubated at 37°C for 6 min (inverting to mix after 3 min). Following this spheroplasting step, 200 μ l extraction buffer (consisting of the following components filter sterilised and mixed in the following order: 50 ml of buffer solution [4 M NaCl, 0.2 M Tris-HCl pH 7.5, 50 mM EDTA], 20 ml 10% (w/v) polyvinyl pyrrolidone 40 and 30 ml 10% (w/v) hexadecyltrimethylammonium bromide [CTAB]; stored at 37°C to prevent precipitation) was added and the cells gently mixed using a pipette tip. 5 μ l of proteinase K (20 mg/ml) was added and the tube inverted gently to mix. Tubes were incubated at 37°C for 15 min, inverting every 5 min. Following incubation, 100 μ l chloroform:isoamyl alcohol (24:1) was added and solutions mixed by gentle shaking until a 'milky' solution was obtained. Samples were incubated at room temperature for 2 min before shaking again and

centrifuging at 13,000 rpm for 5 min. The upper phase was immediately transferred into a clean 1.5 ml microcentrifuge tube, 3 μ l of RNase (10 mg/ml) added and the sample incubated at 37°C for 10 min. 900 μ l of dilution buffer (1% (w/v) CTAB, 50 mM Tris-HCl pH 7.5, 10 mM EDTA pH 8.0) was then layered on top and the tube inverted gently 5 times to mix before being left to stand at room temperature for 10 min. The tubes were then inverted a further 20 times to obtain a precipitate. The supernatant was removed and the precipitate washed twice in ice-cold 1 ml 0.4 M NaCl, 1x TE (10 mM Tris-HCl pH 8.0, 1 mM EDTA pH 8.0). Following washing, the precipitate was completely resuspended in 300 μ l 1.42 M NaCl, 1x TE by gentle shaking. To precipitate the DNA, 600 μ l 100% ethanol was added and the tube incubated at room temperature for 10 min with gentle mixing. DNA was spooled by gentle inversion and then pelleted by centrifugation at 13,000 rpm for 1 min. The DNA was washed twice with 70% ethanol before all traces of ethanol were removed and the pellet left to air-dry briefly. To resuspend, 100-150 μ l (depending upon the size of the pellet) of 1x TE was added and the samples placed at 4°C overnight. The resuspended DNA was then aliquoted into 0.5 ml microcentrifuge tubes and stored at -80°C.

2.2.3 Plasmid DNA preparation

Plasmid DNA was prepared from 5 ml overnight ampicillin-containing LB cultures of *Escherichia coli* using the E.Z.N.A.[™] Plasmid Mini Kit I (Omega Bio-tek) according to the manufacturer's instructions.

2.2.4 Restriction digestion

Restriction enzymes and appropriate buffers were purchased from New England Biolabs and used according to the manufacturer's instructions.

2.2.5 Quantification of DNA

DNA was quantified using 1.5 μ l of each sample on a NanoDrop[™] ND-1000 spectrophotometer according to the manufacturer's instructions.

2.2.6 End-point polymerase chain reaction

2.2.6.1 PCR using *Taq* polymerase

Taq polymerase (Kapa Biosystems) was used for standard DNA amplification. A typical reaction contained template DNA (0.1 – 0.5 ug), 4.5 µl 11.1x PCR buffer (45 mM Tris-HCl pH 8.8, 11 mM ammonium sulphate, 4.5 mM magnesium chloride, 6.7 mM 2-mercaptoethanol, 4.4 M EDTA pH 8.8, dNTPs (1 mM each), 113 µg/ml DNase free BSA, 0.2 µM primers and 5U *Taq* polymerase. Typical cycling conditions were an initial 95°C denaturation for 1 min; 35 cycles of denaturation at 95°C for 30 s, annealing at a primer-dependent temperature for 30 s, extension at 72°C for 1 min/kb; final extension at 72°C for 10 min. Annealing temperatures were optimised for individual primer pairs as required. PCR was carried out using a PTC-225 Peltier Thermal Cycler (MJ Research).

2.2.6.2 Proofreading PCR

When proofreading activity was required, the Phusion high-fidelity polymerase and high-fidelity buffer (Finnzymes) were used according to the manufacturer's instructions.

2.2.6.3 Colony PCR

Colony PCR was performed to check for correct integrations after transformation without the need to first prepare DNA. A small (approximately 0.2 mm²) colony was transferred to a 1.5 ml tube containing 20 µl 0.02 M sodium hydroxide using a sterile pipette tip and resuspended by vortexing. The resulting suspension was heated to 95°C for 10 min then placed on ice for 5 min. Cells were pelleted in a microcentrifuge at 13,000 rpm for 1 min and 2 µl of the supernatant used in a 25 µl PCR reaction composed as in Section 2.2.6.1. PCR cycling conditions were as in Section 2.2.6.1 except that the initial denaturation at 95°C was extended to 3 min.

2.2.7 Quantitative PCR

Quantitative PCR (qPCR) reactions were carried out in a total volume of 10 µl using 1x SensiMix™ SYBR (Bioline), 400 nM forward and reverse oligonucleotides, deionised water and approximately 6 ng of template DNA. Thermocycling was carried out using a LightCycler® 480 Real-Time PCR System (Roche). PCR reactions were initiated by heat activation of the *Taq* polymerase at 95°C for 10 mins,

followed by 40 cycles of 95°C for 15 s and 60°C for 1 min. All reactions were performed in triplicate and no-template controls for each oligonucleotide pair used were included in every run. Amplicons were between 100 and 150 base pairs in length and primer specificity was validated by melt-curve analysis. Standard curves were constructed from a five-point 1 in 10 serial dilution of template DNA. Crossing-point (C_p) values were calculated using the automated C_p-calling algorithm provided by the LightCycler® Analysis Software (based on the second derivative maximum method). For the majority of reactions, the mean C_p value of the three replicates was used for subsequent analysis. However, if a single reaction differed from its duplicates by more than one C_p value it was disregarded and the mean C_p of the remaining two reactions was used. Full details of the experiments performed and the methods used are provided in Chapter 3.

2.2.8 Ethanol precipitation

To concentrate DNA, ethanol precipitation was carried out. 0.1x the starting volume of 3 M sodium acetate (pH 5.2) was added to the DNA solution followed by 2x volume 100% ethanol. For precipitation of small amounts of DNA, 1 µl glycogen (20 mg/ml) was added prior to addition of the ethanol in order to maximise DNA recovery. Samples were placed at -80°C for 10 min before centrifugation in a microcentrifuge at 13,000 rpm for 30 min at 4°C. The supernatant was removed and pellets washed in 1 ml 70% ethanol before a further centrifugation at 13,000 rpm for 5 min. The supernatant was removed and pellets left to air-dry before being resuspended in the required amount of 1x TE (10 mM Tris-HCl pH 8.0, 1 mM EDTA pH 8.0). DNA that did not resuspend easily was incubated at 4°C overnight.

2.2.9 DNA purification

When purification of DNA from an agarose gel was required, the band of interest was visualised under blue light to minimise nicking of the DNA, excised using a clean scalpel and the DNA extracted using the QIAGEN® MinElute Gel Extraction Kit according to the manufacturer's instructions, eluting in 10 µl. When purification of DNA following a PCR reaction was necessary (*e.g.* prior to sequencing analysis), the ChargeSwitch® PCR cleanup kit (Invitrogen) was used according to the manufacturer's instructions, eluting in 50 µl.

2.2.10 Mutagenesis methods

2.2.10.1 PCR-based gene disruption

For analysis of deletion mutants, the open reading frame of the gene of interest was replaced with a drug resistance cassette using the PCR-based method of Wach *et al.* (1994). The primer sequences used are listed in Table 2.4.

2.2.10.2 PCR-based allele replacement

Point mutations were introduced using the method of Erdeniz *et al.* (1997). Amplification of DNA fragments was performed using a proof-reading polymerase (see Section 2.2.6.2) and the desired band purified by gel extraction after each amplification step (see Section 2.2.9). The primer sequences used are listed in Table 2.4.

2.2.10.3 Two-step gene replacement

When a marker was already present on an integrating plasmid with a *URA3* marker and there was no concern about the transfer of additional DNA sequence, the two-step replacement method used was used (based on the method of Scherer and Davis, 1979). This consisted of transforming a *ura3* strain with a linearised plasmid containing both the allele of interest and a *URA3* marker and selecting for “pop-in” transformants in which integration of the plasmid has taken place on synthetic complete medium lacking uracil. This was followed by selection for subsequent “pop-out” events in which the *URA3* gene and the plasmid backbone had looped-out of the genome following recombination on 5'-FOA. The resulting colonies were then screened for those in which the wild-type version of the gene had been replaced by the mutant allele by an appropriate method.

2.2.11 DNA sequencing

DNA was sequenced using the BigDye® V3.1 system (Applied Biosystems). Sequencing reactions were performed in a total volume of 12 µl comprising approximately 200 ng template DNA, 1 µl BigDye®, 3 µl sequencing buffer and 3.2 pmol of the relevant primer. Sequencing reactions consisted of an initial denaturation at 96°C for 1 min followed by 25 cycles of 10 s at 96°C, 5 s at 50°C and 4 mins at 60°C. Excess dye was removed using Performa DTR gel filtration columns (Edge Biosystems) according to the manufacturer's instructions. Samples

were analysed using an Applied Biosystems 3730 sequencer at the Protein Nucleic Acid Chemistry Laboratory, University of Leicester.

2.2.12 Yeast transformation

Yeast was transformed using a modified version of the LiAc/ssDNA/PEG method (Gietz and Schiestl, 2007). For a single transformation reaction, a 5 ml overnight YEPD culture of the cells to be transformed was grown at 30°C. The following morning, 400 µl of the overnight culture was used to inoculate 5 ml of fresh YEPD and the cells were grown for 2 growth cycles (approximately 3-4 hours). Cells were pelleted in a benchtop centrifuge at 1500 xg for 3 mins before resuspension in 1 ml sterile water and transfer to a 1.5 ml tube. Pellets were washed once more with 1 ml water before being resuspended in 1 ml 100 mM lithium acetate. 0.5 ml of the resulting suspension was then transferred to a separate 1.5 ml tube to be used as a no DNA control. Both tubes were subsequently processed in parallel. Cells were pelleted in a microcentrifuge at 13,000 rpm for 1 min and the supernatant removed. The following solutions were then added: 240 µl 50% (w/v) polyethylene glycol, MW 3350, 36 µl 1 M lithium acetate, 50 µl 2 mg/ml single-stranded salmon sperm DNA (denatured at 95°C for 5 mins, then snap chilled on ice) and 34 µl of transformant DNA or 34 µl water for the no DNA control. Once all components had been added, tubes were vortexed thoroughly to mix and heat shocked in a water bath at 42°C for 30 mins. After heat shock, cells were gently washed in sterile water twice, centrifuging at 5,000 rpm each time. When selecting for drug resistance, transformed cells were incubated in YEPD for 3 hours at 30°C prior to plating. Cells were then plated onto selective medium and incubated at 30°C for 3-4 days.

2.2.13 Synchronous liquid sporulation

Diploid strains were patched from frozen glycerol stocks to YEPEG plates and grown overnight at 30°C. Cells from the resulting growth haze were streaked for singles colonies on YEPD plates and incubated at 30°C for two days. A single colony was then selected and used to inoculate 5 ml liquid YEPD, which was grown overnight at 30°C with shaking. The following day, 150 ml SPS was inoculated with the required amount of the overnight YEPD culture. Typically, a 1 in 400 dilution grew to the desired cell density in 18 hours. When the SPS culture reached an $OD_{\lambda 600}$ of 2.1, the cells were pelleted at 1500 xg for 2 min, washed in an equal

volume of 2% (w/v) KAc pre-warmed to the desired sporulation temperature, pelleted as described above and resuspended again in 225 ml of pre-warmed 2% (w/v) KAc. Cultures were transferred to a 2.8 L baffled flask, the t=0 time point taken and the culture incubated with vigorous aeration at the desired temperature.

2.2.13.1 Monitoring meiotic progression by fluorescence microscopy.

To monitor meiotic progression by DAPI (4', 6'-diamidino-2-phenylindoline) staining, 100 μ l of sporulating culture was removed at the desired time points, fixed by the addition of 100 μ l 100% ethanol and stored at 4°C until required. To visualise nuclei, 4 μ l of ethanol-fixed cells were mixed with 4 μ l of DAPI (10 μ g/ml) on a microscope slide and imaged using a Zeiss Axioskop 2 fluorescence microscope with a 100x objective. Cells were scored as being mono-, bi-, or tetranucleate and at least 200 cells were counted for each time point.

2.2.13.2 Monitoring meiotic progression by DNA analysis

To monitor changes in DNA throughout meiosis (either by Southern analysis [Section 2.2.14] or qPCR [Section 2.2.7]), 15 ml of sporulating culture (25 ml for the 0 hour time point) was removed at the desired time point, placed on ice and fixed by the addition of 150 μ l 10% (w/v) NaN_3 (250 μ l for the 0 hour time point). Cells were pelleted at 1500 xg for 2 min, the supernatant removed and cell pellets snap-frozen in a dry ice/ethanol slurry before storing at -80°C. When required, the DNA was extracted using the CTAB method (Section 2.2.2.2).

2.2.14 Southern blotting

2.2.14.1 Preparation of DNA and electrophoresis

DNA for Southern analysis of meiotic DSBs was prepared using the modified CTAB method detailed in Section 2.2.2.2, quantified using the method described in Section 2.2.5 and approximately 3 μ g of DNA from each time-point digested for 3.5 hours with 25 units of restriction enzyme in a total reaction volume of 80 μ l. The digested DNA was ethanol precipitated (Section 2.2.8) and resuspended in 15 μ l 1x TE. 5 μ l of 5x loading buffer was added and the samples loaded into a 0.7% (w/v) agarose gel along with MW markers as described in 2.1.5. Electrophoresis was carried out at 50 volts overnight. The gel was then stained in water supplemented with ethidium

bromide (0.5 $\mu\text{g}/\text{ml}$ final concentration) and incubated with gentle shaking for 30 min before visualisation as described in Section 2.2.1.

2.2.14.2 Southern transfer and cross-linking

Following visualisation, the gel was incubated at room temperature with gentle agitation in denaturation solution (0.5 M NaOH, 1 M NaCl) for 30 min, followed by 30 min in neutralising solution (0.5 M Tris-HCl pH 7.5, 3 M NaCl) and 10 min in 20x SSC buffer (3 M NaCl, 0.3 M sodium citrate). The Southern apparatus was set up as follows: the gel was placed upside-down onto a piece of Whatman 3MM paper which acted as a wick on top of a tank filled with 20x SSC. A piece of MAGNA Nylon membrane (GE Water & Process Technologies) cut to the size of the gel was placed on top and rolled flat with a glass pipette to remove air-bubbles. Two pieces of Whatman paper of the same size were placed on top of that, followed by a stack of paper towels and a weight. DNA was left to transfer onto the membrane overnight by capillary action. After transfer, DNA was UV cross-linked to the membrane at 120 mJ/cm^2 , followed by baking at 80°C for 20 min. Membranes were stored at room temperature if not used immediately.

2.2.14.3 Radioactive labelling of probes

Radio-labelled probes were prepared by the incorporation of α -³²P-dCTP by random prime labelling. 50 ng of template DNA (in a total volume of 16 μl) was denatured at 95°C for 10 min, then snap-chilled on ice. (For visualisation of molecular weight markers, only 10 ng of template DNA was labelled.) 5 μl of oligo-labelling buffer (see below), 1 μl 10 mg/ml BSA, 1 μl Klenow (both from New England Biolabs) and 2.5 μl α -³²P-dCTP were then added and the reaction incubated at 37°C for 1 hour. The probe was then fractionated to remove unincorporated radio-labelled nucleotides using Illustra™ NICK™ columns (GE Healthcare) according to the manufacturer's instructions. Before adding the probe to the hybridisation solution, it was first denatured by heating at 95°C for 10 min, then snap-chilled on ice. The oligo-labelling buffer consisted of solutions A, B and C in the ratio 2:3:3.

Solution A: 100 μl solution O (1.25 M Tris-HCl pH 8.0, 125 mM magnesium chloride), 18 μl 2-mercaptoethanol, 5 μl dATP, 5 μl dTTP and 5 μl dGTP.

Solution B: 2 M HEPES pH 6.6

Solution C: random hexadeoxynucleotides (90 OD units/ml)

2.2.14.4 Hybridisation and stringency washes

Membranes were pre-hybridised in 50 ml pre-hybridisation solution (2x SSPE [20x stock solution composed of 3 M NaCl, 0.2 M NaH₂PO₄, 0.02 M EDTA pH 7.4] 1% (w/v) SDS, 5x Denhardt's [50x stock solution composed of 10 mg/ml Ficoll 400, 10 mg/ml PVP 360, 10 mg/ml BSA fraction V], 0.2 mg/ml denatured salmon sperm DNA) for at least 4 hours at 65°C in roller bottles. The prehybridisation solution was then poured off and 40 ml pre-heated hybridisation solution (2x SSPE, 1% (w/v) SDS, 50 mg/ml dextran sulphate, 0.15 mg/ml denatured salmon sperm DNA) quickly added. The fractionated probe was added directly to the hybridisation solution and the hybridisation reaction allowed to proceed overnight at 65°C with constant rotation. Following hybridisation, the membrane was washed in a large plastic tray with agitation in the following solutions:

- 500ml 2x SSPE, 0.5% (w/v) SDS for 5 mins at room temperature
- 500ml 2x SSPE, 0.5% (w/v) SDS for 20 mins at room temperature
- 500ml 0.2x SSPE, 0.5% (w/v) SDS for 30 mins at room temperature
- 500ml 0.2x SSPE, 0.5% (w/v) SDS for 30 mins at 65°C
- 500ml 0.2x SSPE for 5 mins at room temperature

Membranes were monitored using a Geiger counter: if the edges of the blot gave a signal greater than approximately 2x background signal, the membrane was washed again in 0.2x SSPE, 0.5% (w/v) SDS.

2.2.14.5 Detection and quantification

Membranes were blotted on Whatman 3MM paper to remove excess liquid and wrapped in cling-film to prevent drying out. They were then exposed to a storage phosphor screen (GE Healthcare) for 6 hours to overnight depending upon the exposure time required to give sufficient signal. The phosphor screen was subsequently scanned using a Typhoon Phosphorimager (GE Healthcare) and CellQuant software was used to quantify the amount of DNA present in the bands of interest. To do this, bands were defined by upper and lower boundaries and the area under each peak was used to calculate the amount of DNA contained within.

2.2.15 Genetic procedures

2.2.15.1 Mating and sporulation

When crossing to obtain segregants (*i.e.* not performing recombination analysis), haploid strains of opposite mating types were mixed on a YEPD plate and incubated at 30°C for at least 4 hours. Following mating, cells were replica plated to sporulation medium and incubated at either 23°C or 33°C as required for 24-48 hours. Yeast cells were examined for sporulation using a Zeiss Axiostar phase contrast microscope.

2.2.15.2 Diploid selection

To select for diploid cells (*e.g.* for liquid sporulation), haploid strains were mated as described in Section 2.2.15.1 and cells from the mating mix then streaked for single colonies on minimal media supplemented with any nutrients that both haploid strains were auxotrophic for. Cells were incubated for 2 days at 30°C and single colonies picked. If selection by complementation was not possible, the mating mix was streaked for single colonies on YEPD medium, and after incubation at 30°C for 2 days, large, smooth-looking single colonies (indicative of diploids in the SK1 background) were patched on to YEPD and the cells were determined to be either diploid or haploid using phase contrast microscopy (diploid cells appear considerably larger and a lot less clumpy than haploids).

2.2.15.3 Sporulation protocol for recombination analysis

In order to measure recombination under the same liquid sporulation conditions necessary to achieve the synchronous sporulation required for physical analyses (whilst seeking to avoid potential problems associated with assessing recombination from a single diploid colony) the following strategy was designed: the haploid strains to be crossed were patched onto a YEPEG plate from -80°C stocks and grown for 24-48 hours at 30°C. The two strains were then mixed on a YEPD plate and mating allowed to proceed for 5 hours at 30°C. To enrich for diploids, the cells were then replicated to a minimal medium plate supplemented with 250 µl 0.5% (w/v) adenine hemisulphate and grown overnight at 30°C. A single-colony-sized amount of primarily diploid cells was then used to inoculate a 5 ml YPD culture and the sporulation procedure completed as described for liquid sporulation (Section 2.2.13), incubating at 23°C.

2.2.15.4 Tetrad dissection

Prior to dissection, asci were incubated in 100 μ l dissection buffer (1 M sorbitol, 10 mM EDTA, 10 mM NaPO₄ pH 7.2) supplemented with 5 μ l 5 mg/ml 20T zymolyase for 30 min at 37°C in order to enzymatically remove the ascus wall. Following digestion, a further 400 μ l dissecting buffer was gently added and the cell preparations stored at 4°C for up to one week. Tetrad dissection was carried out on YEPD medium using a Zeiss Axioscope microscope and micromanipulator. Dissecting needles were obtained from Singer Instruments. Spores were allowed to germinate and proliferate on YEPD for 2-3 days at 30°C prior to recombination analysis (Section 2.2.15.7).

2.2.15.5 Mating type testing

To determine the mating type of a particular strain(s), cells were mated on YEPD medium to *MATa* and *MAT α* tester strains for at least 4 hours before replica plating to minimal medium and incubation overnight at 30°C. The mating tester strains contain auxotrophies (*ura2*, *tyr1*) not present in the strains used for analysis. Therefore, following replication to minimal medium, only cells that have mated and henceforth undergone complementation of auxotrophies will be able to grow.

2.2.15.6 Spore viability analysis

Spore viability was assessed by counting the numbers of spores visible to the naked eye. Tetrads were classified as containing 0, 1, 2, 3 or 4 viable spores. To calculate overall viability the following equation was used:

$$\frac{((n \text{ 4-spore tetrads} \times 4) + (n \text{ 3-spore tetrads} \times 3) + (n \text{ 2-spore tetrads} \times 2) + n \text{ 1-spore tetrads})}{(n \text{ 4-spore tetrads} \times 4)} \times 100$$

2.2.15.7 Recombination analysis by tetrad dissection

To determine the recombination events occurring during meiosis in each tetrad, haploid strains were constructed that upon mating form diploids heterozygous for a number of marker mutations at loci on chromosomes III, VII and VIII (see Figure 4.2). Each marker results either in yeast being unable to grow on media lacking specific nutrients or confers the ability to grow on certain drug-containing media. Following replica plating to these selective media, the spore genotypes were scored

and compared to the parental genotypes using MacTetrad 6.9 software (Greene, 1994). This calculates the numbers of parental ditypes (PD), tetratypes (TT) or non-parental ditypes (NPD) and identifies aberrant segregation patterns. The software also calculates a cM value for each genetic interval using the formula of Perkins (1949):

$$cM = \frac{1}{2}(TT + 6NPD)/(TT + NPD + PD)$$

Meiosis I non-disjunction was assessed using the two viable spore tetrad class. The insertion of *URA3* at the centromere of chromosome VIII enabled sister and non-sister spores to be identified. Non-maters indicative of chromosome III non-disjunction were identified by mating type test as described in Section 2.2.15.5.

2.2.15.8 Random Spore Analysis

Diploid strains containing heteroallelic versions of *his4* (see Figure 4.2 for schematic diagram) and heterozygous for the recessive mutations *can1* and *cyh2- α* (conferring resistance to canavanine and cyclohexamide respectively) were sporulated in 50 ml volumes as described in Section 2.2.12. After 24 hours, 200 μ l of culture was removed and transferred to a 1.5 ml microcentrifuge tube. Single spores were generated using a modified version of the protocol described in Jessop *et al.* (2005). Following centrifugation at 13,000 rpm for 1 min, the supernatant was removed and the pellet washed twice with sterile deionised water. After the second wash, the pellet was resuspended in 500 μ l 1 M sorbitol, 10 mM EDTA, 50 mM KPO₄ buffer (pH 7.5), 1% β -mercaptoethanol and 4 mg/ml zymolyase 20T and incubated at 37°C for 15 min. Cells were pelleted at 13,000 rpm for 1 min, the supernatant removed and the pellet resuspended in 1 ml 0.1% Tween 80 (Sigma). Spores were separated by sonication on ice for 15 seconds at a time (followed by 2 min on ice to prevent overheating) until >90% cells were single spores as monitored by phase contrast microscopy. Five 1 in 10 serial dilutions were then made using sterile deionised water and 100 μ l of the 10⁻² to 10⁻⁵ dilutions were plated onto complete medium lacking arginine but supplemented with canavanine and cyclohexamide. Selecting for cells resistant to both canavanine and cyclohexamide ensures that only recombinant haploids are scored. 100 μ l suspensions from the neat solution and the 10⁻¹ and 10⁻² dilutions were plated onto two plates of complete medium lacking histidine and arginine but containing canavanine and cyclohexamide to select for His⁺ spores.

After incubation at 30°C for 3 days, 100 colonies from the non-prototroph selecting medium and 200 colonies from the prototroph-selecting medium from each experiment were picked and patched out onto YEPD plates. After growth overnight, the patches were replicated to media containing either nourseothricin or hygromycin B. Following incubation overnight at 30°C, each patch was scored for growth or lack of growth on the medium containing nourseothricin or hygromycin B in order to assess the amount of recombination taking place. For each strain tested, three independent experiments were performed, each from an independently isolated diploid colony.

2.2.16 Statistical analysis

A variety of statistical tests were performed to investigate the significance of the results obtained. These included the G-test of homogeneity, the Pearson's chi-square (χ^2) test and the Student's t-test (Sokal and Rohlf, 1969). Generally, a P-value of less than 0.05 was considered significant. When multiple comparisons were made, the Dunn-Sidak correction factor was applied to prevent false rejection of the null hypothesis that any deviation observed was due to chance. The relevant P-value used for assessing significance is stated for each test performed where appropriate.

CHAPTER 3

ANALYSING RESECTION AND GENE CONVERSION AT THE *HIS4* HOTSPOT

3.1 Introduction

Following meiotic DSB formation, the broken DNA ends undergo resection and repair. Due to the transient nature of the single-stranded DNA (ssDNA) produced during this process, accurate measurements of resection intermediates have been difficult to provide, meaning that no assessment of the factors contributing to resection has been made in otherwise wild-type cells. Previous attempts to quantify resection tracts have been largely reliant upon the use of Southern blotting. For example, estimation of the amount of smearing visible around the DSB using strand-specific probes is a method that has been employed by several investigators (Bishop *et al.*, 1992; Vedel and Nicolas, 1999). An alternative approach is the use of loss-of-restriction-site assays that take advantage of the fact that many restriction enzymes only cleave dsDNA templates. This means that any DNA present at the restriction site in single-stranded form is protected from cleavage and can thus be separated from the digested dsDNA by gel electrophoresis. Subsequently, Southern blotting (probing for DNA sequence adjacent to the DSB) is used to reveal the fragments of interest (Sun *et al.*, 1991; Manfrini *et al.*, 2010).

In addition to being time-consuming and requiring relatively large amounts of DNA, Southern blotting is also somewhat limited in its ability to distinguish small amounts of target DNA above background meaning that low level resection products may go undetected. Various approaches have been taken to circumvent this inherent limitation including the use of artificially 'hot' Spo11-dependent break sites (Bishop *et al.*, 1992) (such as *HIS4LEU2* which undergoes approximately 1 DSB per cell (Cao *et al.*, 1990; Storlazzi *et al.*, 1995)), non-Spo11-dependent break sites such as that catalysed by the *VMA1*-derived endonuclease (Neale *et al.*, 2002; Johnson *et al.*, 2007) and the employment of the *dmc1* Δ mutation (Tsubouchi and Ogawa, 2000;

Manfrini *et al.*, 2010) in which strand invasion is prevented and hyper-resected DSBs accumulate (Bishop *et al.*, 1992). However, all of these methods affect either the formation or processing of the DSBs meaning that the results obtained may not be representative of normal resection.

Recently, Alastair Goldman and colleagues (University of Sheffield, UK) have developed an alternative approach that combines the loss-of-restriction-site methodology with the use of real-time PCR for DNA quantification, affording greater accuracy and sensitivity. In this technique, PCR primers are designed to flank a suitably placed restriction site. The DNA extracted from cells undergoing meiosis is then subjected to restriction digestion prior to PCR being carried out. If the DNA is double-stranded at the site of interest, enzyme cleavage will act to destroy the PCR template, meaning that amplification from the flanking primers cannot occur. However, if the DNA is single-stranded at the target site, it will not be cut by the restriction enzyme, leaving a template that can be amplified in the subsequent PCR step. A second pair of PCR primers targeted to the rDNA locus (to amplify a region which does not contain target sites for any of the restriction enzymes used) provide an internal control with which to assess the total amount of DNA added to the PCR reaction. The dsDNA-binding dye SYBR[™] Green I fluoresces much more strongly when it is bound to dsDNA than when free in solution. Therefore, if this dye is included within the reaction, the fluorescent signal generated will increase as amplification of the target region occurs. During real-time PCR, fluorescence is monitored each cycle and the number of cycles required to increase the fluorescence signal significantly above the background fluorescence (the crossing-point) thereby provides a measure of the amount of template DNA present at the start of the reaction. Comparison between the crossing-points of the enzyme target PCR and the loading control PCR thus allows the calculation of the proportion of DNA single-stranded at the site of interest (see Section 3.2.3 for details).

We hypothesised that this technique could provide the sensitivity required to detect and quantify small variations in the amounts of ssDNA formed at natural recombination hotspots. In this chapter we sought to test this possibility using the *HIS4* hotspot and if successful, to apply this methodology to assess the contribution

made by Exo1 to meiotic resection and the influence of resection upon hDNA formation during recombination.

3.2 Materials and methods

3.2.1 Strain construction

Strains were designed to provide a number of genetic intervals across three chromosomes in which recombination could be assessed (Figure 4.2). All strains were constructed by transformation or by crossing to SK1 strains provided by Michael Lichten (National Cancer Institute, Bethesda, USA). The *his4-XhoI* and *his4-BglII* alleles represent the cutting and filling-in of the *XhoI* and *BglII* restriction sites situated 96 bp and 1,688 bp downstream of the *HIS4* start codon, respectively. Both mutations result in 4 bp insertions. The *his4-XhoI* allele was obtained by crossing to an existing strain, while *his4-BglII* was inserted using the two-step gene replacement method (Section 2.2.10.3) following linearisation of pRED322 with *XbaI*. The *trp5-S*, *met13-B* and *lys5-P* alleles have been described previously (de los Santos *et al.*, 2003; Martini *et al.*, 2006) and were inserted using the same two-step gene replacement method. The plasmids used were provided by Neil Hunter (University of California, Davis, USA). For insertion of *trp5-S*, plasmid pNH229 was linearised with *BglII*, while the *met13-B* allele was derived from a *BstGI* digest of pNH217. No suitably placed single-cutting enzyme could be identified in the *lys5-P* containing plasmid pNH223; therefore, an *NcoI* partial digest was carried out to obtain product in which the linearised plasmid made up a substantial proportion of the DNA molecules.

CEN8:URA3 was introduced following PCR amplification of the *CEN8:URA3* marker from strain NHY942 (Martini *et al.*, 2006) using oligonucleotides placed a sufficient distance either side of the insert to provide the homology required for homologous recombination. The *ade1-1* allele (*ade1-S240F*) was inserted using a cloning-free PCR-based allele replacement method (Erdeniz *et al.*, 1997; Section 2.2.10.2) using genomic DNA from strain EY97 (Hoffmann *et al.*, 2005) as a template. The *rad50S* mutation was obtained by crossing to an existing strain. The allele used is an A/T point mutation in the *RAD50* gene, which causes an amino acid change from lysine to isoleucine at position 81 (Alani *et al.*, 1990). The remaining markers have been described previously (*leu2-R* (Borts *et al.*, 1986) and *arg4-nsf*

(Nicolas *et al.*, 1989)), and the desired segregants were acquired by standard genetic crossing.

The *exo1-D173A* allele was introduced using the PCR-based allele replacement method (Erdeniz *et al.*, 1997) using plasmid template pEAM71 (Table 2.2). As prior sequencing of the *EXO1* open reading frame in SK1 revealed two non-synonymous polymorphisms compared to the strain background used in the construction of the aforementioned plasmids, only a limited region of *EXO1* surrounding the point mutation was transferred in order to prevent any additional amino acid changes being introduced. The *exo1-D173A* mutation ablates a *DrdI* restriction site, allowing for the screening of successful integrations by restriction digestion. The *EXO1* open reading frame was replaced with the KanMX4 cassette conferring resistance to geneticin using a PCR-based gene replacement method (Wach *et al.*, 1994). All alleles were confirmed by PCR, linkage analysis and DNA sequencing where appropriate. Full genotypes are provided in Table 2.1 and the oligonucleotide sequences used are given in Table 2.4.

3.2.2 Reconstruction experiments for qPCR assay validation

Reconstruction experiments were performed by dividing an aliquot of DNA extracted from pre-meiotic cells into two halves. One half was kept on ice to preserve the native DNA structure while the other half was denatured to produce ssDNA by heating at 95°C for 7 min. The heated sample was then snap chilled on ice for 2 min. The native and denatured DNA was mixed in a 9:1 ratio to produce a sample containing 10% ssDNA. Subsequently, the 5%, 2%, 1% and 0.5% ssDNA samples were made by serial dilution of the 10% ssDNA sample with the appropriate amount of native DNA. These samples were then subjected to the loss-of-restriction-site qPCR assay described below.

3.2.3 Loss of restriction site analysis by qPCR

All DNA samples were extracted from cells using the CTAB method (Section 2.2.2.2). For each sample tested, approximately 750 ng of genomic DNA was digested with 25 units of enzyme for 30 mins at 37°C in a total volume of 50 µl. Following digestion, 20 µl of the digest was diluted into 80 µl of ice-cold water, 2 µl of which was added to each qPCR reaction to give approximately 6 ng of template

DNA per reaction. Quantitative PCR was carried out as described in Section 2.2.9 and was directed to both the target site of interest and the rDNA region. Mean Cp values for each triplicate sample were imported into Microsoft Excel and standard curves were constructed for both the target site primer pair and rDNA primer pair by plotting the mean Cp values obtained against the \log^{10} of the dilution factor used. A line of best fit was drawn and the slope (m) and y intercept (b) of the line calculated. For each experimental sample, a value for the amount of template DNA present at the start of the PCR (x) at both the target and rDNA loci were obtained by reference to the appropriate standard curve using the formula:

$$x = 10^{\left[\frac{Cp \text{ observed} - b}{m} \right]}$$

For the reconstruction experiments, the proportion of ssDNA and dsDNA were then calculated using the equations:

$$\%ssDNA = \frac{x_{TARGET}}{x_{rDNA}} \times 100$$

$$\%dsDNA = 100 - \left[\frac{x_{TARGET}}{x_{rDNA}} \times 100 \right]$$

In order to compare between different target sites and time courses, it was necessary to normalise the data from each experiment to take account of the efficiency with which the digestion of dsDNA had occurred. This was done by reference to the amount of ssDNA measured in the 0 hour time point of that time course (where the 0 hour sample is assumed to represent 100% dsDNA) using the equation:

$$\%ssDNA = \%ssDNA_{MEASURED\ IN\ SAMPLE} - \left[\frac{\%dsDNA_{MEASURED\ IN\ SAMPLE}}{\%dsDNA_{MEASURED\ AT\ 0hr}} \times \%ssDNA_{MEASURED\ AT\ 0hr} \right]$$

Resection was assessed in wild-type (RKD51), *exo1Δ* (RKD52) and *exo1-D173A* (RKD55) strains.

3.2.4 Quantitative Southern blot analysis

Quantitative Southern blotting was carried out as described in Section 2.2.14. Blots were probed with an α -³²P radio-labelled *HIS4* fragment (+523 to +1,547 base-pairs, relative to the *HIS4* open reading frame) amplified from plasmid pVC4 (Table 2.2). The percentage of DSBs present in each time point was calculated using the formula:

$$\%DSBs = \left[\frac{DSB \text{ signal}}{DSB + \text{parental signal}} \right] \times 100$$

3.2.5 Measurements of gene conversion

NMS was assessed at the *bis4-XhoI* allele in wild-type (RK358 x RK392), *exo1* Δ (RK359 x RK394) and *exo1-D173A* strains (RK399 x RK425) and at *bis4-BglII* in wild-type (RK385 x RK392) and *exo1* Δ cells (RK387 x RK394). NMS was scored as any tetrad not exhibiting a 2:2 pattern of segregation at *HIS4* and statistical comparisons were carried out as described in Section 2.2.16.

3.3 Results

3.3.1 Verifying the suitability of the *HIS4* hotspot for resection analysis

Before attempting to use *HIS4* as a site for resection analysis, it was necessary to verify that results obtained at this locus were unlikely to be affected by the processing of DSBs occurring nearby. In order to do this and to confirm the location of the *HIS4* hotspot, DSB formation was monitored in *rad50S* strains in which unresected DSBs accumulate (Alani *et al.*, 1990). Cells were sporulated as described in Section 2.2.13. Consistent with previous studies (Nag and Petes, 1993; Hoffmann *et al.*, 2005), a high frequency of DSBs was observed centring approximately 300 bp upstream of the *HIS4* start codon (Figure 3.1A). To assess the possibility that DSBs downstream of *HIS4* could contribute to the conversion or resection observed at the locus, an *EcoRV* digest was used (Figure 3.1B). Aside from the *HIS4* hotspot, no other DSB sites were seen. Where faint bands were present, they were also visible in the 0 hour time point suggesting that these bands reflect non-specific probe binding. As no other DSB hotspots were observed within a 1.3 kb region upstream or 5.9 kb downstream of *HIS4*, this locus was therefore considered suitable for resection studies. When DSBs were measured in three independent cultures of wild-type, *exo1Δ* and *exo1-D173A* strains, a similar proportion of DSBs were produced in all three genotypes (approximately 13%; Figure 3.1A), demonstrating that the status of Exo1 does not affect DSB formation.

3.3.2 Selection of *HIS4* restriction sites and assay validation

Potential restriction enzyme sites for use in the resection assay were selected according to a range of criteria. Specifically, they had to be commercially available, active at temperatures of 37°C or below (to prevent DNA denaturation) and be free of detectable exonuclease or endonuclease activities upon non-target substrates. These properties were assessed using the product information provided by the manufacturer (New England Biolabs) and several suitable sites were identified within a 2 kb region downstream of *HIS4* (Figure 3.3A). To verify the suitability of these enzymes and to determine whether or not the small amounts of ssDNA expected at the *HIS4* locus were likely to be quantifiable using this approach, reconstruction experiments were performed. In these experiments, a series of known quantities of ssDNA ranging from 10% to 0% were prepared as described in Section 3.2.3. These samples were then subjected to the loss-of-restriction-site qPCR assay in order to

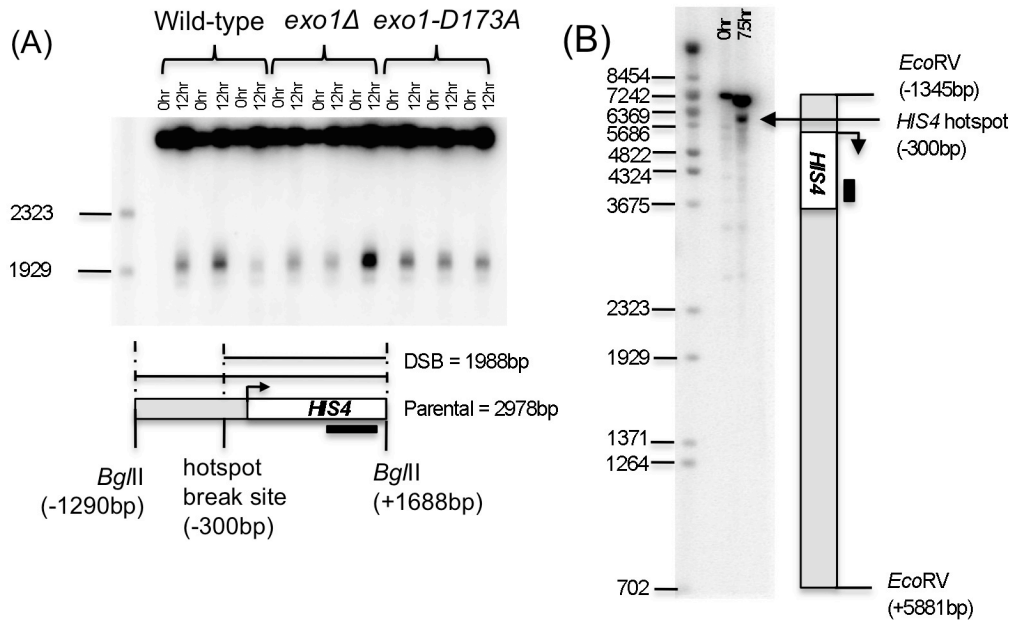


Figure 3.1: Analysis of DSB formation at *HIS4* in *rad50S* strains

(A) DSBs at *HIS4* were assessed after 12 hours in sporulation medium in three independent wild-type, *exo1Δ* and *exo1-D173A* cultures. DNA was digested with *Bgl*II in order to estimate the amount of breaks formed and the position of the break with respect to the *HIS4* start codon. The average amount of DNA present as a DSBs was measured at 12.8% in wild-type, 14.7% in *exo1Δ* cells and 13.2% in the *exo1-D173A* strain. These values were not significantly different from each other ($p > 0.7$, t-test). (B) DNA was digested with *EcoRV* to look for the presence of DSBs downstream of *HIS4*. *BstEII* digested lambda DNA was used as a molecular weight standard and the size of each band is indicated. The black boxes represent the approximate location of the probe used for DSB analysis.

measure the amount of ssDNA at each point in the series (Figure 3.2). This was repeated for each restriction enzyme site of interest. When the proportion of ssDNA measured in these experiments was compared to the proportion of ssDNA expected, a linear correlation between the known and expected proportion of ssDNA was observed at all sites assessed (Figure 3.3B). The greatest source of variation between the different enzymes appeared to be the efficiency with which the dsDNA was digested. For example, when the 0% ssDNA sample was considered, digestion with *ClaI* resulted in 0.41% ssDNA being detected, while digestion with *AatII* produced 1.07% ssDNA. To take account of this variation in enzyme efficiency the data was normalised using the equation outlined in Section 3.2.3. This normalisation assumes that the value measured in the 0% ssDNA sample resulted solely from incomplete digestion.

Following normalisation, a very close correlation between the amount of ssDNA expected and measured was obtained for values between 0% and 5% ssDNA at all four target sites (Figure 3.3C). When ssDNA constituted a greater proportion of the total DNA in the sample, an increased divergence from the expected amount of ssDNA was observed indicating that this technique may become less accurate at higher ratios of ssDNA to total DNA. However, for the amounts of ssDNA expected to occur during a meiotic time course experiment, this approach should provide a reliable and accurate method of quantifying ssDNA. For all primer pairs, melt curve analysis revealed a single peak demonstrating that all pairs specifically amplify a single target site (Figure 3.2C and D; data not shown).

3.3.3 Analysis of meiotic DSB resection at *HIS4*

Following validation of the qPCR loss-of-restriction-site methodology, the assay was applied to samples obtained from cells undergoing meiosis. The data was normalised as described above by assuming that any amplification observed in the 0 hour time point was the result of incomplete digestion. Resection was initially characterised in a wild-type strain and two independent time courses were examined. In both time courses a steep resection gradient was observed whereby the amount of ssDNA detected decreased with increasing distance from the DSB. A considerable amount of ssDNA was observed approximately 0.5 kb from the DSB, and the majority of this DNA also appeared to have been resected as far as 0.8 kb. However, very little

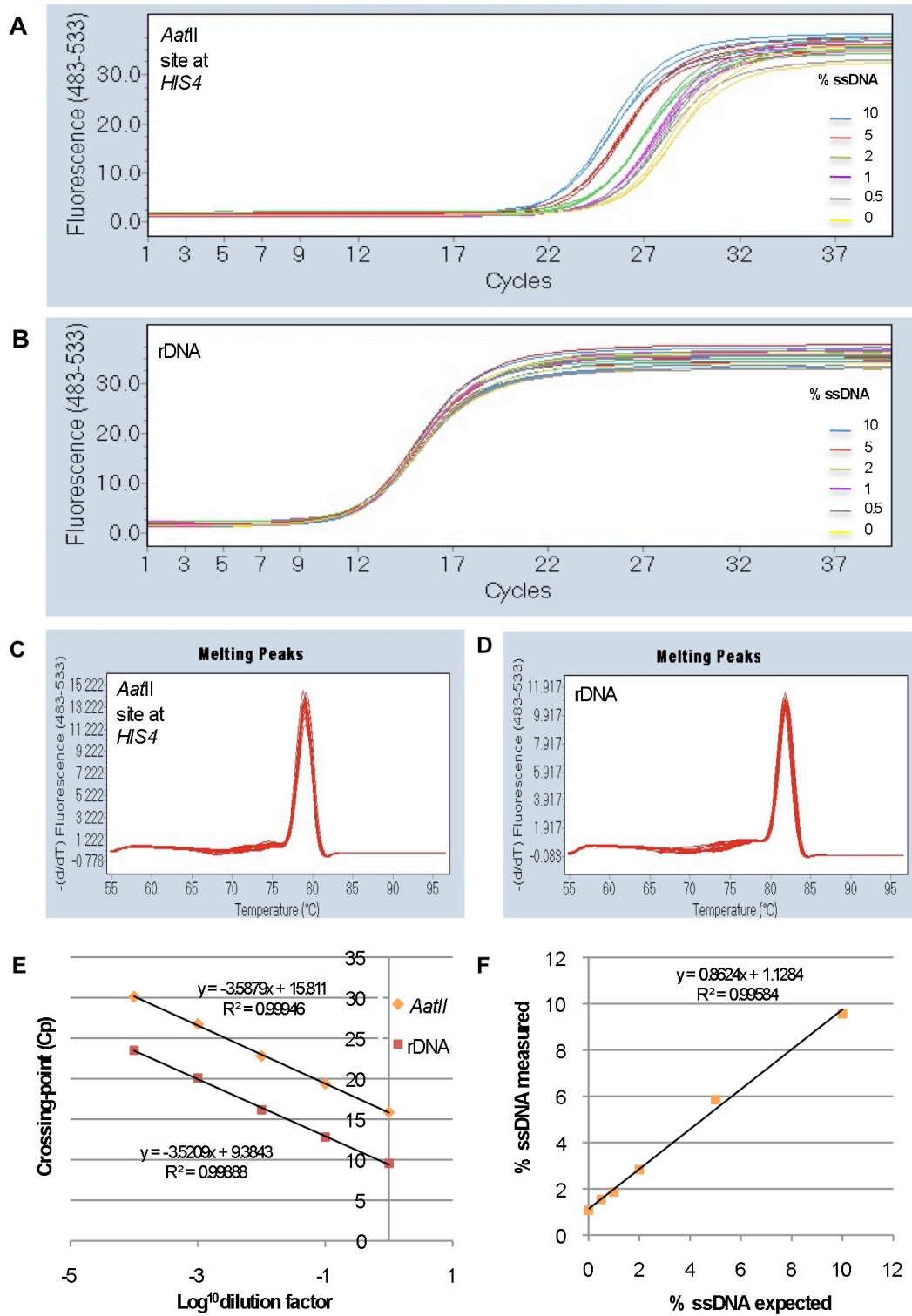


Figure 3.2: Validation of the restriction site suitability – the *AatII* site

(A) Real-time fluorescence amplification plots produced when the indicated proportions of ssDNA were digested with *AatII* prior to qPCR being carried out using primers flanking the *AatII* site at *HIS4*. Triplicate reactions were performed for each sample. (B) Amplification plots of the same digested samples when PCR was directed to the rDNA locus. (C) Melt curve analysis at the *AatII* site demonstrating specific amplification of a single product. (D) Melt curve analysis at the rDNA site demonstrating specific amplification of a single product. (E) Standard curves for both the *AatII* primers and rDNA primers constructed from a DNA serial dilution demonstrating that linear range (F) The amount of ssDNA measured in each sample plotted against the amount expected. The line of best fit between dilutions is shown.

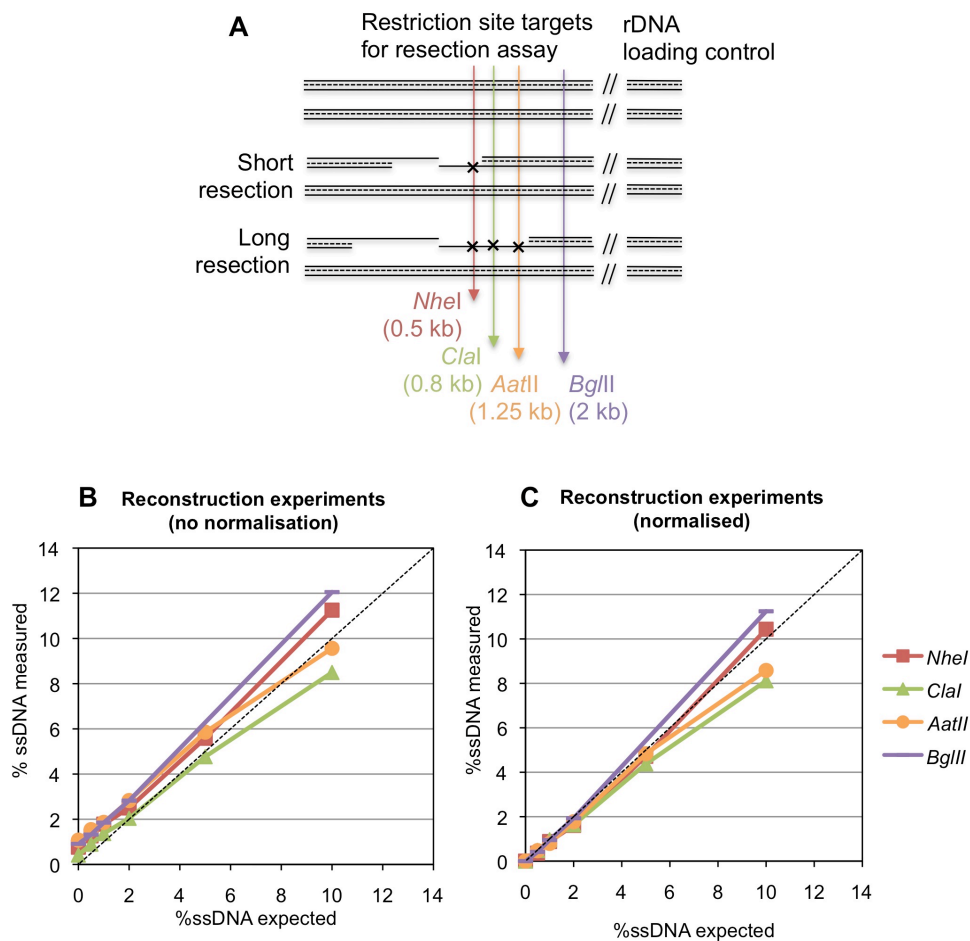


Figure 3.3: Validation of resection assay target sites and data normalisation

(A) Schematic diagram indicating the position of the restriction site targets used in the resection assay with respect to the *HIS4* hotspot. The *HIS4* hotspot is located approximately 300 bp upstream of the start codon. PCR primers were designed to flank each restriction site. A second qPCR reaction was also targeted to the rDNA region in order to quantify the total amount of DNA added to the reaction. (B) Samples containing known quantities of ssDNA were prepared and subject to loss-of-restriction site analysis by qPCR. For each target site, the proportion of ssDNA measured was plotted against the proportion of ssDNA expected. The dashed line indicates a perfect correlation. (C) The same data presented in B after normalisation to account for variations in the efficiency of restriction enzyme digestion.

ssDNA was observed approximately 1.25 kb from the DSB and virtually no ssDNA was observed at the 2 kb site (Figure 3.4A). These lengths are consistent with previous estimates of resection (Sun *et al.*, 1991; Bishop *et al.*, 1992; Vedel and Nicolas, 1999). We also attempted to measure ssDNA at the *AclI* restriction site situated approximately 0.2 kb from the DSB site. However, despite performing well in the reconstruction experiments, this site repeatedly gave inconsistent and poorly reproducible results upon time course samples (data not shown) and hence was excluded from further analysis. We hypothesised that this could be due either to DSBs occurring within the amplicon or degradation of the 3' end. At all target sites, the peak amount of ssDNA was observable after 7 hours in sporulation medium (Figure 3.4A). In the *exo1Δ* time courses, considerably less ssDNA was measured at the *NheI* site (approximately 0.5 kb from the DSB) compared to the wild-type strain and only a small proportion of this ssDNA remained detectable at *ClaI* (approximately 0.8 kb from the DSB). Furthermore, the ssDNA measured at the 0.8 kb site peaked an hour later than the ssDNA measured at the 0.5 kb site, consistent with a reduction in the processivity of resection in the absence of *EXO1*. As the reduction in ssDNA could not be attributed to a reduction in DSB formation, this strongly suggests that Exo1 functions in resecting Spo11-dependent DSBs in otherwise wild-type cells.

The ssDNA detected during meiosis was expected to result from the 5' to 3' resection of the DSB. This effectively removes one DNA strand, leaving only one strand of the original chromatid available to serve as a PCR template. In contrast, both strands of each chromatid are amplifiable at the rDNA locus and at all sites in the reconstruction experiments where the ssDNA was produced by denaturing dsDNA. For this reason, the amount of ssDNA measured as a consequence of resection underestimates the proportion of chromatids resected, preventing direct comparisons with DSB frequency from being made. Accurate calculation of the percent of resected chromatids would require the amplification efficiency associated exclusively with the first PCR cycle (in which only the primer complementary to the unresected strand is able to bind) to be known. Calculation of this is not feasible. However, if the efficiency of amplification in this first cycle is assumed to be equal to the mean efficiency observed when both primers in the reaction are active (as

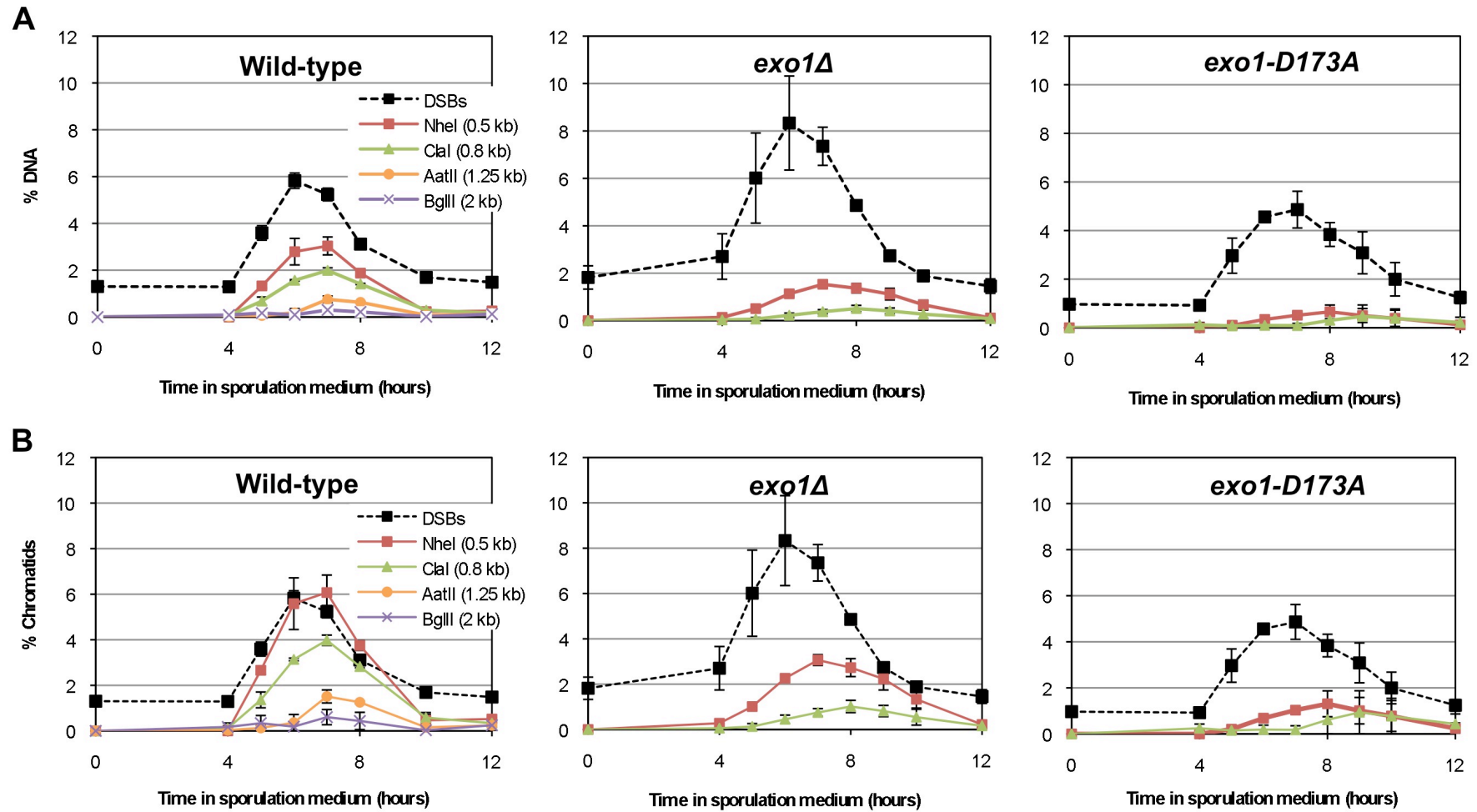


Figure 3.4: Measurements of DSBs and single-stranded DNA in meiotic time course experiments

(A) For each genotype indicated, the amount of ssDNA detected by the loss-of-restriction site qPCR assay at each restriction site and the amount of DSB measured by quantitative Southern blot analysis is plotted at each time point assessed. Each data point represents the mean value measured in two independent time courses. Error bars indicate the range of the data observed. (B) The same data after the amount of ssDNA was doubled to take account of the strand removed by resection.

calculated from the standard curve), the percent of resected chromatids would be equal to twice the amount of ssDNA measured. When this correction was applied and the resulting values were compared to the amount of DSBs measured in the same time courses by Southern blotting, it appeared that resection intermediates accumulated to higher levels than DSBs (Figure 3.4B). This could suggest either that DSBs are underestimated by the Southern blotting approach or that the 2-fold correction factor applied to the ssDNA is inaccurate, resulting in the amount of resection being overestimated. Alternatively, this apparent discrepancy may be due to a difference in the length of time the intermediates take to turnover. If ssDNA persists after DSBs are no longer detectable, the amount of ssDNA produced may appear to be higher. This would argue that only a small proportion of the resected DNA is incorporated upon strand invasion.

3.3.4 Gene conversion at *HIS4* requires *Exo1*

In order to ascertain whether resection determines the extent of hDNA formation, the amount of gene conversion occurring at *HIS4* was assessed under the same sporulation conditions used in the resection analysis. Conversion was measured using DSB proximal (*his4-XhoI*) and distal (*his4-BglII*) alleles. Consistent with a role for resection in determining the extent of hDNA, non-Mendelian segregation was significantly reduced in the *exo1Δ* cells at both alleles when compared to wild-type ($p < 0.007$, G-test; Table 3.1, Figure 3.5). However, while this was similar to the effect that *EXO1* deletion had upon the resection gradient, there did not appear to be a direct correlation between resection and conversion. This was most clearly demonstrated in the wild-type strain in which over one third of the gene conversion tracts that were measured 96 bp from the start codon (approximately 0.4 kb from the DSB) also extended as far as 1,688 bp away (approximately 2 kb from the DSB; Table 3.1). However, despite significant quantities of resection being observed 0.5 kb from the DSB, virtually no ssDNA was detected at the site of the DSB distal allele even though considerable amounts of hDNA must have formed there (Figures 3.4 and 3.5). This argues that more hDNA is produced during meiosis than can be accounted for by detectable resection of the DSB.

Table 3.1: Non-Mendelian Segregation at *HIS4*

Genotype		Allele	
		<i>bis4-XhoI</i>	<i>bis4-BglII</i>
Wild-type	% NMS	29.2 [†]	11.2 [†]
	(NMS/total tetrads)	(275/941)	(38/338)
<i>exo1Δ</i>	% NMS	23.6*	2.5*
	(NMS/total tetrads)	(209/885)	(3/118)
<i>exo1-D173A</i>	% NMS	15.4* [†]	<i>not</i>
	(NMS/total tetrads)	(49/319)	<i>determined</i>

[†]Non-Mendelian segregation includes gene conversion and post-meiotic segregation events. Tetrads exhibiting ≥ 3 NMS events per tetrad were scored as false tetrads and excluded from further analysis. %NMS was calculated as: (number of NMS events/total number of tetrads) x 100. Comparisons were made using the G-test of homogeneity and statistically significant ($p < 0.0169$) differences are indicated as follows: * significantly different from wild-type, [†] significantly different from *exo1Δ*.

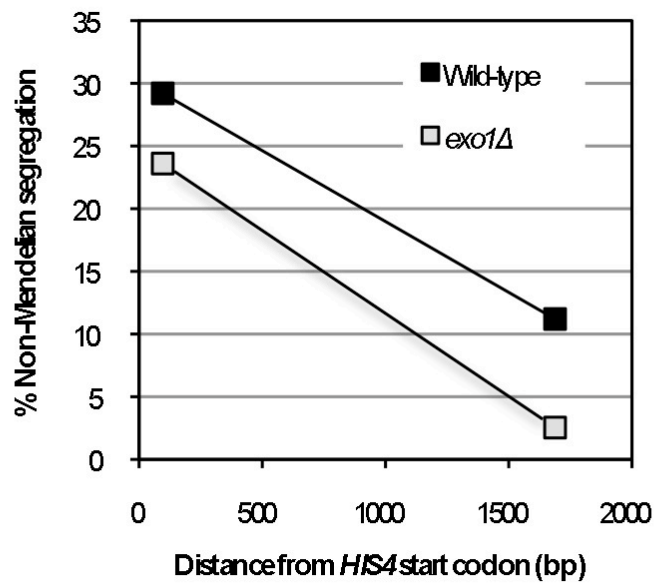


Figure 3.5: The effect of *EXO1* deletion on the *HIS4* gene conversion gradient in the SK1 strain background

Following tetrad dissection, non-Mendelian segregation (NMS) was measured at two alleles situated 96 bp and 1,688 bp from the *HIS4* start codon (approximately 0.4 kb and 2 kb from the *HIS4* hotspot). In the absence of *EXO1*, NMS is significantly reduced at both alleles. See Table 3.1 for raw data.

3.3.5 The functions of Exo1 in DNA resection and hDNA formation are nuclease-dependent

To confirm that the deficient resection and hDNA formation observed in *exo1Δ* was due specifically to a nucleolytic role for Exo1 in these processes, the nuclease deficient allele *exo1-D173A* (Tran *et al.*, 2002) was studied. As shown in Figure 3.4, very little ssDNA was detected in the *exo1-D173A* time courses consistent with reduced resection taking place. As observed previously in *exo1Δ* cells, the peak amount of ssDNA detectable 0.8 kb from the DSB was delayed by an hour compared to the peak amount of ssDNA 0.5 kb away. Furthermore, gene conversion at *bis4-XhoI* was significantly reduced in *exo1-D173A* tetrads compared to the wild-type cells ($p=4 \times 10^{-7}$, G-test). Gene conversion was also reduced in the *exo1-D173A* strain when compared to *exo1Δ* tetrads ($p=0.0016$, G-test), suggesting that the presence of the nuclease-defective protein may partially inhibit either strand invasion or the residual resection observed in *exo1Δ* cells. These results demonstrate that the phenotype observed in *exo1Δ* is not an indirect consequence of the loss of the protein (for example, if the absence of Exo1 destabilised a protein complex involved in these processes). Rather, Exo1 plays a nuclease-dependent role in DSB end resection and hDNA formation.

3.3.6 The *pol3-ct* allele confers a severe mitotic growth defect in the SK1 background

It has been suggested that resection may progress coordinately with recombination-related DNA synthesis (Abdullah *et al.*, 2004; Hoffmann and Borts, 2004; Maloisel *et al.*, 2004) and the results obtained in this study could be accounted for by such a mechanism (see discussion). Therefore, we aimed to test this idea by monitoring resection in strains carrying the *pol3-ct* allele: a short C-terminal truncation removing the last 4 amino acids of the *POL3* gene, which encodes the catalytic subunit of DNA polymerase δ . This allele has been shown to result in decreased gene conversion tract lengths and reduced crossing over during meiosis without exhibiting a mutant phenotype during vegetative growth, leading to the suggestion that *pol3-ct* is specifically defective during meiotic recombination-related DNA synthesis (Section 1.5.2.1; Maloisel *et al.*, 2004). If resection and synthesis are coordinated, it follows that in situations where DNA synthesis is limited, resection would be similarly reduced. Unfortunately, when the *pol3-ct* allele was introduced, it was found to

confer a severe mitotic growth defect in the SK1 strain background. Colonies were small, slow-growing and had ragged edges, consistent with a defect in DNA replication (data not shown). While it is curious that the mutation (which does not show a mitotic defect in either the W303 or BR strain backgrounds (Maloisel *et al.*, 2004)) should cause this phenotype in SK1 strains, it meant that the *pol3-ct* allele could not be used to assess the coordination of resection and DNA synthesis as hoped. Subsequent discussion with Laurent Maloisel (CEA, France) confirmed that this is consistent with his unpublished observations.

3.4 Discussion

3.4.1 A new method with which to study resection at Spo11-dependent DSBs

In this chapter we have demonstrated that a qPCR-based method previously used to measure the amount of ssDNA produced by resection of a *VMA1*-derived endonuclease (VDE) catalysed DSB can also be applied to a Spo11-dependent meiotic hotspot. This method offers several advantages over Southern blotting in that it can provide data more rapidly and allows even very small amounts of ssDNA to be detected. Although target sites are limited by DNA sequence and enzyme suitability, we were able to identify several potential sites within a 2 kb region based upon freely available information. In contrast to previous applications at the *VMA1*-derived endonuclease break site which repairs most commonly by single-strand annealing between flanking regions of homology (Hodgson *et al.*, 2010), the use of this methodology at breaks that preferentially undergo strand invasion mediated repair may provide a more biologically relevant assessment of resection. However, while this technique provides greater sensitivity in detecting ssDNA than is possible employing methods of analysis based on Southern blotting alone, Southern blotting must still be used to estimate DSB formation. In addition, it is difficult to accurately determine the percentage of chromatids undergoing resection. Therefore, while the results of this assay allow resection tract length distributions and the enzymes contributing to ssDNA production to be assessed, the accuracy with which the proportion of DSBs undergoing resection as far as each target site can be calculated is likely to be compromised.

3.4.2 Exo1 is required for full-length resection of meiotic DSBs

Regardless of how the amount of ssDNA is calculated, the resection assay clearly demonstrates that in the absence of Exo1 or the nuclease activity of Exo1, the amount of ssDNA produced is drastically reduced. Furthermore, the data are consistent with all DSBs being resected less in *exo1Δ*, rather than a subset of DSBs being selectively processed. The resection defect observed in *exo1Δ* was more severe when ssDNA was measured approximately 0.8 kb from the DSB compared to 0.5 kb, suggesting that the residual resection occurring in the absence of Exo1 is less processive. A recent study demonstrated a role for Sgs1 and Dna2 in producing the hyper-resected intermediates that form during meiosis in *dmc1Δ* mutants (Manfrini *et al.*, 2010). This is reminiscent of the dual resection pathways mediated by Exo1 and the 5' single-stranded exonuclease Dna2 (in conjunction with the helicase Sgs1 to first unwind the DNA) at DSBs occurring during mitotic growth (Mimitou and Symington, 2008; Zhu *et al.*, 2008). However, if these same enzymes are involved in catalysing normal meiotic resection, they are noticeably less able to compensate for Exo1 during meiosis than in other phases of the cell cycle. Therefore, while the identity of the protein(s) responsible for this remaining resection has not been uncovered, the structure-specific endonuclease Mre11 and/or Sae2 (both of which are required for the initial endonucleolytic cleavage event that releases Spo11 following DSB formation (McKee and Kleckner, 1997; Nairz and Klein, 1997; Prinz *et al.*, 1997; Furuse *et al.*, 1998; Tsubouchi and Ogawa, 1998; Moreau *et al.*, 1999; Neale *et al.*, 2002)) are perhaps the most likely candidates.

3.4.3 Exo1 and DNA synthesis may collaborate in the formation of heteroduplex DNA

While there were similarities between the gene conversion gradients and the single-stranded DNA profiles observed at *HIS4* in the wild-type and *exo1Δ* strains, there did not appear to be a one-to-one relationship between the two. Specifically, gene conversion tracts extended much further than resection tracts. This was most clearly demonstrated in the wild-type strain in which over one third of the number of conversions observed at *his4-XhoI* (approximately 0.4 kb from DSB) were measured at *his4-BglII* (approximately 2 kb from DSB), a distance at which virtually no resection was observed. Branch migration of the dHJ could be responsible for this situation at crossover-designated breaks; however, genetic studies to date have failed

to provide strong evidence of branch migration occurring in *Saccharomyces cerevisiae* meiosis (reviewed in Borts *et al.*, 2000). Therefore, this result implies that DNA synthesis commonly takes place beyond the point reached by resection prior to strand invasion. Although this contradicts a previous study at the *ARG4* locus in which resection and conversion gradients were said to be similar (Sun *et al.*, 1991), it is in accord with the lengths of meiotic recombination-related DNA synthesis observed by Terasawa *et al.* (2007). By monitoring the incorporation of thymidine analogues during meiosis, synthesis tracts associated with a crossover were measured at between 1.5 kb to 1.9 kb, lengths far in excess of those estimated to occur during resection (Sun *et al.*, 1991; Bishop *et al.*, 1992; Vedel and Nicolas, 1999; this study). We cannot rule out the possibility that long resection tracts are not detected because they turn over too rapidly. However, this disparity between the amount of DNA resected and synthesised supports previous observations implying that it is the extent of heteroduplex formed by the combination of DNA synthesis and second-end capture that determines the length of hDNA formed during meiosis, rather than the amount of DNA incorporated upon strand invasion (Hunter and Kleckner, 2001; Merker *et al.*, 2003; Maloisel *et al.*, 2004; Jessop *et al.*, 2005).

Nevertheless, Exo1 evidently influences hDNA tract length in some manner as its absence results in significantly reduced amounts of gene conversion. This reduction could potentially reflect an inability of some DSBs to undergo strand invasion when resection is short. Alternatively, as extensive synthesis past the initial resection point would result in the formation of DNA flaps following second-end capture (Figure 1.7C), the nuclease activity of Exo1 may be required to remove these flaps or to catalyse a second phase of resection as DNA synthesis proceeds. This secondary nucleolytic activity may not be detectable using the loss-of-restriction-site qPCR assay as it would occur within the context of dsDNA, but would allow a longer length of DNA to be incorporated into hDNA, thereby enabling conversion tracts to extend beyond the initial resection. A similar role for Exo1 was previously postulated by Abdullah *et al.* (2004) and such a function fits well with the hDNA extension model proposed by Maloisel *et al.* (2004). In the absence of Exo1, some limited secondary resection may be catalysed by an alternative nuclease. This alternative 5' processing mechanism may also account for the observation that the *exo1-D173A* strain exhibits a lower level of non-Mendelian segregation at the *his4-*

XhoI allele than was observed in *exo1Δ* cells, as substrate binding by the nucleolytically defective protein could reduce the ability of this substitute nuclease to access the DNA end.

3.4.4 Could a reduction in DNA end resection simultaneously account for the reduction in gene conversion and crossing-over observed in *exo1Δ*?

The model described above suggests that resection is required after strand invasion for recombination to proceed as normal and argues that if resection and synthesis are uncoordinated, DNA flaps may result (Figure 1.7). As suggested by Hoffmann and Borts (2004), these flaps could prevent ligation of the dHJ from occurring, thereby preventing crossovers from being formed in the absence of Exo1. This could thus account for the crossover deficit reported to occur in *exo1Δ* cells (Khazanehdari and Borts, 2000; Kirkpatrick *et al.*, 2000; Tsubouchi and Ogawa, 2000). Testing of this hypothesis will be carried out in Chapter 4.

CHAPTER 4

THE ROLE OF EXONUCLEASE I IN CROSSOVER PROMOTION

4.1 Introduction

Exo1 is a member of the evolutionarily conserved Rad2/XPG family of structure-specific nucleases that also includes Rad2 and Rad27 (known as Fen1 in humans and mammals). These proteins feature a conserved N-terminus containing N (N-terminal) and I (Internal) nuclease domains (Figure 4.1; Tishkoff *et al.*, 1997) and exhibit both 5' to 3' dsDNA exonuclease and 5' flap endonuclease activities (Fiorentini *et al.*, 1997; Tran *et al.*, 2002). Several observations suggest that while there is some degree of functional redundancy between these three nucleases (for instance, an *exo1* Δ *rad27* Δ double mutant is synthetically lethal (Tishkoff *et al.*, 1997)), they differ in their preferred biological substrate (Tran *et al.*, 2002; Sun *et al.*, 2003).

Mutation of certain conserved amino acid residues situated in the I nuclease domain can be used to study the various catalytic functions of Rad2 family members. For example, the missense allele *exo1-D173A* used in the previous chapter represents the conversion of the highly conserved aspartate at position 173 to alanine. This results in a protein deficient for both exonuclease and endonuclease activity (Tran *et al.*, 2002). Accordingly, expression of *exo1-D173A* is unable to reduce the increased spontaneous mutation rate and increased MMS sensitivity observed in an *exo1* Δ mutant background and *exo1-D173A* remains synthetically lethal in combination with a *rad27* Δ mutation (Sokolsky and Alani, 2000; Tran *et al.*, 2002). Importantly, the equivalent mutation in human Exo1 (Lee *et al.*, 2002), human Fen1 (Gary *et al.*, 1999), and yeast Rad27 (Shen *et al.*, 1996) does not prevent substrate binding and the ability of *exo1-D173A* to interact with Msh2 is unaffected (Sokolsky and Alani, 2000) suggesting that the protein remains structurally intact.

```

Exo1_S.cerevisiae      MGIQGLLPQLKPIQN PVS----LRRYEGEVL AIDGYAWLHRAACSCAY-----ELAMGK 50
Exo1_H.sapiens        MGIQGLLQFIKEASEPIH----VRKYKGQVVAVD TYCWLHKGAIACAE-----KLAKGE 50
Rad27_S.cerevisiae    MGIKGLN AIISEHVPSAIRKSDIKSFFGRKVAIDASMSLYQFLI AVRQODGGQLTNEAGE 60
Fen1_H.sapiens        MGIQGLAKLIADVAPSAIRENDIKSYFGRKVAIDASMSIYQFLI AVRQ--GGDVLQNEEGE 59
***:** : . : : * . : :* : : : * :

Exo1_S.cerevisiae      PTDKYLQFFIKRFSLLKTFKVEPYLVFDGDAIPVKKSTESKRDRKRKENKAIAERLWACG 110
Exo1_H.sapiens        PTDRYVGFCKM KFNMLLSHGIKPILVFDGCTLP SKKEVERSRRRERQANLLK GKQLLREG 110
Rad27_S.cerevisiae    TTSHLMGMFYRTL RMIDN-GIKPCYVFDGKPPDLK SHELTKRSSRRRVETEKKLA EATT-- 117
Fen1_H.sapiens        TTSHLMGMFYRTIRMMEN-GIKPVYVFDGKPPQLKSGELAKRSERRAEAEKQLQQAQAAG 118
.*. : : : : . : : . : :* **** . * . .* .:* .

Exo1_S.cerevisiae      EKKNAMYDFQKCV DITPEMAKCIICYCKLNGIRYIVAPFEADSQMVYLEQKNIVQGIISE 170
Exo1_H.sapiens        KVSEARECFTRSINITHAMAHKVIKAARSQGV DCLVAPYEADAQLAYLNKAGIVQAIITE 170
Rad27_S.cerevisiae    -ELEKMQERRLVKVSKEHNEEAQKLLGLMGIPYIIAPTEAEAQCAELAKKGKVYAAASE 176
Fen1_H.sapiens        AEQVEVKFTKRLVKVTKQHNDECKHLLSLMGIPYLDAPSEAEASCAALVKAGKVYAAATE 178
: . : : : : . * : : ** ** : : . * : . * . :*

Exo1_S.cerevisiae      DSDLLVFGCRRLITKLN DYGECL EICRDNFIKLPK KFPPLG-SLTNEEIIITMVCLSGCDYT 229
Exo1_H.sapiens        DSDLLAFGCKKVILKMDQFGNGLEIDQA---RLGMCRQLGDVFTEEFKFRYMCILSGCDYL 227
Rad27_S.cerevisiae    DMDTLCYRTP-FLLRH LTFSEAKKEPIHEIDTEL VLRGLD--LTIEQFVDLCIMLGCDYC 233
Fen1_H.sapiens        DMDCLTFGSP-VLMRHLTASEAKKLP IQEFHLSRILQELG--LNQE QFVDLCILLGSDYC 235
* * * : . : : . : : * . : . * : : : * .**

```

Figure 4.1: The Conserved N-terminus of Exonuclease I

N-terminal amino acid sequences from *Saccharomyces cerevisiae* Exo1 and Rad27 and human Exo1 and Fen1 were aligned using ClustalW software (www.ebi.ac.uk/clustalw). Stars, two-dots and one-dot indicate identical residues, conservative and semi-conservative substitutions respectively. The conserved E150 and D173 residues mutated in this study are shaded.

The substitution of glutamate for aspartate at position 150 also causes exonuclease deficiency but in contrast to the D173A mutation, *exo1-E150D* retains approximately 20% of the flap endonuclease activity seen in wild-type Exo1 *in vitro* (Tran *et al.*, 2002). A similar phenotype also results from the equivalent mutation in human Fen1 (Frank *et al.*, 1998) and yeast Rad27 (Negritto *et al.*, 2001). As in the case of the D173A mutant, the binding affinity and structural integrity of *exo1-E150D* are not thought to be affected (Tran *et al.*, 2002).

In addition to the catalytic requirement for Exo1 in various biological processes, there are several lines of evidence that suggest Exo1 may also perform a structural role in mutation avoidance. A homozygous *exo1Δ* mutant exhibits a moderate increase in mutation rate compared to wild-type; however, when diploids heterozygous for certain recessive *pms1* and *mlh1* alleles were assessed, the mutation rate was elevated from wild-type levels in combination with *EXO1* to strongly mutagenic in homozygous *exo1Δ* strains (Amin *et al.*, 2001). The *pms1* and *mlh1* mutations used were situated in the ATP binding and interaction domains of Pms1 and Mlh1 and are thus likely to affect the ability of these two proteins to interact. One possible interpretation of this observation is that Exo1 is required to stabilise the MMR complex in the presence of these otherwise destabilising mutations. A nuclease-independent role for Exo1 is further supported by the demonstration that expression of an allele unable to interact with Mlh1 (*exo1-FF447AA*) results in partially-defective MMR (Tran *et al.*, 2007). Critically, a compound *exo1-D173A-FF447AA* mutant defective for both Mlh1 interaction and nuclease activity displayed a phenotype equivalent to *exo1Δ*, highlighting the requirement for both nuclease dependent and independent functions of Exo1 in MMR.

In the previous chapter, we have shown that decreased resection and reduced hDNA formation occur at the *HIS4* hotspot in *exo1Δ* and *exo1-D173A*. In this chapter we sought to assess whether or not this reduction in hDNA could also account for the crossover deficit observed in *exo1Δ*. Furthermore, we aimed to test whether or not the flap endonuclease activity of Exo1 was required for recombination to occur. In order to do this we carried out genetic experiments designed to characterise the various catalytic and/or structural contributions made by Exo1 in homozygous *exo1-D173A* and *exo1-E150D* strains as compared to *exo1Δ* cells. As described above,

these point mutations result in proteins exhibiting differing levels of nuclease deficiency whilst remaining structurally intact, thereby allowing a more detailed analysis of the role of Exo1 to be carried out.

4.2 Materials and methods

4.2.1 Strain construction

The *E150D* mutation was inserted into the genomic *EXO1* gene using a PCR-based allele replacement method (Erdeniz *et al.*, 1997) from plasmid templates pJM3 (Table 2.2) and transformants were confirmed by DNA sequencing. The *his4-ClaI* allele represents the filling-in of the *ClaI* restriction site located 532 bp from the start codon (resulting in a 2 bp insertion) and was introduced using the two-step allele replacement method (Section 2.2.10.3) following linearisation of pRHB12 by *XbaI*. Correct transformants were identified by their histidine auxotrophy and confirmed by restriction digest following PCR-amplification of *HIS4*. The NatMX4 conferring resistance to nourseothricin was inserted 3,806 bp downstream of *HIS4*, deleting 8 bp, while the HphMX4 cassette conferring resistance to hygromycin B was inserted 5,130 bp upstream of *HIS4*, deleting 7 bp. Both cassettes were introduced using a PCR-based method (Goldstein and McCusker, 1999). The positions and orientations of the drug resistance cassettes were the same as those used by Hoffmann *et al.*, (2005) and Hoffmann and Borts (2005). Successful transformants were confirmed by PCR and linkage analysis. The remaining alleles have been described fully in Section 3.2.1. Full strain genotypes are listed in Table 2.1 and the oligonucleotides used in strain construction are given in Table 2.3.

4.2.2 Tetrad Analysis

Following tetrad dissection, genetic analysis of recombination was carried out upon wild-type (RK358 x RK392), *exo1Δ* (RK359 x RK394) *exo1-D173A* (RK399 x RK425) and *exo1-E150D* (RK409 x RK418) strains using markers on chromosomes III, VII and VIII (Figure 4.2) and analysed as described in Section 2.2.15.7. The results from the separation-of-function mutants were compared to each other, wild-type and *exo1Δ* using the statistical methods outlined in Section 2.2.16. The Dunn Sidak correction was therefore applied for three-way multiple comparisons in order to prevent false rejection of the null-hypothesis and P values less than 0.0169 were considered significant. Over 800 tetrads were dissected for each cross in order to

provide a sufficient number of four-viable spore tetrads with which to assess recombination.

4.2.3 Random Spore Analysis

Random spore analysis was carried out as described in Section 2.2.15.8 and Figure 4.3 using wild-type (RKD62-64, 71-73), *exo1* Δ (RKD65-67, 74-76) and *exo1-D173A* (RKD68-70, 77-79) strains. Strains were examined for the frequency of crossing-over taking place between markers flanking *HIS4* and the association with which gene conversion tract lengths ending between the *bis4-XhoI* and *bis4-ClaI* heteroalleles (96 bp and 532 bp from *HIS4* start codon respectively) and the *bis4-ClaI* and *bis4-BglII* heteroalleles (532 bp and 1,688 bp from the *HIS4* start codon) were associated with crossing-over. The Dunn Sidak correction for two-way/three-way multiple comparisons was applied as appropriate.

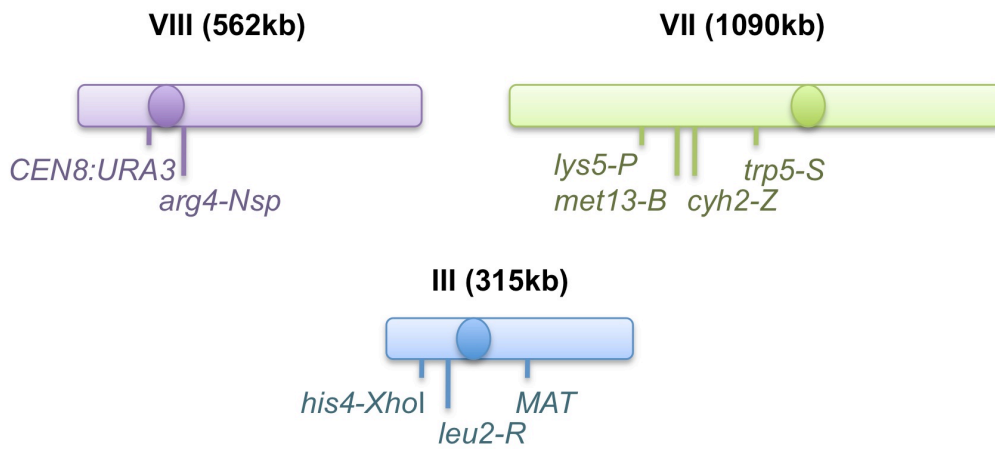


Figure 4.2: Schematic diagram of markers used to assess recombination

Strains were constructed to provide genetically defined intervals on the three chromosomes shown. The chromosome length in kilobases and the approximate position of each marker used is indicated. Drawings are not to scale.

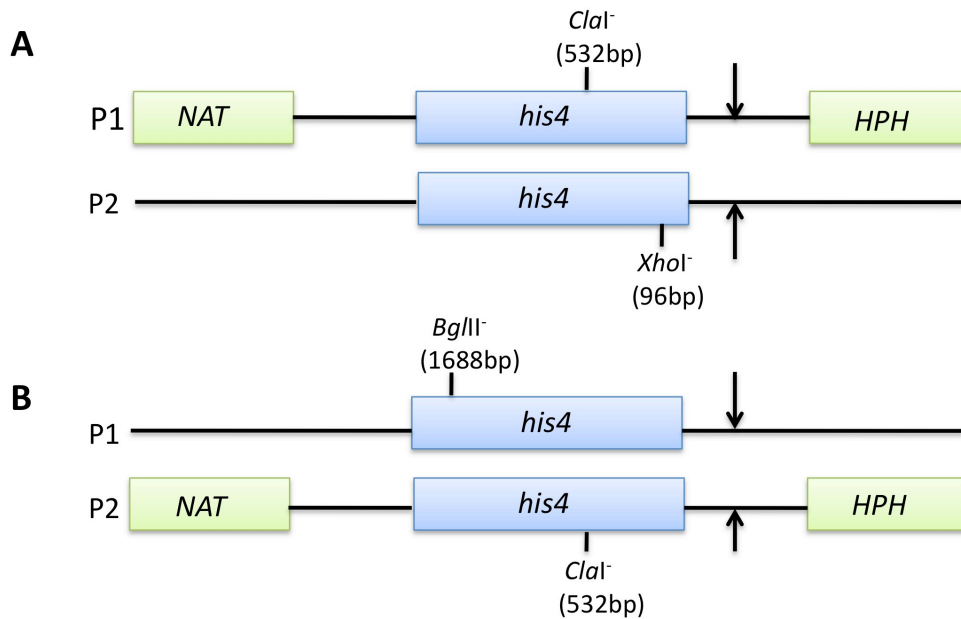


Figure 4.3: Schematic diagram of *HIS4* marker configurations used in random spore analysis

In order to assess recombination associated with the *HIS4* hotspot, two diploids (**A** and **B**) were used containing different pairs of *his4* heteroalleles. The configurations of markers on the two parental chromosomes (P1 and P2) in these diploids are illustrated. The positions of the *his4-XhoI*, *his4-Clal* and *his4-BglII* alleles are given relative to the *HIS4* start codon and the orientations of the flanking nourseothricin (*NAT*) and hygromycin B (*HPH*) drug-resistance cassettes are shown. The *HIS4* hotspot breakpoint is approximately 300 bp upstream of the start codon and is indicated by the arrows.

4.3 Results

4.3.1 Neither the exonuclease nor endonuclease activities of Exo1 are essential for crossing-over

The results of the crossover analysis are presented in Table 4.1. Consistent with previous studies (Khazanehdari and Borts, 2000; Kirkpatrick *et al.*, 2000; Tsubouchi and Ogawa, 2000), *exo1Δ* strains displayed significantly reduced levels of crossing-over in all intervals when compared to wild-type ($p \leq 0.0004$, G-test). Surprisingly, a similar reduction in crossing-over was not observed in the nuclease-deficient *exo1-D173A*. On chromosome VII, crossing-over in all three intervals was maintained at levels equivalent to wild-type ($p \geq 0.03$, G-test) and significantly higher than *exo1Δ* ($p \leq 0.005$, G-test), suggesting that the requirement for Exo1 in crossing-over is a structural one. However, the mechanism by which *exo1-D173A* is able to maintain crossovers may not be as effective at all loci as the map distances measured in intervals on chromosomes III and VIII were intermediate between those observed in wild-type and *exo1Δ*. In the two smaller genetic intervals (*HIS4-LEU2* and *CEN8-ARG4*) this resulted in crossover levels that were not different from either wild-type or *exo1Δ* ($p \geq 0.0947$, G-test), while in the larger *LEU2-MAT* interval, crossing-over was significantly different from both wild-type and *exo1Δ* ($p \leq 0.0136$, G-test).

Crossing-over in *exo1-D173A* and *exo1-E150D* was broadly similar. In five out of the six intervals assessed, crossing-over was decreased in *exo1-E150D* compared to *exo1-D173A* but this was only statistically significant in the *LYS5-MET13* interval ($p = 0.007$, G-test). Only in the *CEN8-ARG4* interval was the observed map distance longer in *exo1-E150D* than in *exo1-D173A* but this difference was not statistically significant ($p = 0.483$, G-test) suggesting that the flap endonuclease activity of Exo1 is not important for crossover production.

4.3.2 Crossover interference in *exo1Δ*

In order to determine whether or not the remaining crossovers that form in *exo1Δ* exhibit crossover interference, two tests were performed. The first of these (referred to as the Malkova method (Malkova *et al.*, 2004)) asks whether the presence of a crossover in one interval reduces the chance that crossing-over will occur in an adjacent interval. For each interval of interest, tetrads were divided into two groups: those in which crossing-over had occurred (tetratypes and nonparental ditypes) and

Table 4.1: Map distances in the separation-of-function mutants

Genotype	Interval											
	<i>HIS4-LEU2</i>				<i>LEU2-MAT</i>				<i>CEN8-ARG4</i>			
	P	NPD	TT	cM ¹	PD	NPD	TT	cM	PD	NPD	TT	cM
Wild-type	449	1	183	14.9 [†]	442	32	425	34.3 [†]	696	2	185	11.2 [†]
<i>exo1Δ</i>	540	1	126	9.9 [*]	622	7	244	16.4 [*]	739	1	119	7.3 [*]
<i>exo1-D173A</i>	206	1	59	12.2	172	3	140	25.1 [†]	248	1	52	9.6
<i>exo1-E150D</i>	245	0	44	7.6 [*]	194	4	128	23.3 [†]	259	0	68	10.4 [†]

¹PD, NPD and TT represent parental ditypes, nonparental ditypes and tetratypes respectively. cM values were calculated according to the formula of (Perkins, 1949). Distributions between tetrad classes were compared using the G-test of homogeneity and statistically significant ($p < 0.0169$) differences are indicated as follows: ^{*} significantly different from wild-type, [†] significantly different from *exo1Δ*.

Table 4.1: (continued)

Genotype	Interval											
	<i>LYS5-MET13</i>				<i>MET13-CYH2</i>				<i>CYH2-TRP5</i>			
	PD ¹	NPD	TT	cM ¹	PD	NPD	TT	cM	PD	NPD	TT	cM
Wild-type	555	8	349	21.8 [†]	738	0	179	9.8 [†]	331	35	557	41.5 [†]
<i>exo1Δ</i>	680	2	186	11.4 [*]	774	0	99	5.7 [*]	539	11	328	22.4 [*]
<i>exo1-D173A</i>	169	5	131	26.4 [†]	257	2	51	10.2 [†]	114	10	189	39.8 [†]
<i>exo1-E150D</i>	206	0	123	18.7 [†]	286	0	45	6.8	138	9	190	36.2 [†]

¹PD, NPD and TT represent parental ditypes, nonparental ditypes and tetratypes respectively. cM values were calculated according to the formula of (Perkins, 1949). Distributions between tetrad classes were compared using the G-test of homogeneity and statistically significant ($p < 0.0169$) differences are indicated as follows: * significantly different from wild-type, [†] significantly different from *exo1Δ*.

those lacking a crossover (parental ditypes). Linkage analysis was then performed on both groups in order to determine the effect that crossing-over had upon recombination in other intervals on the same chromosome. The results of this analysis are presented in Table 4.2. In the wild-type, clear evidence of positive crossover interference was obtained. For example, when a crossover had occurred in the *LYS5-MET13* interval, the map distance in the adjacent *MET13-CYH2* interval was 5.4 cM. This contrasts with the 12.6 cM observed when tetrads were non-recombinant at *LYS5-MET13*. However, similar results were not observed in *exo1Δ*. In no pair of intervals was significant interference detected. While this could be due to an insufficient numbers of tetrads being examined rather than a loss of interference *per se*, it is notable that the map distance ratios calculated remain close to 1 in the intervals along chromosome VII, indicative of a loss of crossover interference.

Curiously, when a second method used to assess interference was applied to the datasets, evidence for positive crossover interference in *exo1Δ* was obtained. The nonparental ditype ratio represents the difference between the observed number of nonparental ditypes (representing double crossovers involving all four chromatids) and the number of nonparental ditypes expected to occur in the absence of interference (based upon the number of single crossovers present in the same interval). The expected frequency of NPDs was calculated using the “better way” proposed by Stahl (2008) and the results are presented in Table 4.3. In all intervals assessed, wild-type and *exo1Δ* strains displayed similar NPD ratios indicating that the strength of interference is unchanged. While a greater number of intervals demonstrated statistically significant levels of interference in the wild-type strain, the lack of significance in *exo1Δ* is likely to be due to the fact that overall numbers of crossovers are reduced, resulting in very low levels of expected NPDs. Supporting this idea is the finding that when the *LYS5-MET13* and *MET13-CYH2* intervals are considered separately, statistical significance is not achieved. However, if *LYS5-CYH2* is treated as a single larger interval, the difference between the number of NPDs observed and expected is highly statistically significant ($p=0.0073$). This suggests that crossover interference is maintained in *exo1Δ*.

Although these two approaches initially appear to yield contradictory results, a potentially reconciliatory explanation is that while interference remains active in *exo1Δ*,

Table 4.2: Interference as measured by the Malkova method

Reference interval:		<i>LYS5-MET13</i>		<i>MET13-CYH2</i>		<i>CYH2-TRP5</i>	
Test interval:		<i>MET13-CYH2</i>	<i>CYH2-TRP5</i>	<i>LYS5-MET13</i>	<i>CYH2-TRP5</i>	<i>LYS5-MET13</i>	<i>MET13-CYH2</i>
Wild-type	PD	415 : 0 : 140	188 : 20 : 343	415 : 7 : 312	244 : 31 : 462	193 : 5 : 134	247 : 0 : 85
	cM	12.6	42	24.1	44	24.7	12.8
	TT + NPD	323 : 0 : 39	141 : 15 : 213	140 : 1 : 37	86 : 4 : 94	362 : 3 : 214	491 : 0 : 94
	cM	5.4	41.1	12.1	32.1	20	8
	p	2E-07	0.39	1E-07	0.002	0.17	0.0025
	Significant?	yes	no	yes	yes	no	yes
	Ratio	0.43	0.98	0.5	0.73	0.81	0.63
Reference interval:		<i>LYS5-MET13</i>		<i>MET13-CYH2</i>		<i>CYH2-TRP5</i>	
Test interval:		<i>MET13-CYH2</i>	<i>CYH2-TRP5</i>	<i>LYS5-MET13</i>	<i>CYH2-TRP5</i>	<i>LYS5-MET13</i>	<i>MET13-CYH2</i>
<i>exo1Δ</i>	PD	600 : 0 : 83	423 : 10 : 253	597 : 1 : 172	476 : 10 : 293	421 : 2 : 112	475 : 0 : 63
	cM	6.1	22.8	11.6	22.7	11.6	5.9
	TT + NPD	173 : 0 : 16	115 : 1 : 75	83 : 1 : 14	63 : 1 : 35	258 : 0 : 74	298 : 0 : 36
	cM	4.2	21.2	10.2	20.7	11.1	5.4
	p	0.35	0.46	0.7	0.88	0.34	0.91
	Significant?	no	no	no	no	no	no
	Ratio	0.69	0.93	0.88	0.91	0.95	0.92

Interference analysis was carried out as described in Malkova *et al.* (2004) and Martini *et al.* (2006). For each genetic interval shown in bold, the tetrad data presented in Table 4.1 was divided into two groups depending upon whether a recombination event had (TT + NPD) or had not (PD) occurred. The map distance in adjacent intervals was then calculated for each group as described previously. Distributions between tetrad classes were analysed by G-test and $p < 0.05$ taken as evidence of significant interference. The ratio between the two map distances is given as an indication of the strength of interference, with smaller ratios indicating stronger interference.

Table 4.2: (continued)

	Reference interval:	<i>HIS4-LEU2</i>	<i>LEU2-MAT</i>
	Test interval:	<i>LEU2-MAT</i>	<i>HIS4-LEU2</i>
wild-type	PD	272 : 23 : 305	199 : 1 : 104
	cM	36.9	18.1
	TT + NPD	170 : 9 : 120	250 : 0 : 79
	cM	29.1	12
	p	0.005	0.008
	Significant?	yes	yes
	Ratio	0.79	0.66
		Reference interval:	<i>HIS4-LEU2</i>
	Test interval:	<i>LEU2-MAT</i>	<i>HIS4-LEU2</i>
exo1Δ	PD	451 : 6 : 195	371 : 0 : 97
	cM	17.7	10.4
	TT + NPD	168 : 1 : 48	169 : 1 : 29
	cM	12.4	8.8
	p	0.06	0.05
	Significant?	no	no
	Ratio	0.7	0.84

Interference analysis was carried out as described in Malkova *et al.* (2004) and Martini *et al.* (2006). For each genetic interval shown in bold, the tetrad data presented in Table 4.1 was divided into two groups depending upon whether a recombination event had (TT + NPD) or had not (PD) occurred. The map distance in adjacent intervals was then calculated for each group as described previously. Distributions between tetrad classes were analysed by G-test and $p < 0.05$ taken as evidence of significant interference. The ratio between the two map distances is given as an indication of the strength of interference, with smaller ratios indicating stronger interference.

Table 4.3: Interference as measured by nonparental ditype ratio

		<i>HIS4-LEU2</i>	<i>LEU2-MAT</i>	<i>LYS5-MET13</i>	<i>MET13-CYH2</i>	<i>LYS5-CYH2</i>	<i>CYH2-TRP5</i>	<i>CEN8-ARG4</i>
Wild-type	NPD ratio	0.141*	0.863	0.406**	0*	0.376**	0.567**	0.381
	(obs/exp)	(1/7.1)	(32/37.1)	(8/19.7)	(0/4.5)	(15/39.9)	(35/61.7)	(2/5.3)
<i>exo1Δ</i>	NPD ratio	0.313	0.693	0.370	0	0.268**	0.585*	0.455
	(obs/exp)	(1/3.2)	(7/10.1)	(2/5.4)	(0/1.4)	(3/11.2)	(11/18.8)	(1/2.2)

The expected number of nonparental ditypes and NPD ratios (observed/expected) were calculated from tetrad data according to (Stahl, 2008) using the Stahl Laboratory Online Tools (<http://molbio.uoregon.edu/~fstahl/>). A ratio of less than 1 indicates positive crossover interference. The statistical significance of the ratio was determined using the Vassarstats Chi Square to P calculator (<http://faculty.vassar.edu/lowry/tabs.html#csq>) and significance thresholds are indicated as follows: * $p < 0.05$, ** $p < 0.01$.

it is weakened or operates over a shorter distance such that it is unable to influence crossing-over in adjacent intervals.

4.3.3 Increased random spore death occurs in the presence of nuclease-deficient *EXO1*

Crossing-over is necessary to ensure chromosome disjunction at the first meiotic division. Therefore, reduced crossing-over often correlates with an increase in the two and zero-viable spore tetrad classes at the expense of four-viable spore tetrads (see Section 1.1 and Figure 1.2). This has been previously observed in *exo1Δ* and is replicated in this study ($p=2 \times 10^{-190}$, G-test). In point of fact, increased meiosis I non-disjunction was observed in *exo1Δ* relative to the previous study carried out in the SK1 background by Tsubouchi *et al.* (2000). This was subsequently shown to be due to the reduced sporulation temperature employed in this work (23°C compared to 30°C, see Chapter 5 for data and discussion). Spore viability data is presented in tabular form in Table 4.4 and graphically in Figure 4.4.

As crossover levels were seen to be considerably higher in *exo1-D173A* and *exo1-E150D* than in *exo1Δ*, it was expected that spore viability would also be improved in these mutants relative to *exo1Δ*. However, although a significant improvement in overall spore viability was observed ($p \leq 0.012$, G-test), this rescue was not as great as suggested by the crossover analysis and the spores of both strains remained considerably less viable than wild-type ($p \leq 2 \times 10^{-215}$, G-test). Close examination of the distributions of tetrad classes seen in *exo1-D173A* and *exo1-E150D* revealed an increase in the three and one-viable-spore tetrad classes but decreases in the four and zero-viable spore classes when compared to *exo1Δ* ($p \leq 7 \times 10^{-13}$, G-test). This viability pattern is consistent with decreased meiosis I non-disjunction but increased random spore death.

To verify whether or not lower levels of meiosis I non-disjunction were indeed occurring in the nuclease-deficient alleles, the two-viable-spore tetrad class was analysed in more detail. As described in Section 1.1 and shown in Figure 1.2, the two-viable-spores that result from a non-disjunction event should share the same genotype for any centromere-linked marker. Furthermore, instances of disomy for chromosome III result in non-mating spores. When the centromeric *CEN8:URA3*

Table 4.4: Distribution of viable spores per tetrad class and overall viability of the separation-of-function mutants

Genotype		Viable spores per tetrad class					Total tetrads	% overall spore viability ¹
		4	3	2	1	0		
Wild-type	<i>n</i>	941	54	41	2	8	1046	95.8 [†]
	(%)	(89.9)	(5.2)	(3.9)	(0.2)	(0.8)		
<i>exo1Δ</i>	<i>n</i>	885	231	472	136	476	2200	60.4 [*]
	(%)	(40.2)	(10.5)	(21.5)	(6.2)	(21.6)		
<i>exo1-D173A</i>	<i>n</i>	319	198	199	66	49	831	70.2 ^{*†}
	(%)	(38.3)	(23.8)	(23.9)	(7.9)	(5.9)		
<i>exo1-E150D</i>	<i>n</i>	341	186	236	78	144	985	62.7 ^{*†}
	(%)	(34.6)	(18.9)	(24.0)	(7.9)	(14.6)		

¹ Calculated as ((4 x no. 4-spore tetrads) + (3 x no. 3-spore tetrads) + (2 x no. 2-spore tetrads) + no. 1-spore tetrads)/(4 x total number of tetrads) x100. Distributions between spore classes were compared using the G-test of homogeneity and statistically significant (p<0.0169) differences are indicated as follows: * significantly different from wild-type, [†] significantly different from *exo1Δ*.

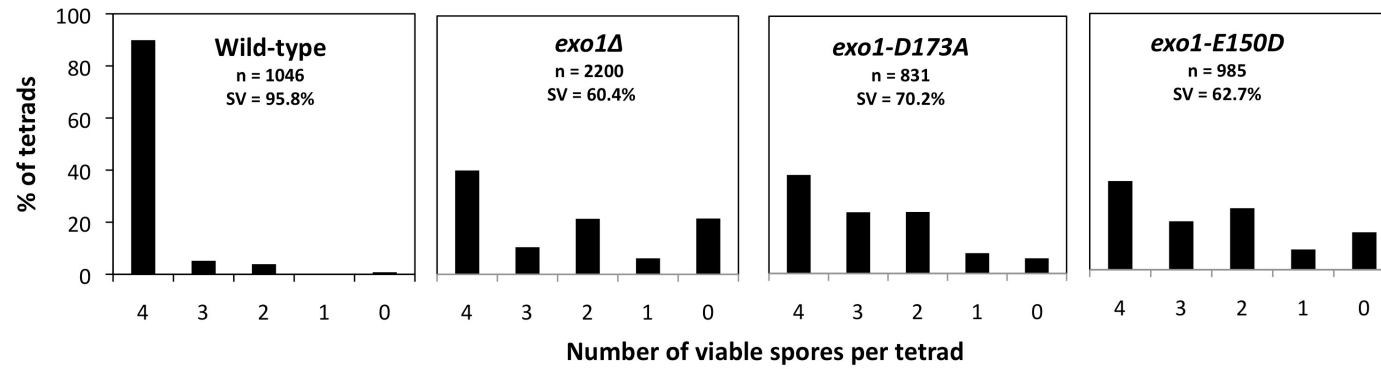


Figure 4.4: Distributions of viable spores in separation of function mutants

The data provided in Table 4.4 is presented graphically. The number of tetrads dissected and the overall spore viability are given.

allele was used to estimate the incidence of disomy (Table 4.5), *exo1Δ* displayed an 8-fold increase in non-disjunction compared to wild-type ($p=1 \times 10^{-35}$, G-test). This was reduced by over half in the *exo1-E150D* mutant ($p=7 \times 10^{-12}$, G-test) whilst *exo1-D173A* did not exhibit an excess of sister spores compared to non-sisters, perhaps suggesting that non-disjunction did not occur in this strain. However, when rates of chromosome III disomy were analysed (Table 4.6), elevated non-disjunction was apparent in *exo1-D173A* when compared to wild-type ($p<0.005$, G-test), albeit at lower levels than were observed in *exo1Δ* ($p<0.001$, G-test).

In summary, the increased levels of crossing-over seen in the nuclease-deficient mutants appear to promote more accurate chromosome disjunction at the first meiotic division. Interestingly, the *exo1-D173A* mutant displays a phenotype consistent with low levels of genome-wide non-disjunction but elevated levels of chromosome III disomy, matching well with the results of the crossover analysis that suggested crossing-over was less efficient on chromosome III. Despite decreased non-disjunction however, overall spore viability remains relatively low due to increased levels of seemingly random spore death occurring in *exo1-D173A* and *exo1-E150D*.

4.3.4 Wild-type levels of non-Mendelian segregation at *HIS4* are dependent upon the exonucleolytic activity of *EXO1*

As described in Chapter 3, reduced gene conversion of alleles downstream of the *HIS4* hotspot occurs in both *exo1Δ* and *exo1-D173A*. When the frequency of gene conversion occurring at *bis4-XhoI* (approximately 400 bp from the *HIS4* recombination initiation site) was assessed in *exo1-E150D*, an equivalent amount of NMS to that seen in *exo1-D173A* was observed ($p=0.26$, G-test). *In vitro*, Exo1-E150D was shown to maintain approximately 20% of the flap endonuclease activity associated with Exo1 (Tran *et al.*, 2002). Therefore, the lack of an improvement in NMS in *exo1-E150D* compared to *exo1-D173A* suggests either that the 20% of flap endonuclease remaining is insufficient to have any effect or that NMS is dependent upon the exonuclease activity of Exo1. In both point mutants, the rates of NMS were significantly lower than both wild-type and *exo1Δ* (Table 4.7; $p<0.002$, G-test). Possible reasons for this were explored in Chapter 3. While NMS was significantly reduced in *exo1Δ* at both *leu2-R* and *arg4-nsp* compared to wild-type, there was no

Table 4.5: Rates of meiosis I non-disjunction in the separation-of-function mutants

Genotype	Number of sister spores ¹	Number of non-sister spores ¹	Total tetrads	% Non-disjunction ²
Wild-type	<i>30</i>	<i>11</i>	1046	1.8 [†]
<i>exo1Δ</i>	<i>394</i>	<i>78</i>	2200	14.4 [*]
<i>exo1-D173A</i>	99	100	832	0 [†]
<i>exo1-E150D</i>	<i>149</i>	<i>87</i>	985	6.3 ^{*†}

¹ Two-viable-spore tetrads were categorised as sisters (same uracil phenotype) or non-sisters (different uracil phenotype) based upon the segregation of the centromere-linked *CEN8:URA3* marker. Emboldened italics indicate distributions of sister to non-sister spores that are significantly different ($p < 0.05$) from a 50:50 distribution as determined by χ^2 test. ² Non-disjunction was calculated as: ((number of sister spores - number of non-sister spores)/total tetrads) x100. Comparisons were made using the G-test of homogeneity and statistically significant ($p < 0.0169$) differences are indicated as follows: * significantly different from wild-type, [†] significantly different from *exo1Δ*.

Table 4.6: Rate of chromosome III non-disjunction at meiosis I in the separation-of-function mutants

Genotype	Number of non-maters ¹	Total tetrads	% Non-disjunction ²
Wild-type	1	1046	0.1 [†]
<i>exo1Δ</i>	61	2200	2.8 [*]
<i>exo1-D173A</i>	8	832	1.0 [†]
<i>exo1-E150D</i>	18	985	1.8 [*]

¹ The number of two-viable-spore tetrads containing two non-mating spores (indicative of chromosome III non-disjunction). ² Non-disjunction was calculated as: (number of non-maters/total number of tetrads) x100. Comparisons were made using the G-test of homogeneity and statistically significant ($p < 0.0169$) differences are indicated as follows: * significantly different from wild-type, [†] significantly different from *exo1Δ*.

Table 4.7: Non-Mendelian Segregation of 9 Alleles

Genotype		Allele								
		<i>bis4-XhoI</i>	<i>leu2-R</i>	<i>MAT</i>	<i>lys5-P</i>	<i>met13-B</i>	<i>cyb2-Z</i>	<i>trp5-S</i>	<i>CEN8:URA3</i>	<i>arg4-Nsp</i>
Wild-type	%NMS ¹	29.2 [†]	3.6 [†]	0.9	1.4	1.8	0.7	1.3	0	6.1 [†]
	(NMS/total tetrads)	(275/941)	(34/941)	(8/941)	(13/941)	(17/941)	(7/941)	(12/941)	(0/941)	(58/941)
<i>exo1Δ</i>	%NMS	23.6*	1.1*	0.2	0.9	1.0	0.5	0.3	0	2.9*
	(NMS/total tetrads)	(209/885)	(10/885)	(2/885)	(8/885)	(9/885)	(4/885)	(3/885)	(0/885)	(26/885)
<i>exo1-D173A</i>	%NMS	15.4 ^{††}	1.3	0	1.9	2.5	0.3	1.6	0	5.6
	(NMS/total tetrads)	(49/319)	(4/319)	(0/319)	(6/319)	(8/319)	(1/319)	(5/319)	(0/319)	(18/319)
<i>exo1-E150D</i>	%NMS	12.3 [†]	2.9	1.5	0.6	2.9	0	1.1	0.3	3.8
	(NMS/total tetrads)	(42/341)	(10/341)	(5/341)	(2/341)	(10/341)	(0/341)	(4/341)	(1/341)	(13/341)

¹Non-Mendelian segregation includes gene conversion and post-meiotic segregation events. Tetrads exhibiting ≥ 3 NMS events per tetrad were scored as false tetrads and excluded from further analysis. %NMS was calculated as: (number of NMS events/total number of tetrads) x 100. Comparisons were made using the G-test of homogeneity and statistically significant ($p < 0.0169$) differences are indicated as follows: * significantly different from wild-type, [†] significantly different from *exo1Δ*.

significant difference at any remaining allele in *exo1-D173A* or *exo1-E150D*, perhaps due to the numbers of tetrads assessed.

4.3.5 Crossing-over at the *HIS4* hotspot mirrors other intervals on chromosome III

The tetrad analysis described above demonstrated that at many breaks, the presence of a non-catalytically active version of Exo1 is sufficient to enable crossovers to form as normal. However, the intermediate crossover frequency observed at some intervals suggested that this was not the case at all breaks and that at some loci, the nuclease activity of Exo1 was required for a proportion of crossovers. This raised the possibility that two classes of breaks were occurring. As the resection and hDNA analysis (Chapter 3) was only carried out at the *HIS4* hotspot, it remains possible that *HIS4* represents a nuclease-requiring locus in which crossing-over is influenced by hDNA tract length alone. For this reason, it was of interest to ascertain whether or not crossovers associated with breaks at *HIS4* exclusively were reduced when *exo1-D173A* was expressed. It was not possible to determine this from the tetrad analysis as markers closely flanking the break site were not used. Therefore, an alternative strategy was employed. In this approach, strains containing drug resistance cassettes flanking the *HIS4* hotspot were sporulated (Figure 4.3). Following meiosis, 600 spores were chosen at random and the configuration of the *HIS4* flanking markers determined in order to estimate the frequency with which a crossover had taken place between them.

The amount of crossing-over in *exo1Δ* was reduced compared to wild-type as expected (Table 4.8; $p=0.03$, G-test); however, this difference was not statistically significant after the Dunn-Sidak correction to the significance threshold was imposed (for two-way multiple comparisons, P values less than 0.0253 were considered to be significant). The recombination frequency observed in *exo1-D173A* was intermediate between wild-type and *exo1Δ* consistent with the results obtained in the *HIS4-LEU2* and *LEU2-MAT* intervals by tetrad analysis. This implies that both the catalytic and structural functions of Exo1 are required for normal levels of crossing-over at the *HIS4* hotspot. However, a larger number of spores would be required to confirm this result.

Table 4.8: Crossing-over between flanking markers at the *HIS4* hotspot

Genotype	Configuration of <i>NAT/HPH</i> markers ¹		Recombination Frequency ²
	Parental	Recombinant	
Wild-type	549	51	8.5
<i>exo1</i> Δ	568	32	5.3
<i>exo1-D173A</i>	558	42	7

¹ For each genotype, a total of 600 colonies growing on the non-selective (histidine-containing) medium were patched out, tested for their ability to grow on media containing either nourseothricin or hygromycin and classified as either parental (same configuration of *NAT/HPH* markers as a parental strain) or recombinant (different configuration of *NAT/HPH* markers to either parental strain). Data was pooled from 6 independent cultures for each genotype. ² Recombination frequencies were calculated as: (number of recombinants/total number of colonies tested) x 100.

4.3.6 The nuclease-independent function of Exo1 increases the association of short hDNA tracts with crossing-over

In order to further investigate the apparent non-relatedness between gene conversion and crossing-over, the random spore approach was also used to assess the association between the two. The assay devised was similar to that employed by Martini *et al.* (2006) to demonstrate the existence of crossover homeostasis at the *ARG4* hotspot. While diploids heterozygous for the *bis4-XhoI*, *bis4-ClaI* or *bis4-BglII* alleles (Figure 4.3) are unable to grow on histidine-lacking medium, meiotic recombination can produce a functional *HIS4* gene when hDNA terminates between the two alleles (Figure 4.5). These events were selected for by growth on medium lacking histidine and the genotypes of the flanking markers determined by replica plating to media containing nourseothricin or hygromycin B. The configuration of these flanking markers thus revealed whether or not a crossover had occurred. As conversion of the DSB-proximal allele to wild-type was the most common source of His⁺ spores, prototrophs generally resulted from breaks occurring on the chromosome mutant for the DSB-proximal allele. This was reflected in the linkage of the flanking markers (*eg*: the majority of His⁺ non-crossovers arising from the *bis4-XhoI/bis4-ClaI* heteroalleles were sensitive to nourseothricin and hygromycin B as the *bis4-XhoI* chromosome did not contain either drug resistance cassette). The data presented in Table 4.9 is consistent with this mechanism.

As the tetrad analysis of the *exo1-D173A* strain had shown lower than wild-type levels of gene conversion without an equivalent decrease in crossing-over, it was predicted that crossover association in *exo1-D173A* spores would be higher than in wild-type. In agreement with this, a significant increase in crossovers was observed when both the *bis4-XhoI/bis4-ClaI* heteroalleles (selecting for 'short' hDNA tracts) and *bis4-ClaI/bis4-BglII* heteroalleles (selecting for 'long' hDNA tracts) were used ($p \leq 0.002$, G-test). Furthermore, a significant increase in crossover association was observed in *exo1-D173A* compared to *exo1Δ* when 'short' hDNAs were selected for ($p = 5 \times 10^{-9}$, G-test). This suggests that the non-catalytic function of Exo1 is important for ensuring 'short' hDNA tracts undergo crossing-over at *HIS4*. Surprisingly, when 'long' hDNA tracts were selected for, no such reduction in association was observed in the *exo1Δ* strain ($p = 0.81$, G-test), arguing that longer hDNA tracts are resolved into crossovers via an Exo1-independent mechanism.

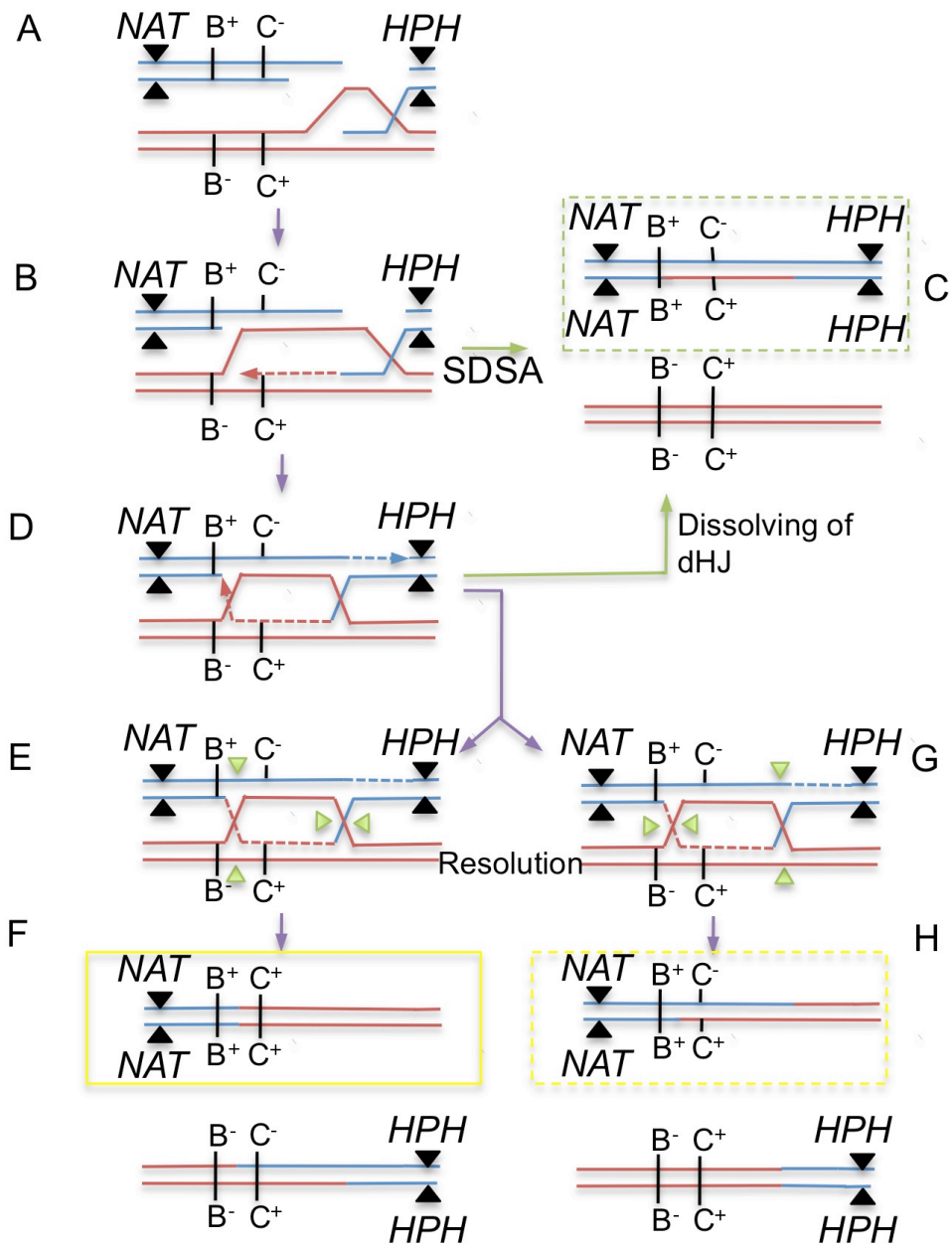


Figure 4.5: An example illustrating prototroph formation between heteroalleles

In this example, a *bis4-ClaI/bis4-BglII* heteroallelic cross is presented. Cassettes conferring resistance to nourseothricin and hygromycin B are inserted on the *bis4-ClaI* chromosome. **(A)** In such crosses, prototrophs most commonly arise when DSBs occur on the chromosome containing the mutant allele situated closest to the break site (in this case, *bis4-ClaI*). **(B)** Following strand invasion, DNA synthesis then takes place using the *bis4-BglII* strand as a template. If this synthesis terminates between the *bis4-ClaI* and *bis4-BglII* sites, a *HIS4* strand is produced. **(C)** If the invading strand is then displaced to form a non-crossover, a His⁺ spore may result depending upon the direction of mismatch repair. This spore will be both Nat^R and Hyg^R. **(D)** Alternatively, if the break is to be repaired as a crossover, a dHJ intermediate will be produced. **(E)** Resolution of this dHJ in one orientation (indicated by green triangles) will yield a His⁺ spore **(F)**. **(G)** Resolution in the alternative orientation may also produce a His⁺ spore **(H)**, depending upon the directionality of mismatch repair. In both cases, the His⁺ spore will be Nat^R Hyg^S. Boxes indicate potential sources of His⁺ spores.

Table 4.9: Association of prototroph formation with crossing-over at *HIS4*

Heteroalleles	Genotype	Parental ¹		Recombinant ¹		Total	% Crossover associated ²
		<i>Nat</i> ^R <i>Hpb</i> ^R	<i>Nat</i> ^S <i>Hpb</i> ^S	<i>Nat</i> ^R <i>Hpb</i> ^S	<i>Nat</i> ^S <i>Hpb</i> ^R		
<i>XhoI/ClaI</i>	Wild-type	34	308	32	226	600	43
	<i>exo1Δ</i>	43	320	34	203	600	39.5
	<i>exo1-D173A</i>	17	245	22	316	600	56.3 [†]
<i>ClaI/BglII</i>	Wild-type	123	24	447	5	599	75.5 [†]
	<i>exo1Δ</i>	78	15	503	4	600	84.5 [*]
	<i>exo1-D173A</i>	83	13	501	3	600	84 [*]

¹ For each genotype tested, approximately 600 colonies from the prototroph-selecting (histidine-lacking) medium were patched out and tested for their ability to grow on media containing either nourseothricin or hygromycin to determine the configuration of the drug-resistance genes. For each genotype, data from 3 independent cultures were pooled. ² Crossover association was calculated as: (number of recombinants/total number of colonies tested) x 100. For both sets of heteroalleles, the proportions of recombinant and parental spores were compared using the G-test of homogeneity and statistically significant ($p \leq 0.0169$ for 3-way multiple comparisons) differences are indicated as follows: * significantly different from wild-type and [†]significantly different from *exo1Δ*. All genotypes displayed a significant increase in crossover association when the *ClaI/BglII* heteroalleles were used compared to the *XhoI/ClaI* heteroalleles.

4.3.7 Longer hDNA tracts are preferentially associated with crossovers

In all three genotypes, longer hDNA tracts were significantly more likely to be associated with a crossover than shorter hDNA tracts ($p \leq 2 \times 10^{-26}$, G-test). It has been suggested that the likelihood of a mismatch being repaired to yield a conversion rather than undergoing restoration-type repair decreases with increasing distance from the DSB (Nicolas and Petes, 1994; Kirkpatrick *et al.*, 1998). Therefore, the possibility that such a conversion bias could account for the observed change in association was considered. As demonstrated in Figure 4.3, if the DSB proximal allele does not undergo gene conversion, a His⁺ spore may still be obtained by crossing-over if the resolution point of the dHJ is situated between the two heteroalleles. However, non-crossovers would not be detectable. The *bis4-ClaI* allele is situated further away from the DSB site than *bis4-XhoI*, meaning that an increased proportion of *bis4-ClaI* alleles incorporated into hDNA may undergo restoration-type repair compared to *bis4-XhoI*. This could thus result in an apparent increase in the association of His⁺ spores with crossing-over when the *bis4-ClaI/bis4-BglII* heteroalleles were used compared to the *bis4-XhoI/bis4-ClaI* heteroalleles. However, the assessment of the *HIS4* gene conversion gradient in Chapter 3 demonstrates that significant amounts of gene conversion occur at the even more distally located *bis4-BglII* allele in the wild-type strain. Indeed, if the amount of NMS measured at *bis4-XhoI* and *bis4-BglII* are plotted on a graph (Figure 3.5), the line of best fit drawn between them predicts that 24.3% NMS would occur at *bis4-ClaI*. This is 16.8% lower than the 29.2% observed at *bis4-XhoI* ($100 - (24.3/29.2 \times 100)$). If we assume that 16.8% fewer non-crossovers would be detectable in the *bis4-ClaI/bis4-BglII* diploid, this would reduce the percentage of non-crossover His⁺ spores detected from 57% to 47.4% ($57 - (0.57 \times 16.8)$), resulting in an apparent crossover association of 52.6% in the *bis4-XhoI/bis4-ClaI* strain ($100 - 47.4$). Nevertheless, 52.6% remains significantly lower than the 75.5% observed ($p = 1 \times 10^{-16}$, G-test) suggesting that longer hDNA tracts either influence or reflect whether a break is repaired to yield a crossover or non-crossover. This is consistent with a number of previous inferences from studies in yeast, mice and humans (Jeffreys and May, 2004; Guillon *et al.*, 2005; Terasawa *et al.*, 2007; Chen *et al.*, 2008; Mancera *et al.*, 2008). The correlation between hDNA tract length and crossover propensity was observed in all three strains tested arguing that the underlying mechanism responsible is independent of *EXO1*.

4.4 Discussion

4.4.1 Resection may influence crossing-over in a locus-dependent manner

In Chapter 3, it was demonstrated that the nuclease activity of Exo1 is essential for normal strand resection and hDNA formation following the creation of DSBs at the *HIS4* hotspot. However, the genetic analysis presented in this chapter reveals that despite these defects, crossing-over in the presence of the nuclease-deficient *exo1* alleles is maintained at levels either equivalent to wild-type or intermediate between wild-type and *exo1Δ* depending upon the locus of interest. This argues that resection length is not a major factor determining the propensity for crossing-over. Importantly, this finding contradicts a number of earlier models (presented in 1.5.2.2) proposed to account for the crossover deficit observed in *exo1Δ*. In these models, it was suggested that shorter resection tracts would produce less stable strand invasions and consequently, fewer crossovers.

However, the finding that *exo1-D173A* crossover levels are intermediate between wild-type and *exo1Δ* in some intervals (such as those assessed on chromosomes III and VIII) argues that at some loci, the nuclease activity of Exo1 *is* necessary for a sub-class of crossovers to occur. The *HIS4* hotspot appears to belong to this class of breaks. The reason for a locus-specific requirement for the nucleolytic function of Exo1 is unclear; perhaps in some regions of the genome, more extensive resection is essential to guarantee stable strand invasion. Alternatively, some loci may be more prone to unwinding of crossover-designated intermediates than others, an activity which could be exacerbated by the shorter hDNA tracts seen in the absence of the nuclease activity of Exo1.

Although only a few intervals were tested and thus reliable conclusions cannot be drawn, it is perhaps interesting to note that in this study, the crossover and non-disjunction phenotypes observed in *exo1-D173A* appear to correlate well with chromosome size. Specifically, on the larger chromosome VII, wild-type crossover frequencies were detected compared to the intermediate levels produced on the smaller chromosomes III and VIII. Additionally, non-disjunction in *exo1-D173A* was lower in comparison to *exo1Δ* when assessed genome-wide than when instances of chromosome III non-disjunction alone were considered. Whilst it remains possible that resection on chromosome VII is less dependent on Exo1, other

differences could also be responsible. For example, if crossover designation results from the build-up of stress along the chromosome axis (Kleckner *et al.*, 2004), the stronger crossover interference in operation along larger chromosomes (Chen *et al.*, 2008) could perhaps better constrain instability-prone intermediates to the crossover pathway. However, testing of this hypothesis would require a genome-wide approach to measuring recombination.

4.4.2 A structural role for Exo1 in crossover promotion

The increased levels of crossing-over observed in the nuclease-deficient mutants when compared to *exo1* Δ (despite equivalent or greater defects in resection and hDNA formation) argue that relatively short resection tracts remain largely proficient for strand invasion at most loci. Similar observations have been made previously at mitotic DSBs (Mimitou and Symington, 2008; Zhu *et al.*, 2008). Furthermore, it can be argued that dHJ formation is also largely unaffected by the reduction in nucleolytic processing. In light of this and the finding that the non-catalytic function of Exo1 appears to be most important when short hDNA tracts have occurred, it is possible that Exo1 is required to stabilise either the strand invasion structure or the dHJ intermediate, allowing it to be resolved as a crossover.

As described in Section 4.1, a nuclease-independent role for Exo1 has previously been shown to be important during mitotic DNA mismatch-repair (MMR). In MMR, this nuclease-independent function requires Exo1 to physically interact with Mlh1 (Tran *et al.*, 2007). A five amino acid motif R/S-S-K-(Y/F)-F known as the Mlh1 interacting protein (MIP) box in Exo1 (also found in Ntg2 and Sgs1) mediates this interaction by binding a conserved S2 binding motif in Mlh1 (Tran *et al.*, 2007; Dherin *et al.*, 2009). This non-catalytic role was hypothesised to be important for the stabilisation of Mlh1 and Pms1, supporting the formation of a larger multi-protein complex involved in MMR (Amin *et al.*, 2001). It is therefore tempting to speculate that Exo1 may behave similarly during meiosis by supporting the formation/function of the Mlh1/Mlh3 complex. Such a function for Exo1 fits well with observations from *Exo1*^{-/-} mice in which synapsis occurs normally but chiasmata are not maintained (Kan *et al.*, 2008). However, in the Y55 strain background, a MIP box mutant *exo1-S445A F447A F448A* that is defective in Mlh1 binding was found to exhibit an entirely wild-type meiotic phenotype (Cotton, 2007) arguing that this same

interaction is not essential for the non-catalytic function of Exo1 during crossover promotion.

4.4.3 The *exo1-D173A* and *exo1-e150D* alleles are not equivalent

Both *exo1-D173A* and *exo1-E150D* mutations were assessed in order to test whether the 20% flap endonuclease activity remaining in *exo1-E150D* was able to ameliorate the meiotic defects expected in *exo1-D173A*. However, in all aspects assessed, the phenotype of *exo1-E150D* was equivalent to or worse than that observed in *exo1-D173A*. This suggests that the flap endonuclease activity of Exo1 does not function to promote recombination and furthermore argues that *exo1-E150D* is less able to support crossing-over than *exo1-D173A*. When the substrate binding affinities of three different human Exo1 alleles (D78A, D173A and D225A) were assayed *in vitro*, the residue mutated appeared to influence the strength of substrate binding. While the D173A mutant was equivalent to wild-type, the D78A protein exhibited a 5-fold reduction in binding affinity and the D225A mutant bound the substrate with a 5-fold greater affinity than the wild-type (Lee *et al.*, 2002). Therefore, the reduced ability of *exo1-E150D* to promote recombination compared to *exo1-D173A* may be due to an alteration in substrate binding affinity.

4.4.4 The nature of the spore death in the separation-of-function mutants

Analysis of the spore viability data demonstrated that an increased level of seemingly random spore death takes place in the nuclease-deficient alleles. There are several possible reasons for this. For instance, it could be due to an increased accumulation of haplo-lethal mutations during the vegetative growth phase, resulting in inviable spores being produced following meiosis. However, this seems unlikely given that the mutation frequencies measured in *exo1-D173A* cells are not significantly elevated when compared to *exo1Δ* strains and furthermore, *exo1-D173A* over-expression in wild-type does not result in a dominant negative phenotype (Sokolsky and Alani, 2000; Tran *et al.*, 2002; Tran *et al.*, 2007). Therefore, alternative possibilities must be considered. Another potential source of spore death is the persistence of unrepaired DSBs. This could occur as a consequence of reduced resection resulting in a small number of breaks incapable of undergoing strand invasion or alternatively, if the lengths of resection that occur are sufficient to enable strand invasion but insufficient to allow strand capture. If strand capture were unsuccessful, a single

broken chromatid would result leading to the death of the spore inheriting the broken chromatid. This may be associated with the formation of a half crossover. Similar situations have been suggested to occur in the absence of the strand annealing activity of Rad52 (Lao *et al.*, 2008) and during heteroduplex rejection of the second-end capture during homeologous recombination (Chambers *et al.*, 1996). The differential ability of a break to undergo strand invasion and strand capture could be explained either by differing amounts of resection either side of the DSB or if the length of resection required for strand capture is greater than that necessary for strand invasion. Given that such an event need only occur at a single DSB to cause the death of one spore within a tetrad and each cell is estimated to undergo approximately 150 DSBs per meiosis (Buhler *et al.*, 2007), only a very low frequency of these aberrant events would be required to produce the viability pattern observed in *exo1-D173A* and *exo1-E150D* meioses. Broken chromatids may similarly arise in *exo1Δ* cells but the high levels of meiosis I non-disjunction that occur may mask this phenotype.

CHAPTER 5

ANALYSIS OF PUTATIVE DNA REPAIR MUTANTS IN MEIOSIS

5.1 Introduction

The measurement of single-stranded DNA presented in Chapter 3 demonstrated that some resection of meiotic DSBs still takes place in the absence of *EXO1*. Potential nuclease candidates include Mre11, Sae2, Trm2 and Dna2 in conjunction with the helicase activity of Sgs1 (discussed in greater detail in Section 1.2.3.1). Both Mre11 and Sae2 are essential for the removal of Spo11 following DSB formation, preventing mutant analysis from being carried out for these genes. This is not the case for Sgs1 and Trm2. Therefore, in this chapter, we aimed to carry out a genetic characterisation of *sgs1* and *trm2* mutants alone and in combination with *exo1Δ* to assess the relative contributions made by these enzymes to meiotic DSB repair. It was predicted that if resection were worsened by the loss of these proteins, reduced gene conversion, crossing-over and spore viability would result.

Examination of the *sgs1 exo1Δ* meiotic phenotype was also of interest for a second reason. Previous research has demonstrated that deletion of *SGS1* in *zip1Δ*, *zip2Δ*, *zip3Δ*, *mer3Δ*, *msh4Δ*, *msh5Δ* and *mlh3Δ* mutants restores crossovers to near wild-type levels (Jessop *et al.*, 2006; Oh *et al.*, 2007). This was associated with an improvement in spore viability. Therefore, it is argued that one of the roles of these crossover-promoting factors is to antagonise the anti-recombination activity of Sgs1, shielding crossover-designated recombinants from Sgs1-catalysed unwinding/dissolution. The results presented in Chapter 4 of this thesis suggest that Exo1 plays a structural role in supporting crossing-over and thus may also function to protect recombination intermediates from Sgs1. If this were the case, an improvement in spore viability and crossing-over in *sgs1 exo1Δ* cells compared to the *exo1Δ* strain would be expected.

5.2 Materials and Methods

5.2.1 Strain Construction

The *TRM2* ORF was replaced with the KanMX4 cassette conferring resistance to geneticin as described by Wach *et al.* (1994). As an *sgs1Δ exo1Δ* double mutant confers a severe mitotic resection defect (Mimitou and Symington, 2008; Zhu *et al.*, 2008), a meiotic null allele of *SGS1* (*sgs1-mn*) was constructed by bringing expression of *SGS1* under the control of the *CLB2* promoter as described by Lee & Amon (2003). This construct allows gene expression during mitotic growth but strongly represses transcription upon entry into meiosis, thereby enabling the meiosis-specific effects caused by the absence of the protein to be assessed. Transformants were initially checked by PCR and the integrity of the *CLB2* promoter sequence upstream of *SGS1* was confirmed by DNA sequencing. As *sgs1Δ* mutants are sensitive to MMS, the expression of *SGS1* during mitotic growth in the resulting *sgs1-mn* strain was confirmed by growth testing on MMS-containing medium (Figure 5.1). The *sgs1-mn exo1Δ* and *trm2Δ exo1Δ* double mutants were produced by crossing. Genotypes of the resulting strains are listed in Table 2.1 and the oligonucleotides used in strain construction are given in Table 2.2.

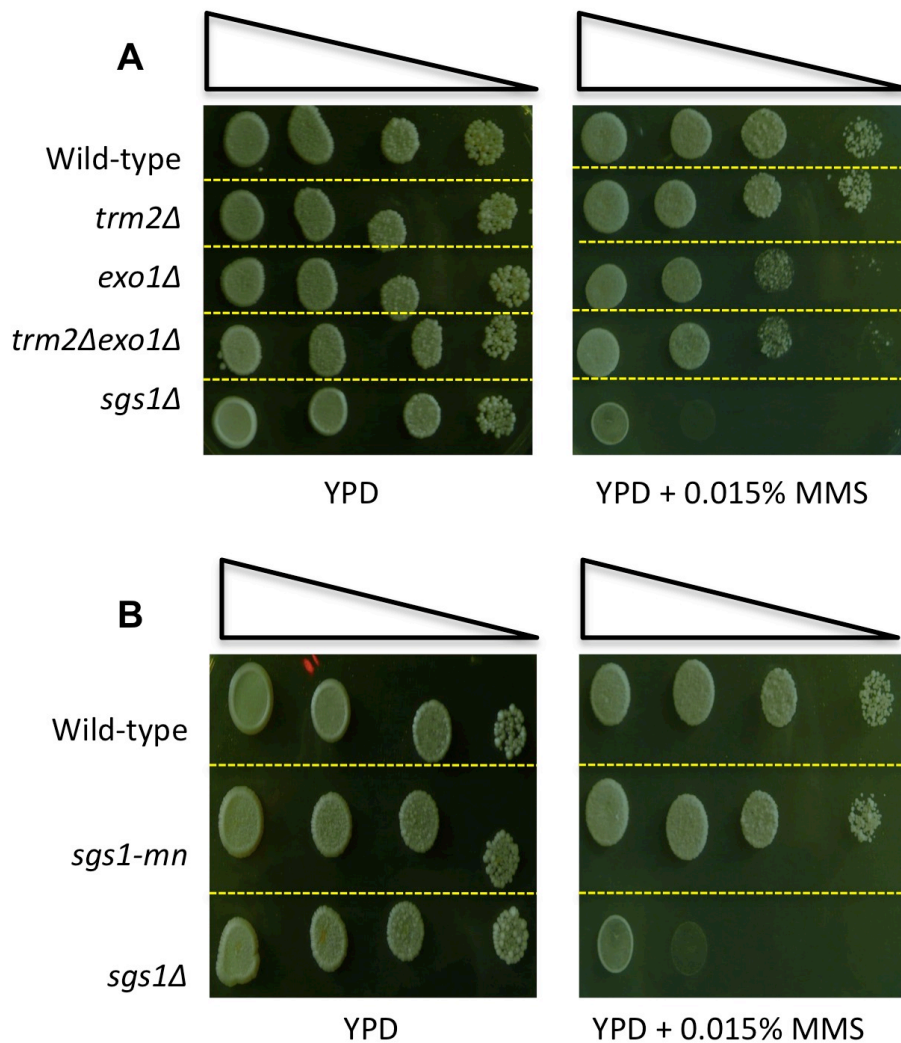


Figure 5.1: MMS sensitivity testing

Serial 10-fold dilutions of overnight cultures were spotted onto both unsupplemented YPD medium and YPD containing 0.015% (v/v) MMS and were allowed to grow for 2 days at 30°C. The sensitivity of *exo1Δ*, *trm2Δ* and *exo1Δ trm2Δ* mutants were tested in (A), while the *sgs1-mn* allele was assessed in (B). Wild-type and *sgs1Δ* strains were included on all plates as positive and negative controls.

5.3 Results

5.3.1 Trm2 does not function in meiotic recombination

In all but one of the phenotypes assessed (spore viability, non-Mendelian segregation, chromosome non-disjunction and crossing-over; Tables 5.1-5.5), the *trm2Δ* strain was indistinguishable from wild-type. Only when recombination was measured in the *LEU-MAT* interval was a significantly reduced crossover frequency observed in *trm2Δ* cells ($p=0.008$, G-test; Table 5.4). Furthermore, the *trm2Δ exo1Δ* double mutant was not significantly different from the *exo1Δ* single mutant in any test performed. These results suggest that Trm2 does not function to promote meiotic recombination, in either the presence or absence of Exo1. This is in contrast to the synergistic relationship between Trm2 and Exo1 proposed to take place at mitotic DSBs by Choudhury *et al.* (2007a). However, we were also unable to replicate the increased MMS sensitivity reported to occur in *trm2Δ* (Figure 5.1) by the same authors (Choudhury *et al.*, 2007b). Therefore, our results are more comparable to those of Nordlund *et al.* (2000) who were similarly unable to detect an increase in MMS sensitivity in a *trm2* mutant strain. In addition, Nordlund *et al.* (2000) failed to detect any nuclease activity associated with Trm2 during mitotic growth, raising the possibility that a secondary mutation in the strains used by Choudhury *et al.* (2007a) may be responsible for the phenotype observed.

5.3.2 Spore viability distributions in the absence of *SGS1* and *EXO1*

In order to investigate the genetic interaction between *EXO1* and *SGS1* in meiosis, *sgs1-mn* and *sgs1-mn exo1Δ* strains were assessed. As shown in Table 5.1 and Figure 5.2, the *sgs1-mn* strain displayed a significant reduction in spore viability compared to wild-type cells ($p=3 \times 10^{-27}$, G-test; Table 5.1). The pattern of spore death in these cells (in contrast to the crossover-deficient *exo1Δ* mutant) was indicative of random spore death, consistent with previous studies (Watt *et al.*, 1995; Jessop *et al.*, 2006). In the *sgs1-mn exo1Δ* double mutant, a further reduction in viability was observed, resulting in an overall viability of 53.6% ($p=6 \times 10^{-96}$, G-test). This agrees well the 52.5% predicted to occur from the additive effect of two independent sources of spore death in *sgs1-mn* and *exo1Δ* ($p=0.48$, G-test). However, when the pattern of viable spores contained within each tetrad was examined more closely, a significant alteration from the predicted pattern was observed ($p=4 \times 10^{-9}$, contingency chi-square test; Figure 5.2). Specifically, there appeared to be a slight increase in three

Table 5.1: Spore viability in the putative DNA repair mutants at 23°C

		Viable spores per tetrad class					Total tetrads	% overall spore viability ¹
		4	3	2	1	0		
Wild-type ²	<i>n</i>	941	54	41	2	8	1046	95.8 [†]
	(%)	(89.9)	(5.2)	(3.9)	(0.2)	(0.8)		
<i>exo1Δ</i> ²	<i>n</i>	885	231	472	136	476	2200	60.4*
	(%)	(40.2)	(10.5)	(21.5)	(6.2)	(21.6)		
<i>trm2Δ</i>	<i>n</i>	252	17	3	0	2	274	97.2 [†]
	(%)	(92.0)	(6.2)	(1.1)	(0.0)	(0.7)		
<i>trm2Δ</i>	<i>n</i>	156	32	90	18	74	370	62.0*
	(%)	(42.2)	(8.6)	(24.3)	(4.9)	(20.0)		
<i>sgs1-mn</i>	<i>n</i>	219	66	34	5	6	330	86.9 [†]
	(%)	(66.4)	(20)	(10.3)	(1.5)	(1.8)		
<i>sgs1-mn</i>	<i>n</i>	108	108	119	82	85	502	53.6* [†]
	(%)	(21.5)	(21.5)	(23.7)	(16.3)	(16.9)		
Predicted								
if additive:	<i>n</i>	134	78	116	52	122	502	52.5
	(%)	(26.7)	(15.5)	(23.0)	(10.4)	(24.3)		
	<i>sgs1-mn</i>							
	<i>exo1Δ</i>							

¹ Calculated as ((4 x no. 4-spore tetrads) + (3 x no. 3-spore tetrads) + (2 x no. 2-spore tetrads) + no. 1-spore tetrads)/(4 x total number of tetrads) x100. Comparisons of the distributions between spore classes were made using the G-test of homogeneity and statistically significant (p<0.0102, for four-way comparisons) differences are indicated as follows: * significantly different from wild-type at same temperature, [†] significantly different from *exo1Δ* at same temperature. ² Data presented previously in Chapter 4.

Table 5.2: Crossing-over in the putative DNA repair mutants at 23°C

	Wild-type ²	<i>exo1Δ</i> ²	<i>trm2Δ</i>	<i>trm2Δ</i> <i>exo1Δ</i>	<i>sgs1-mn</i>	<i>sgs1-mn</i> <i>exo1Δ</i>
<i>HIS4-LEU2</i>						
PD ¹	449	540	133	99	85	76
NPD	1	1	0	2	0	0
TT	183	126	48	16	52	17
cM	14.9 [†]	9.9*	13.3	12*	19 [†]	9.1
<i>LEU2-MAT</i>						
PD	442	622	146	105	98	70
NPD	32	7	5	1	18	2
TT	425	244	92	44	92	34
cM	34.3 [†]	16.4*	25.1*	16.7*	48.1	21.7*
<i>CEN8-ARG4</i>						
PD	696	739	194	135	149	83
NPD	2	1	0	0	0	0
TT	185	119	46	16	47	18
cM	11.2 [†]	7.3*	9.6	5.3*	12 [†]	8.9
<i>LYS5-MET13</i>						
PD	555	680	172	120	144	80
NPD	8	2	2	0	2	1
TT	349	186	72	27	68	22
cM	21.8 [†]	11.4*	17.1	9.2*	18.7 [†]	13.6*
<i>MET13-CYH2</i>						
PD	738	774	203	138	180	88
NPD	0	0	0	0	0	0
TT	179	99	43	14	33	18
cM	9.8 [†]	5.7*	8.7	4.6*	7.7	8.5
<i>CYH2-TRP5</i>						
PD	331	539	99	97	102	61
NPD	35	11	5	2	9	1
TT	557	328	146	57	102	43
cM	41.5 [†]	22.4*	35.2 [†]	22.1*	36.6 ^{††}	23.3*

¹PD, NPD and TT represent parental ditypes, nonparental ditypes and tetratypes respectively. cM values were calculated according to the formula of Perkins (1949). Distributions between tetrad classes were compared using the G-test of homogeneity and statistically significant ($p < 0.0102$) differences are indicated as follows: * significantly different from wild-type, [†] significantly different from *exo1Δ*. ² Data presented previously in Chapter 4.

Table 5.3: Rates of meiosis I chromosome III non-disjunction in the putative DNA repair mutants at 23°C

Genotype	Number of non-maters ¹	Total tetrads	% Non-disjunction ²
Wild-type ³	1	1046	0.1 [†]
<i>exo1Δ</i> ³	61	2200	2.8*
<i>trm2Δ</i>	0	274	0.0 [†]
<i>trm2Δ exo1Δ</i>	11	370	3.0*
<i>sgs1-mn</i>	3	330	0.9
<i>sgs1-mn exo1Δ</i>	6	502	1.2*

¹The number of two-viable-spore tetrads containing two non-mating spores (indicative of chromosome III non-disjunction). ²Non-disjunction was calculated as: (number of non-maters/total number of tetrads) x100. Comparisons were made using the G-test of homogeneity and statistically significant ($p < 0.0102$) differences are indicated as follows: * significantly different from wild-type, [†] significantly different from *exo1Δ*. ³ Data presented previously in Chapter 4.

Table 5.4: Rates of meiosis I non-disjunction in the putative DNA repair mutants at 23°C

Genotype	Number of sister spores ¹	Number of non-sister spores ¹	Total tetrads	% Non-disjunction ²
Wild-type ³	<i>30</i>	<i>11</i>	1046	1.8 [†]
<i>exo1Δ</i> ³	<i>394</i>	<i>78</i>	2200	14.4*
<i>trm2Δ</i>	3	0	274	1.1 [†]
<i>trm2Δ exo1Δ</i>	<i>73</i>	<i>17</i>	370	19.7*
<i>sgs1-mn</i>	19	15	330	1.2 [†]
<i>sgs1-mn exo1Δ</i>	64	55	502	1.8 [†]

¹Two-viable-spore tetrads were categorised as sisters (same uracil phenotype) or non-sisters (different uracil phenotype) based upon the segregation of the centromere-linked *CEN8:URA3* marker. Emboldened italics indicate distributions of sister to non-sister spores that are significantly different ($p < 0.05$) from a 50:50 distribution as determined by χ^2 test. ²Non-disjunction was calculated as: ((number of sister spores - number of non-sister spores)/total tetrads) x100. Comparisons were made using the G-test of homogeneity and statistically significant ($p < 0.0102$) differences are indicated as follows: * significantly different from wild-type, [†] significantly different from *exo1Δ*. ³ Data presented previously in Chapter 4.

Table 5.5: Non-Mendelian segregation in the putative DNA repair mutants at 23°C

Genotype		Allele								
		<i>his4-XhoI</i>	<i>leu2-R</i>	<i>MAT</i>	<i>lys5-P</i>	<i>met13-B</i>	<i>cyb2-Z</i>	<i>trp5-S</i>	<i>CEN8:URA3</i>	<i>arg4-nsp</i>
Wild-type ²	%NMS ¹	29.2 [†]	3.6 [†]	0.9	1.4	1.8	0.7	1.3	0	6.1 [†]
	(NMS/total tetrads)	(275/941)	(34/941)	(8/941)	(13/941)	(17/941)	(7/941)	(12/941)	(0/941)	(58/941)
<i>exo1Δ</i> ²	%NMS	23.6*	1.1*	0.2	0.9	1.0	0.5	0.3	0	2.9*
	(NMS/total tetrads)	(209/885)	(10/885)	(2/885)	(8/885)	(9/885)	(4/885)	(3/885)	(0/885)	(26/885)
<i>trm2Δ</i>	%NMS	27.0	1.6	2.0	0	2.4	0	0.8	0	4.8
	(NMS/total tetrads)	(68/252)	(4/252)	(5/252)	(0/252)	(6/252)	(0/252)	(2/252)	(0/252)	(12/252)
<i>trm2Δ exo1Δ</i>	%NMS	23.7	1.9	1.9	3.2	2.6	0	0	0.6	2.6
	(NMS/total tetrads)	(37/156)	(3/156)	(3/156)	(5/156)	(4/156)	(0/156)	(0/156)	(1/156)	(4/156)
<i>sgs1-mn</i>	%NMS	34.7 [†]	3.7	1.4	0.5	1.8	0.9	1.8	0	10.5 [†]
	(NMS/total tetrads)	(76/219)	(8/219)	(3/219)	(1/219)	(4/219)	(2/219)	(4/219)	(0/219)	(23/219)
<i>sgs1-mn exo1Δ</i>	%NMS	14*	0*	1.9	2.8	1.9	0	2.8	0	6.5
	(NMS/total tetrads)	(15/108)	(0/158)	(2/158)	(3/158)	(2/158)	(0/158)	(3/108)	(0/108)	(7/108)

¹Non-Mendelian segregation includes gene conversion and post-meiotic segregation events. Tetrads exhibiting ≥ 3 NMS events per tetrad were scored as false tetrads and excluded from further analysis. %NMS was calculated as: (number of NMS events/total number of tetrads) x 100. Comparisons were made using the G-test of homogeneity and statistically significant ($p < 0.0102$) differences are indicated as follows: * significantly different from wild-type, [†] significantly different from *exo1Δ*. ² Data presented previously in Chapter 4.

and one viable spore tetrads at the expense of the four and zero viable spore tetrad classes. The decrease in tetrads containing zero viable spores in particular is suggestive of improved chromosome disjunction.

5.3.3 Crossing-over is not restored in *sgs1-mn exo1Δ* at 23°C

In order to investigate whether increased recombination was occurring in the *sgs1 exo1Δ* strain, crossing-over was measured in the 6 genetic intervals used previously in Chapter 4 (Table 5.2). In five of the six intervals, a slight increase in crossing-over was observed in the *sgs1-mn exo1Δ* tetrads compared to the *exo1Δ* cells. However, this increase was small in all cases and was not statistically significant in any interval. Furthermore, in three intervals, recombination remained significantly lower than in the wild-type strain ($p < 0.004$, G-test). Therefore, while a small increase in recombination may account for the apparent improvement in chromosome segregation, a large-scale rescue of crossing-over does not appear to take place in *sgs1-mn exo1Δ* cells. The finding that significantly higher rates of chromosome III non-disjunction occurred in *sgs1-mn exo1Δ* tetrads compared to wild-type cells ($p = 0.0034$, G-test) supports this conclusion. However, when non-disjunction was assessed genome-wide, the opposite situation was observed (Table 5.3). The overall rate of meiosis I non-disjunction in the *sgs1-mn exo1Δ* strain was significantly reduced compared to *exo1Δ* ($p = 3 \times 10^{-20}$, G-test). In the *sgs1-mn* single mutant, the proportions of sister and non-sister spores did not deviate significantly from a 50:50 distribution suggesting that they did not result from non-disjunction (see Figure 1.2). Therefore, the non-sister spores produced as a result of *SGS1* mutation may act to decrease the apparent level of non-disjunction detected in *sgs1-mn exo1Δ*.

5.3.4 Gene conversion is not significantly reduced in *sgs1-mn exo1Δ*

In order to rule out the possibility that the opposing effects of reduced unwinding of crossover-designated intermediates and decreased resection operating at the same time could be responsible for the comparable amount of crossing-over observed in *sgs1-mn exo1Δ* and *exo1Δ* strains, the levels of NMS were calculated (Table 5.5). If decreased resection were occurring this should result in a decrease in gene conversion. In the *sgs1-mn* single mutant, NMS was slightly increased compared to wild-type at the majority of loci and was significantly higher than the *exo1Δ* strain at both *HIS4* and *ARG4* ($p < 0.001$, G-test). This supports the theory that deletion of

SGS1 alone does not result in a resection defect. NMS was reduced at *HIS4* from 23.6% in the *exo1Δ* single mutant to 14% in the *sgs1-mn exo1Δ* strain. Contrastingly, at *ARG4*, NMS was increased from 2.9% in *exo1Δ* cells to 6.5% in the *sgs1-mn exo1Δ* strain. Neither change was statistically significant with the number of tetrads studied ($p > 0.017$, G-test). Therefore, while a role for Sgs1 in catalysing some resection at certain loci cannot be ruled out, it does not appear to be responsible for the majority of resection that occurs in *exo1Δ*.

5.3.5 A differential requirement for *SGS1* in *exo1Δ* cells at 23°C and 33°C

The finding that crossing-over was not improved in *sgs1-mn exo1Δ* cells compared to *exo1Δ* tetrads was somewhat surprising given that other mutants defective in forming crossovers via the same pathway (*zip1Δ*, *zip2Δ*, *zip3Δ*, *mer3Δ*, *msb4Δ*, *msh5Δ* and *mlh3Δ*) all exhibited an increase in crossover frequency upon deletion of *SGS1* (Jessop *et al.*, 2006; Oh *et al.*, 2007). These previous studies were carried out at 30°C. Therefore, we considered whether the reduced sporulation temperature employed in the experiments presented here (23°C) could account for this apparently anomalous result. It has been proposed that recombination in *zmm* mutants proceeds via one of two ‘modes’ depending upon whether the cells are sporulated at 23°C or 33°C, while experiments performed at 30°C represent a mixture of the two modes (Borner *et al.*, 2004; see Section 1.3.2 for further details). We hypothesised that any potential influence of temperature may thus be more obvious at 33°C. Unlike *zmm* mutants, *exo1Δ* cells in the SK1 strain background sporulate efficiently at both temperatures (data not shown), allowing tetrad analysis at 33°C to be carried out.

When recombination was analysed at the elevated temperature, an apparent improvement in crossing-over in *sgs1-mn exo1Δ* cells was indeed observed. At 33°C, the map distance measured in the *sgs1-mn exo1Δ* tetrads was longer (indicating increased recombination) than in the *exo1Δ* strain in all but one interval (Table 5.6). Furthermore, the change in recombination frequency was statistically significantly in four intervals ($p < 0.0145$, G-test). When the *sgs1-mn* and *sgs1-mn exo1Δ* strains were compared, a slight decrease in crossing-over was observed in the *sgs1-mn exo1Δ* cells but this difference was only statistically significant in the *LYS5-MET13* interval ($p = 0.0021$, G-test), arguing that the *exo1Δ* mutation does not confer a severe

Table 5.6: Crossing-over in the putative DNA repair mutants at 33°C

	Wild-type	<i>exo1Δ</i>	<i>sgs1-mn</i>	<i>sgs1-mn exo1Δ</i>
<i>HIS4-LEU2</i>				
PD ¹	195	166	109	150
NPD	1	0	3	1
TT	92	31	51	56
cM	17 [†]	7.9*	21.2 [†]	15 [†]
<i>LEU2-MAT</i>				
PD	130	140	73	111
NPD	18	3	7	7
TT	142	72	97	94
cM	43.1 [†]	20.9*	39.3 [†]	32.1
<i>CEN8-ARG4</i>				
PD	202	186	111	148
NPD	0	0	3	1
TT	86	25	57	54
cM	14.9 [†]	5.9*	21.9 [†]	14.8 [†]
<i>LYS5-MET13</i>				
PD	172	171	99	150
NPD	1	1	1	5
TT	114	38	76	58
cM	20.9 [†]	10.5*	23.3 [†]	20.7 [†]
<i>MET13-CYH2</i>				
PD	229	185	148	188
NPD	0	0	0	0
TT	61	26	30	26
cM	10.5	6.2	8.4	6.1
<i>CYH2-TRP5</i>				
PD	93	138	82	99
NPD	11	1	14	13
TT	202	81	88	102
cM	43.8 [†]	19.8*	46.7 [†]	42.1 [†]

¹PD, NPD and TT represent parental ditypes, nonparental ditypes and tetratypes respectively. cM values were calculated according to the formula of Perkins (1949). Distributions between tetrad classes were compared using the G-test of homogeneity and statistically significant ($p < 0.0169$) differences are indicated as follows: * significantly different from wild-type, [†] significantly different from *exo1Δ*.

crossover defect in the absence of *SGS1* at 33°C. As expected from an improvement in crossing-over upon *SGS1* deletion, the 77.3% spore viability observed in the *sgs1-mn exo1Δ* strain at 33°C was significantly higher than the 73.2% predicted if the *exo1Δ* and *sgs1-mn* mutations had an additive effect on spore death (Table 5.7, Figure 5.2; $p=0.0029$, G-test). This suggests that at 33°C (in contrast to the situation observed at 23°C), Sgs1 acts antagonistically to Exo1 in crossover production.

5.3.6 Increasing temperature promotes chromosome disjunction in *exo1Δ* strains

Increasing the temperature of sporulation was also seen to have an effect upon the *exo1Δ* single mutant. Spore viability in *exo1Δ* strains was improved from 60.4% at 23°C to 81.5% at 33°C (Tables 5.1 and 5.7, Figure 5.2; $p=6 \times 10^{-55}$, G-test). This overall improvement resulted from an increase in the number of tetrads containing four viable spores, while the two and zero viable spore tetrad classes were decreased ($p=4 \times 10^{-20}$, G-test) suggesting that chromosome disjunction is improved at the higher temperature. However, in contrast to the *sgs1-mn exo1Δ* strain, the improvement in viability in the *exo1Δ* cells did not appear to occur as a result of increased crossovers as no interval exhibited a statistically significant increase in crossing-over (Tables 5.1 and 5.6). In fact, in five of the six intervals tested there was a slight reduction in crossing-over at 33°C compared to 23°C. This argues that temperature affects chromosome disjunction via a crossover-independent backup system as described previously in *msb4Δ*, *msb5Δ* and *pch2Δ* mutant cells (Chan *et al.*, 2009; Joshi *et al.*, 2009). In support of this, spore death in the *sgs1-mn* strain (which did not exhibit high levels of non-disjunction at 23°C) was not significantly affected by temperature ($p=0.028$; G-test).

Table 5.7: Spore viability of putative DNA repair mutants at 33°C

Genotype		Viable spores per tetrad class					Total tetrads	% overall spore viability ¹
		4	3	2	1	0		
Wild-type	<i>n</i>	309	21	2	0	2	334	97.5 [†]
	(%)	(92.2)	(6.3)	(0.6)	(0.0)	(0.6)		
<i>exo1Δ</i>	<i>n</i>	220	33	45	10	23	331	81.5*
	(%)	(66.3)	(9.9)	(13.6)	(3)	(6.9)		
<i>sgs1-mn</i>	<i>n</i>	187	46	22	4	1	260	89.8 [†]
	(%)	(71.6)	(17.6)	(8.4)	(1.5)	(0.4)		
<i>sgs1-mn</i> <i>exo1Δ</i>	<i>n</i>	216	149	94	25	9	493	77.3 [†]
	(%)	(43.8)	(30.2)	(19.1)	(5.1)	(1.8)		
Predicted	<i>n</i>	235.7	95.5	91.4	31.3	39.1	493	73.2
if additive:	(%)	(47.8)	(19.4)	(18.5)	(6.4)	(7.9)		
<i>sgs1-mn</i> <i>exo1Δ</i>								

¹ Calculated as ((4 x no. 4-spore tetrads) + (3 x no. 3-spore tetrads) + (2 x no. 2-spore tetrads) + no. 1-spore tetrads)/(4 x total number of tetrads) x100. Comparisons of the distributions between spore classes were made using the G-test of homogeneity and statistically significant ($p < 0.0169$, for four-way comparisons) differences are indicated as follows: * significantly different from wild-type at same temperature, [†] significantly different from *exo1Δ* at same temperature.

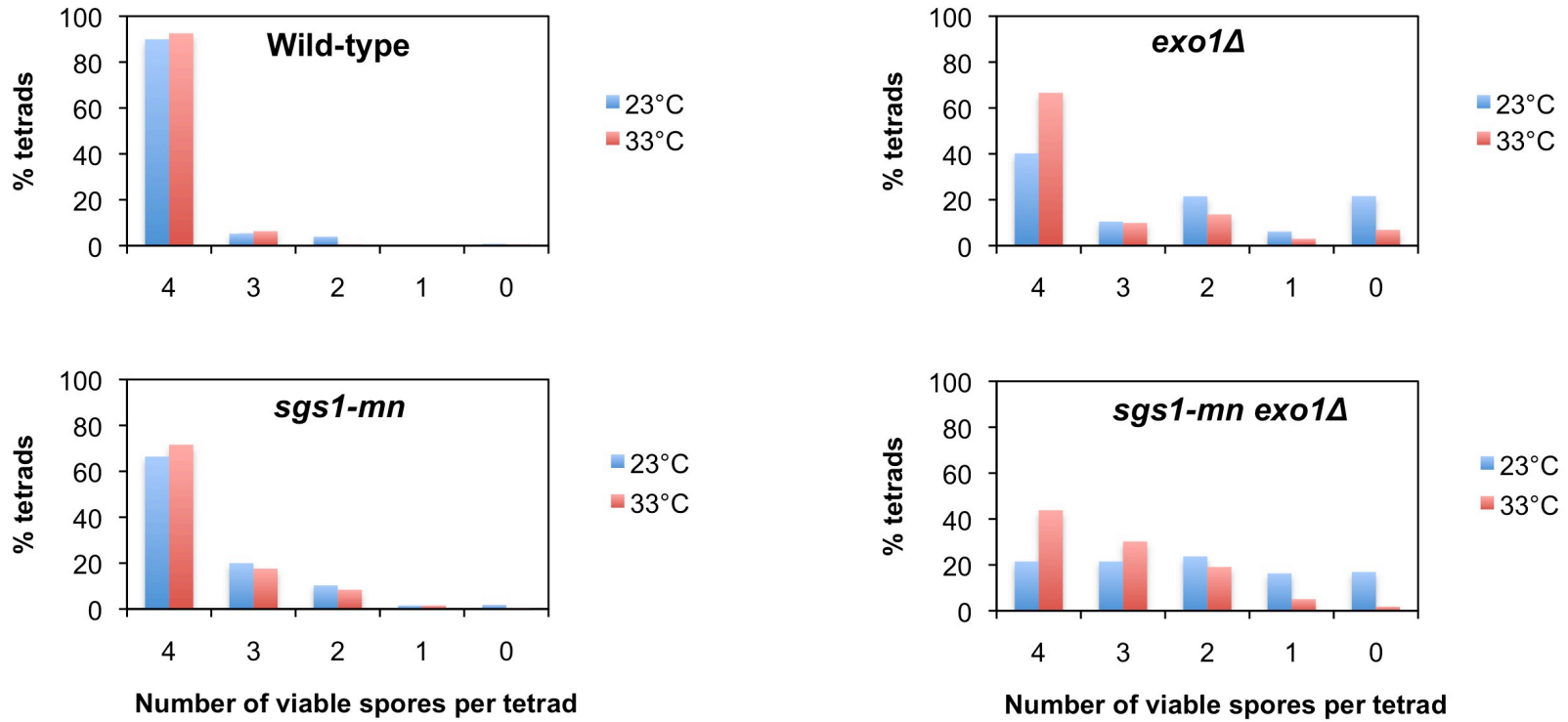


Figure 5.2: The effect of temperature upon spore viability

The data presented in Tables and is presented graphically.

5.4 Discussion

5.4.1 Neither Sgs1 nor Trm2 contribute to meiotic DSB processing

The results presented in Chapters 3 and 4 of this thesis suggest that resection influences heteroduplex tract length and that at some loci (such as those on chromosome III) extensive resection is required in order to maintain normal levels of crossing-over. Therefore, it was predicted that a further reduction in resection tract length would result in decreased levels of inter-homologue recombination and decreased spore viability. Spore viability assays are more sensitive than measurements of crossing-over and gene conversion as they reflect the amount of recombination occurring genome-wide and report upon the status of all four cells contained within each tetrad. Furthermore, crossing-over and gene conversion can only be accurately assessed in tetrads containing four viable spores and only provide information about a small region of the genome. In this chapter, it was demonstrated that deletion of *TRM2* has no effect upon spore viability while the decreased spore viability observed in an *sgs1-mn exo1Δ* strain is no worse than that predicted to result from the additive effect of two independent sources of spore death. Recombination was not significantly reduced below the level seen in *exo1Δ* cells in either *trm2Δ exo1Δ* or *sgs1-mn exo1Δ* strains. Therefore, neither Sgs1 nor Trm2 appear to contribute significantly to producing the residual resection observable in *exo1Δ* mutants. As studies of resection in *dmc1Δ* strains had indicated a role for Sgs1 in producing the hyper-resected DSBs that accumulate in this mutant (Manfrini *et al.*, 2010), these results argue that the resection that takes place at later time points in *dmc1Δ* cells is not representative of normal meiotic resection. Instead, hyper-resection in *dmc1Δ* appears to more closely resemble the mitotic DSB processing described by Mimitou & Symington (2008) and Zhu *et al.* (2008).

It remains possible that Sgs1 and Trm2 are able to functionally compensate for each other and that deletion of all three genes (*SGS1*, *TRM2* and *EXO1*) would be required to affect resection in otherwise wild-type cells. However, given the conflicting evidence that Trm2 possesses a nuclease activity, a perhaps more likely explanation is that the MRX complex and/or Sae2 is responsible for catalysing resection in the absence of *EXO1*. In mitotic cells, it is proposed that MRX/Sae2 normally acts to remove 100 bp of DNA adjacent to the break site prior to extensive resection by Exo1 or Sgs1/Dna2 (Mimitou and Symington, 2008; Zhu *et al.*, 2008).

In the absence of Exo1 and Sgs1/Dna2, MRX/Sae2 is also responsible for producing a limited amount of further resection. This process is slow and appears to pause at discrete sites separated by approximately 100 bp. It is therefore possible that MRX/Sae2 functions analogously in *exo1Δ* cells during meiosis (Figure 5.3). This agrees well with recent data produced by Hodgson *et al.* (2010) suggesting that Mre11 is important for the initiation and processivity of resection at a *VDE* catalysed meiotic DSB.

5.4.2 The nature of the crossover deficit in *exo1Δ* and the effect of temperature

The finding that crossing-over is not significantly improved in *sgs1-mn exo1Δ* cells compared to the *exo1Δ* single mutant at 23°C argues that the crossover deficit observed in the absence of *EXO1* is not due the action of Sgs1 upon crossover designated intermediates at this temperature. However, at 33°C, deletion of *SGS1* does appear able to restore a substantial amount of crossing-over to the *exo1Δ* cells. This could potentially be due to an increased number of inter-homologue interactions occurring at high temperature that require Sgs1 to be unwound/dissolved. However, if this were the case, an increase in crossing-over at 33°C compared to 23°C in the *sgs1-mn* single mutant would also be expected. As only one interval (*CEN8-ARG4*) displayed such an increase (p=0.0112, G-test), a perhaps more likely explanation is that the same number of recombination intermediates are formed at both temperatures in *exo1Δ* yeast but these intermediates are inherently less stable at 23°C. Therefore, Sgs1 would not be required at the lower temperature in order for dissolution to occur. It would be interesting to ascertain whether the other mutants in which *SGS1* deletion was previously shown to restore crossing-over at 30°C share the same temperature-dependent phenotype. Temperature has previously been shown to influence meiotic progression, checkpoint robustness, chromosome segregation and crossover interference in meiosis (Borner *et al.*, 2004; Chan *et al.*, 2009; Joshi *et al.*, 2009) and it is thus conceivable that changes in temperature may also influence the stability of recombination intermediates. The finding that spore viability is improved by temperature in the *exo1Δ* mutant strain without an improvement in crossing-over provides further support for the theory that higher temperature acts to promote accurate chromosome disjunction at the first meiotic division when the crossover-

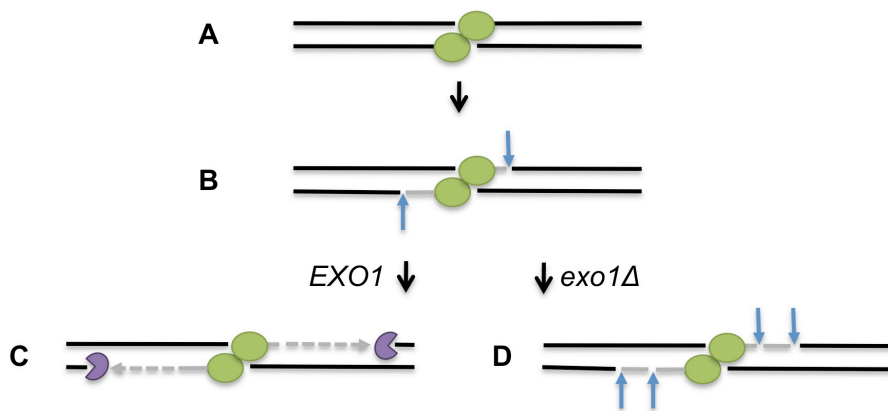


Figure 5.3: A model describing resection at meiotic DSBs

(A) Following DSB formation catalysed by a Spo11 dimer (shown in green), the MRX complex and/or Sae2, acts to endonucleolytically cleave the DNA (B), producing single-stranded gaps (sites of endonucleolytic activity are indicated by arrows). (C) Exo1 (shown in purple) loads onto the DNA at these sites and carries out processive resection. (D) In the absence of *EXO1*, slower, limited resection catalysed by MRX/Sae2 takes place. This may utilise the endonuclease activity of MRX/Sae2 in conjunction with a helicase to unwind the DNA or alternatively, following endonucleolytic cleavage, the 3' to 5' exonuclease activity of Mre11 could act to remove the DNA. Adapted from Neale *et al.* (2005) and Hodgson *et al.* (2010).

mediated disjunction pathway is compromised. The mechanism that promotes the accurate disjunction of chromosomes in the absence of crossing-over is known as distributive segregation. Such systems are essential in certain organisms such as *Drosophila melanogaster* (Cooper, 1945) and are likely to become of increasing importance in other organisms when recombination is prevented due to mutation or high levels of sequence divergence. Given that yeast in the wild may encounter a greater degree of sequence divergence during reproduction than isogenic laboratory strains, a distributive segregation pathway may have increased significance in the natural environment. Therefore, the ability of temperature to improve the reliability of this pathway provides an example of how environmental factors may influence the reproductive abilities of certain species. Whether or not this improved segregation is linked to the apparent increase in the stability of recombination intermediates at higher temperature remains unclear.

CHAPTER 6

DISCUSSION & FUTURE DIRECTIONS

6.1 Multiple functions for Exonuclease I in meiotic recombination

In yeasts, *Drosophila*, mice and humans, homologues of Exonuclease I are up-regulated in cells undergoing meiosis (Szankasi and Smith, 1995; Digilio *et al.*, 1996; Chu *et al.*, 1998; Tishkoff *et al.*, 1998; Lee *et al.*, 1999). This suggests that there is a highly conserved requirement for the protein during the recombination process. Prior to the work described in this thesis, experiments in yeast had demonstrated that Exo1 is essential for the formation of crossovers in the Msh4/Msh5 pathway but the molecular mechanism by which this occurred remained uncertain (Khazanehdari and Borts, 2000; Kirkpatrick *et al.*, 2000; Tsubouchi and Ogawa, 2000). In this study, evidence was presented that suggests Exo1 performs at least two functions during the repair of meiotic DSBs in *Saccharomyces cerevisiae*. A model describing these roles is presented in Figure 6.1 (see text below for details).

6.1.1 Meiotic DSB end resection

Exo1 appears to be the principal nuclease responsible for producing the 3' single-stranded tails found at DSB sites during meiosis. These tails form the basis of the nucleoprotein filaments that initiate recombination by invading the homologous chromosome. Two observations suggest that the processing of meiotic DSBs differs significantly from that of endonucleolytically induced mitotic DSBs where dual resection pathways mediated by Exo1 and Sgs1/Dna2 are thought to operate (see Mimitou and Symington, 2008; Zhu *et al.*, 2008 for mitotic experiments). Firstly, physical assessments of resection in meiotic cells revealed a considerable resection defect in the *exo1Δ* single mutant compared to wild type. This was not seen in the mitotic resection assays where deletion of both *EXO1* and *SGS1* was necessary to produce a strong resection phenotype. Secondly, an *sgs1 exo1* double mutant did not exhibit any additional reduction in homologous recombination or spore viability

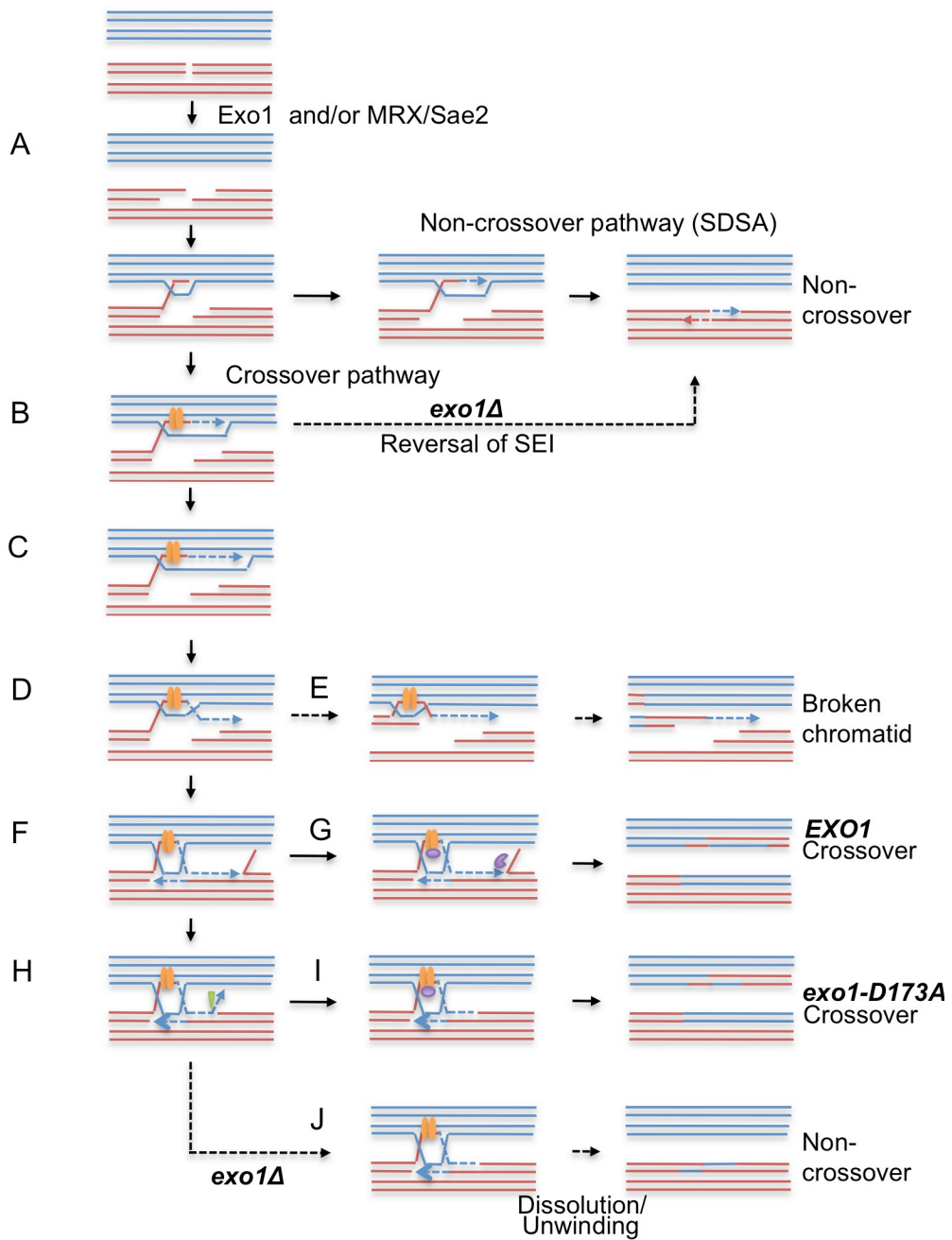


Figure 6.1: Model demonstrating multiple roles for Exo1 during meiotic recombination

(A) Following DSB formation, Exo1 acts to resect the DNA ends in a 5' to 3' direction. When Exo1 nuclease activity is absent, limited resection may be catalysed by Mre11 and/or Sae2. The overhanging 3' strands can then begin to interact with the homologous chromosome and a D-loop is produced upon invasion. If a break is to be repaired as a non-crossover, DNA synthesis and strand displacement will follow. (B) Along the crossover pathway, the D-loop requires stabilisation by proteins such as Msh4/Msh5 (shown in orange). If Exo1 also performs an early stabilising function, its absence may lead to displacement of the SEI, collapsing the D-loop. A non-crossover can be formed by SDSA. (C) With a stable SEI, extensive DNA synthesis then takes place, which may or may not be coordinated with processive resection. (D) The synthesised end is eventually displaced and attempts to anneal to the strand uncovered by resection on the opposite side of the break. (E) If there is insufficient resection for this annealing to occur, a half crossover and a single broken chromatid could result. (F) Upon successful annealing, if DNA synthesis and resection do not occur at the same rate, DNA flaps could be formed from displacement of the unresected region. (G) These flaps normally require the exonuclease activity of Exo1 for removal, allowing dHJs to form and undergo subsequent resolution to form crossovers. (H) When Exo1 nuclease activity is absent, 3' flaps could be produced that may serve as substrates for Mus81/Mms4 (indicated by green triangle). This would then permit ligation and completion of the dHJ. (I) If instead of/in addition to an early stabilising role, the nuclease-independent function of Exo1 (shown in purple) acts to stabilise the dHJ structure, crossovers would form as normal in *exo1-D173A*. (J) Without this stabilising activity in *exo1Δ*, crossovers would not be produced.

compared to the *exo1Δ* single mutant. The basis for this meiosis-specific regulation is not known; however, evidence from mitotic cells implies that Mre11 may be important.

When yeast cells are subjected to ionising irradiation (IR), DSB formation ensues (Ward, 1990 and references therein). Vegetative *mre11Δ* cells are highly sensitive to IR, demonstrating the essential role played by Mre11 in repairing this type of DNA damage (Bressan *et al.*, 1999; Moreau *et al.*, 1999). The sensitivity of *mre11Δ* strains is partially suppressed by the absence of yKu70, which together with yKu80 forms the Ku complex (Bressan *et al.*, 1999). Ku and Mre11 seemingly compete for DSB ends (Clerici *et al.*, 2008) and while Mre11 acts to facilitate end processing (allowing further resection and HR to follow), Ku targets breaks for repair via non-homologous end-joining (NHEJ). In contrast to HR, NHEJ directly rejoins the DNA ends in a manner that can be imprecise and subject to errors (Daley *et al.*, 2005). Furthermore, the ‘ragged’ DSB ends produced by IR are not readily ligatable; therefore if Ku binding prevents DNA end resection and HR in *mre11Δ* cells, these breaks can be lethal. Interestingly, the suppression of IR sensitivity in *mre11Δ* yeast by *yku70Δ* appears to require Exo1 but not Sgs1, arguing that DSB ends not bound by either Mre11 or Ku can only be processed by the Exo1-dependent resection pathway (Mimitou and Symington, 2010). Conversely, when the MRX complex is present but catalytically impaired (either by the *mre11-H125N* point mutation or the absence of *SAE2*), both Sgs1 and Exo1 are able to assist in DNA end processing, leading to the suggestion that an intact Mre11 protein/MRX complex is required for Sgs1 recruitment (Mimitou and Symington, 2010). Further support for this idea is provided by Chiolo *et al.* (2005) who demonstrated that a physical interaction between Mre11 and Sgs1 occurs following activation of the DNA damage checkpoint. Therefore, it is possible that the inability of Sgs1 to function in meiotic resection in *exo1Δ* cells is due to a failure of Mre11 to recruit Sgs1 during meiosis.

It is tempting to speculate that Mre11 could be specifically defective in Sgs1 recruitment during meiosis if the same interaction(s)/modification(s) that allow Mre11 to perform its meiosis-specific functions (*e.g.* in Spo11-catalysed DSB formation/Spo11 removal) also prevent any association with Sgs1. If this were the case it would mean that once removal of Spo11 were achieved, Mre11 would not be

able to recruit Sgs1, leaving Exo1 as the main nuclease available to resect the DSB ends. This theory is somewhat difficult to substantiate experimentally; however, evidence suggesting that this block can be overcome at later time points in *dmc1Δ* meiotic time courses (Manfrini *et al.*, 2010) may provide a useful starting point. For example, co-immunoprecipitation experiments could be performed to determine if an interaction between Mre11 and Sgs1 becomes detectable at these later time points. Alternatively, it may be the case that Sgs1 *is* able to access the DNA ends but its nucleolytic partner, Dna2, cannot. A potential molecular basis for this is not clear. In the future, the delineation of the mechanism(s) preventing Sgs1/Dna2 from participating in meiotic resection could be of great interest as it may provide further insight into the factors that determine which resection pathway is utilised in mitotically cycling cells.

A second noticeable feature of meiotic resection is that even in wild-type cells, the resection tract lengths measured remain relatively short (almost always shorter than 1.25kb in this study) when compared to estimates of mitotic resection. For example, when resection was monitored at an HO endonuclease-induced mitotic DSB capable of undergoing allelic recombination, over half of the cells analysed exhibited resection tracts extending as far as 2.6kb (Chung *et al.*, 2010). This difference could potentially result from the lack of Sgs1 involvement during meiotic repair. However, given that the absence of *SGS1* does not generally confer a resection defect when Exo1 is present, this seems somewhat unlikely. Therefore, a perhaps more probable explanation is that the reduced resection is a consequence of the large number of DSBs that are induced in each cell concomitantly during meiosis. This inevitably places a much higher demand upon the repair machinery of the cell than would be the case when a single mitotic DSB occurs, meaning that the amount of resection that any individual break undergoes is likely to be reduced (Neale *et al.*, 2002; Johnson *et al.*, 2007). Short tracts may be beneficial to the cell for several reasons. For instance, limiting the amount of ssDNA uncovered could help to prevent repetitive sequences located close to the DSB from becoming involved in the search for homology (Inbar and Kupiec, 1999). Such sequences would have the potential to initiate non-allelic recombination, leading to genomic rearrangements. Additionally, the uncovering of homology situated on either side of the break could facilitate

repair via single-strand annealing (SSA). This would result in a potentially lethal deletion of the intervening region.

6.1.2 The influence of resection upon recombination

How the cell determines which DSBs are repaired to yield a crossover and which produce non-crossovers remains an area of active research. It has been suggested that the amount of DNA included within the initial strand invasion intermediate may be important (Khazanehdari and Borts, 2000). Indeed, the only physically assayable strand invasion intermediates detected to date are thought to belong exclusively to the crossover pathway (Hunter and Kleckner, 2001). The extent of resection could in turn determine the amount of DNA available for this invasion event, thereby influencing whether or not crossing-over will take place. For this reason, one of the aims of this study was to test whether the crossover deficient phenotype of *exo1* Δ cells arises as a direct consequence of decreased resection. Contrary to this idea however, the analysis of point mutations affecting the nucleolytic activity of Exo1 revealed that a resection defect does not necessarily confer an equivalent reduction in crossing-over. In fact, in several intervals, crossing-over was maintained at wild-type levels in the nuclease deficient *exo1-D173A*, arguing that resection *per se* does not greatly influence the crossover/non-crossover decision. More recently, it has also been proposed that the extent of resection determines whether DSBs are repaired as crossovers or non-crossovers during mitotic growth (Mitchel *et al.*, 2010). In light of the results presented here, it would be interesting to test whether or not this is the case by analysing whether resection mutants are able to influence the ratio of crossovers to non-crossovers during the mitotic cell cycle.

The ability of the nucleolytically inactive Exo1 protein to support crossing-over demonstrates a novel non-catalytic function for Exo1 in crossover promotion. It was not possible to determine the precise stage at which Exo1's structural role is required from the experiments performed in this study. However, this could be established in the future using 2D gel analysis of crossover-specific recombination intermediates produced at the *HIS4LEU2* hotspot. Evidence from mice *Exo1*^{-/-} models is consistent with a post-Msh4/5 role for Exo1 in supporting crossing-over, important at around the same stage as Mlh1/Mlh3 (Wei *et al.*, 2003; Kan *et al.*, 2008).

In order to confirm that this function is similarly nuclease-independent in higher eukaryotes, the fertility of a mouse line expressing *exo1-D173A* could be assessed.

While resection does not appear to affect crossing-over, the results obtained in this study argue that it may be important in determining gene conversion tract lengths. In the absence of Exo1 or the exonuclease activity of Exo1, both gene conversion tracts and resection tracts are shortened. However, physical analysis of single-stranded DNA suggests that resection gradients and gene conversion gradients do not directly correlate and that hDNA can extend further than resection. Given that resection occurring within the context of dsDNA may not be detectable using the assay employed in this study, these findings are therefore compatible with a role for resection after strand invasion in determining hDNA tract length (Figure 6.1). Such a situation is consistent with the models proposed by Maloisel *et al.* (2004) and Abdullah *et al.* (2004). It has been claimed that meiotic recombination-related DNA synthesis extends further at crossover-designated sites (Terasawa *et al.*, 2007); therefore, if this later resection is coordinated with DNA synthesis, this model can also account for the observation that crossovers are associated with longer hDNA tracts than non-crossovers. We attempted to test this possibility by measuring resection in synthesis deficient *pol3-ct* cells. However the unexpected mitotic growth defect displayed by these cells in the SK1 background prevented such an analysis from being carried out. An alternative approach would be to measure the amount of meiotic recombination-related DNA synthesis that takes place in a resection deficient strain. This could be achieved using the method employed by Terasawa *et al.* (2007), which involved assessing the pattern of thymidine analogue incorporation. As recent genome-wide recombination studies have suggested that up to 1% of the yeast genome undergoes gene conversion in each meiosis (Mancera *et al.*, 2008) and the human genome is estimated to undergo meiotic gene conversion at 4-15 times the frequency that it undergoes crossing-over (Jeffreys and May, 2004), understanding the mechanisms underlying this process is likely to be of vital importance in understanding genetic variation.

6.1.3 Coordinating the multiple roles of Exo1

The identification of separable functions for Exo1 during meiosis raises the question as to how Exo1's participation in these roles is regulated. Previous studies have

demonstrated that both yeast Exo1 and human EXO1 undergo phosphorylation in response to DNA damage (El-Shemerly *et al.*, 2005; Smolka *et al.*, 2007; El-Shemerly *et al.*, 2008; Morin *et al.*, 2008). In these studies, phosphorylation of Exo1 was associated with a down-regulation of Exo1 activity. Protein modifications such as phosphorylation are also known to be important in regulating the ability of proteins to interact with their binding partners. If such a modification were necessary for Exo1 to interact with the proteins necessary to perform its structural function, this could allow the early nuclease-dependent and late nuclease-independent roles of Exo1 to be coordinated. For this reason, it would be of interest to determine if Exo1 undergoes phosphorylation during meiosis. If phosphorylation were detectable, determining the timing of this phosphorylation with respect to meiotic progression may also be informative. Furthermore, co-immunoprecipitation experiments could be employed to test the association of Exo1 with other proteins such as Mre11, Msh4 and Mlh1.

6.2 Conclusions

In conclusion, the work presented in this thesis provides a better insight into the role of Exo1 in meiotic recombination and the mechanics of the meiotic resection process. However, the results of these experiments raise several important questions. For example, why is the Sgs1-mediated resection pathway unable to compensate for the loss of Exo1 during meiotic resection? Is resection coordinated with DNA synthesis? And how is Exo1 regulated in order to be able to perform its multiple functions? In order to further explore these and other issues, a number of potential experiments have been proposed. These include both physical analyses (*e.g.* determining the amount of meiotic recombination-related DNA synthesis that takes place in the *exo1Δ* mutant) and genetic experiments (*e.g.* measuring the ratio of mitotic crossovers to non-crossovers in resection deficient strains). Given the paucity of information available regarding the regulation of meiosis at the proteomic level, it is likely that the analysis of protein-protein interactions and post-translational modifications will also be important in furthering our understanding of the complexities governing the meiotic recombination process.

REFERENCES

- ABDULLAH, M. F., HOFFMANN, E. R., COTTON, V. E. & BORTS, R. H. (2004) A role for the MutL homologue *MLH2* in controlling heteroduplex formation and in regulating between two different crossover pathways in budding yeast. *Cytogenet Genome Res*, 107, 180-90.
- ABDULLAH, M. F. & BORTS, R. H. (2001) Meiotic recombination frequencies are affected by nutritional states in *Saccharomyces cerevisiae*. *Proc Natl Acad Sci USA*, 98, 14524-14529.
- ALANI, E., PADMORE, R. & KLECKNER, N. (1990) Analysis of wild-type and *rad50* mutants of yeast suggests an intimate relationship between meiotic chromosome synapsis and recombination. *Cell*, 61, 419-436.
- ALANI, E., REENAN, R. A. & KOLODNER, R. D. (1994) Interaction between mismatch repair and genetic recombination in *Saccharomyces cerevisiae*. *Genetics*, 137, 19-39.
- ALLERS, T. & LICHTEN, M. (2000) A method for preparing genomic DNA that restrains branch migration of Holliday junctions. *Nucl Acids Res*, 28, e6.
- ALLERS, T. & LICHTEN, M. (2001) Differential timing and control of noncrossover and crossover recombination during meiosis. *Cell*, 106, 47-57.
- AMIN, N. S., NGUYEN, M. N., OH, S. & KOLODNER, R. D. (2001) *exo1*-dependent mutator mutations: model system for studying functional interactions in mismatch repair. *Mol Cell Biol*, 21, 5142-55.
- ARGUESO, J. L., WANAT, J., GEMICI, Z. & ALANI, E. (2004) Competing crossover pathways act during meiosis in *Saccharomyces cerevisiae*. *Genetics*, 168, 1805-1816.
- ASEFA, B., KAULER, P., COURNOYER, D., LEHNERT, S. & CHOW, T. Y. K. (1998) Genetic analysis of the yeast *NUD1* endo-exonuclease: a role in the repair of DNA double-strand breaks. *Curr Genet*, 34, 360-367.
- BAE, S.-H. & SEO, Y.-S. (2000) Characterization of the enzymatic properties of the yeast Dna2 helicase/endonuclease suggests a new model for Okazaki fragment processing. *J Biol Chem*, 275, 38022-38031.
- BAKER, S. M., PLUG, A. W., PROLLA, T. A., BRONNER, C. E., HARRIS, A. C., YAO, X., CHRISTIE, D. M., MONELL, C., ARNHEIM, N., BRADLEY, A., ASHLEY, T. & LISKAY, R. M. (1996) Involvement of mouse Mlh1 in DNA mismatch repair and meiotic crossing over. *Nat Genet*, 13, 336-342.

- BAUDAT, F. & NICOLAS, A. (1997) Clustering of meiotic double-strand breaks on yeast chromosome III. *Proc Natl Acad Sci USA*, 94, 5213-5218.
- BISHOP, D. K., PARK, D., XU, L. & KLECKNER, N. (1992) *DMC1*: A meiosis-specific yeast homolog of *E. coli* recA required for recombination, synaptonemal complex formation, and cell cycle progression. *Cell*, 69, 439-456.
- BISHOP, D. K. & ZICKLER, D. (2004) Early decision: meiotic crossover interference prior to stable strand exchange and synapsis. *Cell*, 117, 9-15.
- BLITZBLAU, H. G., BELL, G. W., RODRIGUEZ, J., BELL, S. P. & HOCHWAGEN, A. (2007) Mapping of meiotic single-stranded DNA reveals double-stranded-break hotspots near centromeres and telomeres. *Curr Biol*, 17, 2003-12.
- BODDY, M. N., GAILLARD, P. H., MCDONALD, W. H., SHANAHAN, P., YATES, J. R., 3RD & RUSSELL, P. (2001) Mus81-Eme1 are essential components of a Holliday junction resolvase. *Cell*, 107, 537-48.
- BOLDERSON, E., TOMIMATSU, N., RICHARD, D. J., BOUCHER, D., KUMAR, R., PANDITA, T. K., BURMA, S. & KHANNA, K. K. (2009) Phosphorylation of Exo1 modulates homologous recombination repair of DNA double-strand breaks. *Nucl Acids Res* 1-11.
- BORDE, V. & COBB, J. (2009) Double functions for the Mre11 complex during DNA double-strand break repair and replication. *Int J Biochem Cell Biol*, 41, 1249-1253.
- BORDE, V., GOLDMAN, A. S. & LICHTEN, M. (2000) Direct coupling between meiotic DNA replication and recombination initiation. *Science*, 290, 806-9.
- BORDE, V., ROBINE, N., LIN, W., BONFILS, S., GELI, V. & NICOLAS, A. (2009) Histone H3 lysine 4 trimethylation marks meiotic recombination initiation sites. *Embo J*, 28, 99-111.
- BORNER, G. V., KLECKNER, N. & HUNTER, N. (2004) Crossover/noncrossover differentiation, synaptonemal complex formation, and regulatory surveillance at the leptotene/zygotene transition of meiosis. *Cell*, 117, 29-45.
- BORTS, R. H., CHAMBERS, S. R. & ABDULLAH, M. F. (2000) The many faces of mismatch repair in meiosis. *Mutat Res*, 451, 129-50.
- BORTS, R. H. & HABER, J. E. (1989) Length and distribution of meiotic gene conversion tracts and crossovers in *Saccharomyces cerevisiae*. *Genetics*, 123, 69-80.
- BORTS, R. H., LICHTEN, M. & HABER, J. E. (1986) Analysis of meiosis-defective mutations in yeast by physical monitoring of recombination. *Genetics*, 113, 551-67.

- BRESSAN, D. A., BAXTER, B. K. & PETRINI, J. H. J. (1999) The Mre11-Rad50-Xrs2 protein complex facilitates homologous recombination-based double-strand break repair in *Saccharomyces cerevisiae*. *Mol Cell Biol*, 19, 7681-7687.
- BUHLER, C., BORDE, V. & LICHTEN, M. (2007) Mapping meiotic single-strand DNA reveals a new landscape of DNA double-strand breaks in *Saccharomyces cerevisiae*. *PLoS Biol*, 5, e324.
- CAO, L., ALANI, E. & KLECKNER, N. (1990) A pathway for generation and processing of double-strand breaks during meiotic recombination in *S. cerevisiae*. *Cell*, 61, 1089-1101.
- CARBALLO, J. S. A., JOHNSON, A. L., SEDGWICK, S. G. & CHA, R. S. (2008) Phosphorylation of the axial element protein Hop1 by Mec1/Tel1 ensures meiotic interhomolog recombination. *Cell*, 132, 758-770.
- CARTAGENA-LIROLA, H., GUERINI, I., MANFRINI, N., LUCCHINI, G. & LONGHESE, M. P. (2008) Role of the *Saccharomyces cerevisiae* Rad53 checkpoint kinase in signaling double-strand breaks during the meiotic cell cycle. *Mol Cell Biol*, 28, 4480-4493.
- CARTAGENA-LIROLA, H., GUERINI, I., VISCARDI, V., LUCCHINI, G. & LONGHESE, M. P. (2006) Budding yeast Sae2 is an in vivo target of the Mec1 and Tel1 checkpoint kinases during meiosis. *Cell Cycle*, 5, 1549-1559.
- CHAIX, A. (2007) Genetic analysis and meiotic role of the *Saccharomyces cerevisiae* RecQ helicase *SGS1*. *Department of Genetics*. PhD thesis. University of Leicester.
- CHAMBERS, S. R., HUNTER, N., LOUIS, E. J. & BORTS, R. H. (1996) The mismatch repair system reduces meiotic homeologous recombination and stimulates recombination-dependent chromosome loss. *Mol Cell Biol*, 16, 6110-20.
- CHAN, A. C.-H., BORTS, R. H. & HOFFMANN, E. (2009) Temperature-dependent modulation of chromosome segregation in *msb4* mutants of budding yeast. *PLoS ONE*, 4, e7284.
- CHEN, S. Y., TSUBOUCHI, T., ROCKMILL, B., SANDLER, J. S., RICHARDS, D. R., VADER, G., HOCHWAGEN, A., ROEDER, G. S. & FUNG, J. C. (2008) Global analysis of the meiotic crossover landscape. *Dev Cell*, 15, 401-415.
- CHIOLO, I., CAROTENUTO, W., MAFFIOLETTI, G., PETRINI, J. H. J., FOIANI, M. & LIBERI, G. (2005) Srs2 and Sgs1 DNA helicases associate with Mre11 in different subcomplexes following checkpoint activation and CDK1-mediated Srs2 phosphorylation. *Mol Cell Biol*, 25, 5738-5751.
- CHOUDHURY, S., ASEFA, B., KAULER, P. & CHOW, T. (2007a) Synergistic effect of *TRM2/RNC1* and *EXO1* in DNA double-strand break repair in *Saccharomyces cerevisiae*. *Mol Cell Biochem*, 304, 127-134.

- CHOUDHURY, S. A., ASEFA, B., WEBB, A., RAMOTAR, D. & CHOW, T. Y. K. (2007b) Functional and genetic analysis of the *Saccharomyces cerevisiae* RNC1/TRM2: evidences for its involvement in DNA double-strand break repair. *Mol Cell Biochem*, 300, 215-226.
- CHU, S., DERISI, J., EISEN, M., MULHOLLAND, J., BOTSTEIN, D., BROWN, P. O. & HERSKOWITZ, I. (1998) The transcriptional program of sporulation in budding yeast. *Science*, 282, 699-705.
- CHU, W. K. & HICKSON, I. D. (2009) RecQ helicases: multifunctional genome caretakers. *Nat Rev Cancer*, 9, 644-654.
- CHUA, P. R. & ROEDER, G. S. (1997) Tam1, a telomere-associated meiotic protein, functions in chromosome synapsis and crossover interference. *Genes Dev*, 11, 1786-1800.
- CHUNG, W.-H., ZHU, Z., PAPUSHA, A., MALKOVA, A. & IRA, G. (2010) Defective resection at DNA double-strand breaks leads to *de novo* telomere formation and enhances gene targeting. *PLoS Genet*, 6, e1000948.
- CLERICI, M., MANTIERO, D., GUERINI, I., LUCCHINI, G. & LONGHESE, M. P. (2008) The YKu70-YKu80 complex contributes to regulate double-strand break processing and checkpoint activation during the cell cycle. *Embo Rep*, 9, 810-818.
- CLERICI, M., MANTIERO, D., LUCCHINI, G. & LONGHESE, M. P. (2005) The *Saccharomyces cerevisiae* Sae2 protein promotes resection and bridging of double strand break ends. *J Biol Chem*, 280, 38631-38638.
- CONSTANTIN, N., DZANTIEV, L., KADYROV, F. A. & MODRICH, P. (2005) Human mismatch repair: reconstitution of a nick-directed bidirectional reaction. *J Biol Chem*, 280, 39752-61.
- COOPER, K. W. (1945) Normal segregation without chiasmata in *Drosophila melanogaster*. *Genetics*, 30, 472-484.
- COTTON, V. E. (2007) A structural and functional analysis of mismatch repair proteins in meiosis. *Department of Genetics*. PhD thesis. University of Leicester.
- COTTON, V. E., HOFFMANN, E. R., ABDULLAH, M. F. & BORTS, R. H. (2009) Interaction of genetic and environmental factors in *Saccharomyces cerevisiae* meiosis: The devil is in the details. IN KEENEY, S. (Ed.) *Meiosis: Volume 1, Molecular and Genetic Methods*. Totowa, Humana Press.
- COTTON, V. E., HOFFMANN, E. R. & BORTS, R. H. (2010) Distinct regulation of Mlh1p heterodimers in meiosis and mitosis in *Saccharomyces cerevisiae*. *Genetics*, 185, 459-467.
- DALEY, J. M., PALMBOS, P. L., WU, D. & WILSON, T. E. (2005) Nonhomologous end joining in yeast. *Annu Rev Genet*, 39, 431-451.
- DE LOS SANTOS, T., HUNTER, N., LEE, C., LARKIN, B., LOIDL, J. & HOLLINGSWORTH, N. M. (2003) The Mus81/Mms4 endonuclease acts

- independently of double-Holliday junction resolution to promote a distinct subset of crossovers during meiosis in budding yeast. *Genetics*, 164, 81-94.
- DE LOS SANTOS, T., LOIDL, J., LARKIN, B. & HOLLINGSWORTH, N. M. (2001) A role for *MMS4* in the processing of recombination intermediates during meiosis in *Saccharomyces cerevisiae*. *Genetics*, 159, 1511-25.
- DETLOFF, P. & PETES, T. D. (1992) Measurements of excision repair tracts formed during meiotic recombination in *Saccharomyces cerevisiae*. *Mol Cell Biol*, 12, 1805-1814.
- DETLOFF, P., SIEBER, J. & PETES, T. D. (1991) Repair of specific base pair mismatches formed during meiotic recombination in the yeast *Saccharomyces cerevisiae*. *Mol Cell Biol*, 11, 737-745.
- DETLOFF, P., WHITE, M. A. & PETES, T. D. (1992) Analysis of a gene conversion gradient at the *HIS4* locus in *Saccharomyces cerevisiae*. *Genetics*, 132, 113-123.
- DERIN, C., GUENEAU, E., FRANCIN, M., NUNEZ, M., MIRON, S., LIBERTI, S. E., RASMUSSEN, L. J., ZINN-JUSTIN, S., GILQUIN, B., CHARBONNIER, J.-B. & BOITEUX, S. (2009) Characterization of a highly conserved binding site of Mlh1 required for Exonuclease I-dependent mismatch repair. *Mol Cell Biol*, 29, 907-918.
- DIGILIO, F. A., PANNUTI, A., LUCCHESI, J. C., FURIA, M. & POLITO, L. (1996) Tosca: A *Drosophila* gene encoding a nuclease specifically expressed in the female germline. *Dev Biol*, 178, 90-100.
- DZANTIEV, L., CONSTANTIN, N., GENSCHER, J., IYER, R. R., BURGERS, P. M. & MODRICH, P. (2004) A defined human system that supports bidirectional mismatch-provoked excision. *Mol Cell*, 15, 31-41.
- EDELMANN, W., COHEN, P. E., KANE, M., LAU, K., MORROW, B., BENNETT, S., UMAR, A., KUNKEL, T., CATTORETTI, G., CHAGANTI, R., POLLARD, J. W., KOLODNER, R. D. & KUCHERLAPATI, R. (1996) Meiotic pachytene arrest in MLH1-deficient mice. *Cell*, 85, 1125-1134.
- EGEL, R. (1978) Synaptonemal complex and crossing-over: structural support or interference? *Heredity*, 41, 233-237.
- EGEL-MITANI, M. O., LAURITZ W.; EGEL,RICHARD (1982) Meiosis in *Aspergillus nidulans*: Another example for lacking synaptonemal complexes in the absence of crossover interference. *Hereditas*, 97, 179-187.
- EGYDIO DE CARVALHO, C. & COLAIACOVO, M. P. (2006) SUMO-mediated regulation of synaptonemal complex formation during meiosis. *Genes Dev*, 20, 1986-1992.
- EL-SHEMERLY, M., HESS, D., PYAKUREL, A. K., MOSELHY, S. & FERRARI, S. (2008) ATR-dependent pathways control hEXO1 stability in response to stalled forks. *Nucl Acids Res*, 36, 511-519.

- EL-SHEMERLY, M., JANSČAK, P., HESS, D., JIRICNY, J. & FERRARI, S. (2005) Degradation of human Exonuclease 1b upon DNA synthesis inhibition. *Cancer Res*, 65, 3604-3609.
- ERDENIZ, N., MORTENSEN, U. H. & ROTHSTEIN, R. (1997) Cloning-free PCR-based allele replacement methods. *Genome Res*, 7, 1174-83.
- FAN, Q., XU, F. & PETES, T. D. (1995) Meiosis-specific double-strand DNA breaks at the *HIS4* recombination hot spot in the yeast *Saccharomyces cerevisiae*: control in cis and trans. *Mol Cell Biol*, 15, 1679-88.
- FAN, Q. Q. & PETES, T. D. (1996) Relationship between nuclease-hypersensitive sites and meiotic recombination hot spot activity at the *HIS4* locus of *Saccharomyces cerevisiae*. *Mol Cell Biol*, 16, 2037-2043.
- FIORENTINI, P., HUANG, K. N., TISHKOFF, D. X., KOLODNER, R. D. & SYMINGTON, L. S. (1997) Exonuclease I of *Saccharomyces cerevisiae* functions in mitotic recombination in vivo and in vitro. *Mol Cell Biol*, 17, 2764-73.
- FLORES-ROZAS, H. & KOLODNER, R. D. (1998) The *Saccharomyces cerevisiae* *MLH3* gene functions in *MSH3*-dependent suppression of frameshift mutations. *Proc Natl Acad Sci USA*, 95, 12404-9.
- FOSS, E., LANDE, R., STAHL, F. W. & STEINBERG, C. M. (1993) Chiasma interference as a function of genetic distance. *Genetics*, 133, 681-691.
- FOSS, E. J. & STAHL, F. W. (1995) A test of a counting model for chiasma interference. *Genetics*, 139, 1201-1209.
- FRANK, G., QIU, J., SOMSOUK, M., WENG, Y., SOMSOUK, L., NOLAN, J. P. & SHEN, B. (1998) Partial functional deficiency of E160D flap endonuclease-1 mutant *in vitro* and *in vivo* is due to defective cleavage of DNA substrates. *J Biol Chem*, 273, 33064-33072.
- FRICKE, W. M. & BRILL, S. J. (2003) Slx1-Slx4 is a second structure-specific endonuclease functionally redundant with Sgs1-Top3. *Genes Dev*, 17, 1768-1778.
- FUNG, J. C., ROCKMILL, B., ODELL, M. & ROEDER, G. S. (2004) Imposition of crossover interference through the nonrandom distribution of synapsis initiation complexes. *Cell*, 116, 795-802.
- FURUSE, M., NAGASE, Y., TSUBOUCHI, H., MURAKAMI-MUROFUSHI, K., SHIBATA, T. & OHTA, K. (1998) Distinct roles of two separable *in vitro* activities of yeast Mre11 in mitotic and meiotic recombination. *Embo J*, 17, 6412-25.
- GARY, R., PARK, M. S., NOLAN, J. P., CORNELIUS, H. L., KOZYREVA, O. G., TRAN, H. T., LOBACHEV, K. S., RESNICK, M. A. & GORDENIN, D. A. (1999) A novel role in DNA metabolism for the binding of Fen1/Rad27 to PCNA and implications for genetic risk. *Mol Cell Biol*, 19, 5373-5382.

- GASIOR, S. L., OLIVARES, H., EAR, U., HARI, D. M., WEICHSELBAUM, R. & BISHOP, D. K. (2001) Assembly of RecA-like recombinases: Distinct roles for mediator proteins in mitosis and meiosis. *Proc Natl Acad Sci USA*, 98, 8411-8418.
- GERTON, J. L., DERISI, J., SHROFF, R., LICHTEN, M., BROWN, P. O. & PETES, T. D. (2000) Global mapping of meiotic recombination hotspots and coldspots in the yeast *Saccharomyces cerevisiae*. *Proc Natl Acad Sci USA*, 97, 11383-11390.
- GIETZ, R. D. & SCHIESTL, R. H. (2007) High-efficiency yeast transformation using the LiAc/SS carrier DNA/PEG method. *Nat Protoc*, 2, 31-34.
- GILBERTSON, L. A. & STAHL, F. W. (1996) A test of the double-strand break repair model for meiotic recombination in *Saccharomyces cerevisiae*. *Genetics*, 144, 27-41.
- GOLDSTEIN, A. L. & MCCUSKER, J. H. (1999) Three new dominant drug resistance cassettes for gene disruption in *Saccharomyces cerevisiae*. *Yeast*, 15, 1541-1553.
- GRAVEL, S., CHAPMAN, J. R., MAGILL, C. & JACKSON, S. P. (2008) DNA helicases Sgs1 and BLM promote DNA double-strand break resection. *Genes Dev*, 22, 2767-2772.
- GREENE, J., VOTH, W., AND STILLMAN, D. (1994) MacTetrad 6.9 and MacTetrad 6.7.3, in *Gopher*, from www.merlot.welch.jhu.edu.
- GUILLOIN, H., BAUDAT, F., GREY, C., LISKAY, R. M. & DE MASSY, B. (2005) Crossover and noncrossover pathways in mouse meiosis. *Mol Cell*, 20, 563-73.
- HABRAKEN, Y., SUNG, P., PRAKASH, L. & PRAKASH, S. (1997) Enhancement of *MSH2-MSH3*-mediated mismatch recognition by the yeast *MLH1-PMS1* complex. *Curr Biol*, 7, 790-3.
- HARFE, B. D., MINESINGER, B. K. & JINKS-ROBERTSON, S. (2000) Discrete *in vivo* roles for the MutL homologs Mlh2p and Mlh3p in the removal of frameshift intermediates in budding yeast. *Curr Biol*, 10, 145-8.
- HARRISON, J. C. & HABER, J. E. (2006) Surviving the breakup: The DNA damage checkpoint. *Annu Rev Genet*, 40, 209-235.
- HASSOLD, T. & HUNT, P. (2001) To err (meiotically) is human: the genesis of human aneuploidy. *Nat Rev Genet*, 2, 280-291.
- HENDERSON, K. A. & KEENEY, S. (2004) Tying synaptonemal complex initiation to the formation and programmed repair of DNA double-strand breaks. *Proc Natl Acad Sci USA*, 101, 4519-24.
- HILLERS, K. J. (2004) Crossover interference. *Curr Biol*, 14, R1036-7.

- HILLERS, K. J. & STAHL, F. W. (1999) The conversion gradient at *HIS4* of *Saccharomyces cerevisiae*. I. Heteroduplex rejection and restoration of Mendelian segregation. *Genetics*, 153, 555-572.
- HINNEBUSCH, A. G. & NATARAJAN, K. (2002) Gcn4p, a master regulator of gene expression, is controlled at multiple levels by diverse signals of starvation and stress. *Eukaryot Cell*, 1, 22-32.
- HODGSON, A., TERYTYEV, Y., JOHNSON, R. A., BISHOP-BAILEY, A. & GOLDMAN, A. S. H. (2010) Mre11 and Exo1 contribute to the initiation and processivity of resection at meiotic double-strand breaks made independently of Spo11. *Submitted*.
- HOFFMANN, E. R. & BORTS, R. H. (2004) Meiotic recombination intermediates and mismatch repair proteins. *Cytogenet Genome Res*, 107, 232-48.
- HOFFMANN, E. R. & BORTS, R. H. (2005) Trans events associated with crossovers are revealed in the absence of mismatch repair genes in *Saccharomyces cerevisiae*. *Genetics*, 169, 1305-10.
- HOFFMANN, E. R., ERIKSSON, E., HERBERT, B. J. & BORTS, R. H. (2005) *MLH1* and *MSH2* promote the symmetry of double-strand break repair events at the *HIS4* hotspot in *Saccharomyces cerevisiae*. *Genetics*, 169, 1291-303.
- HOFFMANN, E. R., SHCHERBAKOVA, P. V., KUNKEL, T. A. & BORTS, R. H. (2003) *MLH1* mutations differentially affect meiotic functions in *Saccharomyces cerevisiae*. *Genetics*, 163, 515-26.
- HOLLINGSWORTH, N. M. & BRILL, S. J. (2004) The Mus81 solution to resolution: Generating meiotic crossovers without Holliday junctions. *Genes Dev*, 18, 117-125.
- HOLLOWAY, J. K., BOOTH, J., EDELMANN, W., MCGOWAN, C. H. & COHEN, P. E. (2008) MUS81 generates a subset of MLH1-MLH3 independent crossovers in mammalian meiosis. *PLoS Genet*, 4, e1000186.
- HOPKINS, B. B. & PAULL, T. T. (2008) The *P. furiosus* Mre11/Rad50 complex promotes 5' strand resection at a DNA double-strand break. *Cell*, 135, 250-260.
- HUNTER, N. (2006) Meiotic Recombination. IN AGUILERA, A. & ROTHSTEIN, R. (Eds.) *Molecular Genetics of Recombination*. Heidelberg, Springer-Verlag.
- HUNTER, N. & BORTS, R. H. (1997) Mlh1 is unique among mismatch repair proteins in its ability to promote crossing-over during meiosis. *Genes Dev*, 11, 1573-82.
- HUNTER, N. & KLECKNER, N. (2001) The single-end invasion: An asymmetric intermediate at the double-strand break to double-Holliday junction transition of meiotic recombination. *Cell*, 106, 59-70.
- INBAR, O. & KUPIEC, M. (1999) Homology search and choice of homologous partner during mitotic recombination. *Mol Cell Biol*, 19, 4134-4142.

- IP, S. C. Y., RASS, U., BLANCO, M. G., FLYNN, H. R., SKEHEL, J. M. & WEST, S. C. (2008) Identification of Holliday junction resolvases from humans and yeast. *Nature*, 456, 357-361.
- IRA, G. & HABER, J. E. (2002) Characterization of *RAD51*-independent break-induced replication that acts preferentially with short homologous sequences. *Mol Cell Biol*, 22, 6384-6392.
- IRA, G., MALKOVA, A., LIBERI, G., FOIANI, M. & HABER, J. E. (2003) Srs2 and Sgs1-Top3 suppress crossovers during double-strand break repair in yeast. *Cell*, 115, 401-11.
- JEFFREYS, A. J. & MAY, C. A. (2004) Intense and highly localized gene conversion activity in human meiotic crossover hot spots. *Nat Genet*, 36, 151-6.
- JESSOP, L., ALLERS, T. & LICHTEN, M. (2005) Infrequent co-conversion of markers flanking a meiotic recombination initiation site in *Saccharomyces cerevisiae*. *Genetics*, 169, 1353-1367.
- JESSOP, L. & LICHTEN, M. (2008) Mus81/Mms4 endonuclease and Sgs1 helicase collaborate to ensure proper recombination intermediate metabolism during meiosis. *Mol Cell*, 31, 313-323.
- JESSOP, L., ROCKMILL, B., ROEDER, G. S. & LICHTEN, M. (2006) Meiotic chromosome synapsis-promoting proteins antagonize the anti-crossover activity of Sgs1. *PLoS Genet*, 2, e155.
- JINKS-ROBERTSON, S., MICHELITCH, M. & RAMCHARAN, S. (1993) Substrate length requirements for efficient mitotic recombination in *Saccharomyces cerevisiae*. *Mol Cell Biol*, 13, 3937-3950.
- JIRICNY, J. (2006) The multifaceted mismatch-repair system. *Nat Rev Mol Cell Biol*, 7, 335-46.
- JOHNSON, R., BORDE, V., NEALE, M. J., BISHOP-BAILEY, A., NORTH, M., HARRIS, S., NICOLAS, A. & GOLDMAN, A. S. H. (2007) Excess single-stranded DNA inhibits meiotic double-strand break repair. *PLoS Genet*, 3, e223.
- JOHZUKA, K. & OGAWA, H. (1995) Interaction of Mre11 and Rad50: two proteins required for DNA repair and meiosis-specific double-strand break formation in *Saccharomyces cerevisiae*. *Genetics*, 139, 1521-1532.
- JOSHI, N., BAROT, A., JAMISON, C. & BORNER, G. V. (2009) Pch2 links chromosome axis remodeling at future crossover sites and crossover distribution during yeast meiosis. *PLoS Genet*, 5, e1000557.
- KADYROV, F. A., DZANTIEV, L., CONSTANTIN, N. & MODRICH, P. (2006) Endonucleolytic function of MutLalpha in human mismatch repair. *Cell*, 126, 297-308.
- KADYROV, F. A., GENSCHEL, J., FANG, Y., PENLAND, E., EDELMANN, W. & MODRICH, P. (2009) A possible mechanism for Exonuclease 1-

- independent eukaryotic mismatch repair. *Proc Natl Acad Sci USA*, 106, 8495-8500.
- KADYROV, F. A., HOLMES, S. F., ARANA, M. E., LUKIANOVA, O. A., O'DONNELL, M., KUNKEL, T. A. & MODRICH, P. (2007) *Saccharomyces cerevisiae* MutL α is a mismatch repair endonuclease. *J Biol Chem*, 282, 37181-37190.
- KAN, R., SUN, X., KOLAS, N. K., AVDIEVICH, E., KNEITZ, B., EDELMANN, W. & COHEN, P. E. (2008) Comparative analysis of meiotic progression in female mice bearing mutations in genes of the DNA mismatch repair pathway. *Biol Reprod*, 78, 462-471.
- KANE, S. M. & ROTH, R. (1974) Carbohydrate metabolism during ascospore development in yeast. *J Bacteriol*, 118, 8-14.
- KEENEY, S., GIROUX, C. N. & KLECKNER, N. (1997) Meiosis-specific DNA double-strand breaks are catalyzed by Spo11, a member of a widely conserved protein family. *Cell*, 88, 375-384.
- KEENEY, S. & KLECKNER, N. (1995) Covalent protein-DNA complexes at the 5' strand termini of meiosis-specific double-strand breaks in yeast. *Proc Natl Acad Sci USA*, 92, 11274-11278.
- KEENEY, S. & NEALE, M. J. (2006) Initiation of meiotic recombination by formation of DNA double-strand breaks: mechanism and regulation. *Biochem Soc Trans*, 34, 523-5.
- KHAZANEHDARI, K. A. & BORTS, R. H. (2000) *EXO1* and *MSH4* differentially affect crossing-over and segregation. *Chromosoma*, 109, 94-102.
- KIM, H.-S., VIJAYAKUMAR, S., REGER, M., HARRISON, J. C., HABER, J. E., WEIL, C. & PETRINI, J. H. J. (2008) Functional interactions between Sae2 and the Mre11 complex. *Genetics*, 178, 711-723.
- KIRKPATRICK, D. T., DOMINSKA, M. & PETES, T. D. (1998) Conversion-type and restoration-type repair of DNA mismatches formed during meiotic recombination in *Saccharomyces cerevisiae*. *Genetics*, 149, 1693-705.
- KIRKPATRICK, D. T., FERGUSON, J. R., PETES, T. D. & SYMINGTON, L. S. (2000) Decreased meiotic intergenic recombination and increased meiosis I nondisjunction in *exo1* mutants of *Saccharomyces cerevisiae*. *Genetics*, 156, 1549-1557.
- KIRKPATRICK, D. T., WANG, Y. H., DOMINSKA, M., GRIFFITH, J. D. & PETES, T. D. (1999) Control of meiotic recombination and gene expression in yeast by a simple repetitive DNA sequence that excludes nucleosomes. *Mol Cell Biol*, 19, 7661-71.
- KLECKNER, N., ZICKLER, D., JONES, G. H., DEKKER, J., PADMORE, R., HENLE, J. & HUTCHINSON, J. (2004) A mechanical basis for chromosome function. *Proc Natl Acad Sci USA*, 101, 12592-12597.

- KNIEWEL, R. & KEENEY, S. (2009) Histone methylation sets the stage for meiotic DNA breaks. *Embo J*, 28, 81-83.
- KROGH, B. O. & SYMINGTON, L. S. (2004) Recombination proteins in yeast. *Annu Rev Genet*, 38, 233-271.
- KUNKEL, T. A. & ERIE, D. A. (2005) DNA mismatch repair. *Annu Rev Biochem*, 74, 681-710.
- LAO, J. P., OH, S. D., SHINOHARA, M., SHINOHARA, A. & HUNTER, N. (2008) Rad52 promotes postinvasion steps of meiotic double-strand-break repair. *Mol Cell*, 29, 517-524.
- LEE, B., SHANNON, M., STUBBS, L. & WILSON, D., 3RD (1999) Expression specificity of the mouse Exonuclease 1 (mExo1) gene. *Nucl Acids Res*, 27, 4114-4120.
- LEE, B. H. & AMON, A. (2003) Role of polo-like kinase *CDC5* in programming meiosis I chromosome segregation. *Science*, 300, 482-486.
- LEE, B. I., NGUYEN, L. H., BARSKY, D., FERNANDES, M. & WILSON, D. M., 3RD (2002) Molecular interactions of human Exo1 with DNA. *Nucl Acids Res*, 30, 942-9.
- LENGSFELD, B. M., RATTRAY, A. J., BHASKARA, V., GHIRLANDO, R. & PAULL, T. T. (2007) Sae2 is an endonuclease that processes hairpin DNA cooperatively with the Mre11/Rad50/Xrs2 complex. *Mol Cell*, 28, 638-651.
- LIAO, S., TOCZYLOWSKI, T. & YAN, H. (2008) Identification of the *Xenopus* DNA2 protein as a major nuclease for the 5' to 3' strand-specific processing of DNA ends. *Nucl Acids Res*, 36, 6091-6100.
- LIPKIN, S. M., MOENS, P. B., WANG, V., LENZI, M., SHANMUGARAJAH, D., GILGEOUS, A., THOMAS, J., CHENG, J., TOUCHMAN, J. W., GREEN, E. D., SCHWARTZBERG, P., COLLINS, F. S. & COHEN, P. E. (2002) Meiotic arrest and aneuploidy in MLH3-deficient mice. *Nat Genet*, 31, 385-90.
- LIU, J., WU, T. C. & LICHTEN, M. (1995) The location and structure of double-strand DNA breaks induced during yeast meiosis: evidence for a covalently linked DNA-protein intermediate. *Embo J*, 14, 4599-608.
- LYNN, A., SOUCEK, R. & BÖRNER, G. (2007) ZMM proteins during meiosis: Crossover artists at work. *Chromosome Res*, 15, 591-605.
- MALKOVA, A., SWANSON, J., GERMAN, M., MCCUSKER, J. H., HOUSWORTH, E. A., STAHL, F. W. & HABER, J. E. (2004) Gene conversion and crossing over along the 405-kb left arm of *Saccharomyces cerevisiae* chromosome VII. *Genetics*, 168, 49-63.
- MALOISEL, L., BHARGAVA, J. & ROEDER, G. S. (2004) A role for DNA polymerase delta in gene conversion and crossing over during meiosis in *Saccharomyces cerevisiae*. *Genetics*, 167, 1133-1142.

- MALONE, R. E., BULLARD, S., LUNDQUIST, S., KIM, S. & TARKOWSKI, T. (1992) A meiotic gene conversion gradient opposite to the direction of transcription. *Nature*, 359, 154-155.
- MANCERA, E., BOURGON, R., BROZZI, A., HUBER, W. & STEINMETZ, L. M. (2008) High-resolution mapping of meiotic crossovers and non-crossovers in yeast. *Nature*, 454, 479-485.
- MANFRINI, N., GUERINI, I., CITTERIO, A., LUCCHINI, G. & LONGHESE, M. P. (2010) Processing of meiotic DNA double strand breaks requires cyclin-dependent kinase and multiple nucleases. *J Biol Chem*, 285, 11628-37.
- MARSISCHKY, G. T., FILOSI, N., KANE, M. F. & KOLODNER, R. (1996) Redundancy of *Saccharomyces cerevisiae* *MSH3* and *MSH6* in *MSH2*-dependent mismatch repair. *Genes Dev*, 10, 407-20.
- MARTINI, E., DIAZ, R. L., HUNTER, N. & KEENEY, S. (2006) Crossover homeostasis in yeast meiosis. *Cell*, 126, 285-295.
- MAZINA, O. M., MAZIN, A. V., NAKAGAWA, T., KOLODNER, R. D. & KOWALCZYKOWSKI, S. C. (2004) *Saccharomyces cerevisiae* Mer3 helicase stimulates 3'-5' heteroduplex extension by Rad51: Implications for crossover control in meiotic recombination. *Cell*, 117, 47-56.
- MCKEE, A. & KLECKNER, N. (1997) A general method for identifying recessive diploid-specific mutations in *Saccharomyces cerevisiae*, its application to the isolation of mutants blocked at intermediate stages of meiotic prophase and characterization of a new gene *SAE2*. *Genetics*, 146, 797-816.
- MCMAHILL, M. S., SHAM, C. W. & BISHOP, D. K. (2007) Synthesis-dependent strand annealing in meiosis. *PLoS Biol*, 5, e299.
- MERKER, J. D., DOMINSKA, M. & PETES, T. D. (2003) Patterns of heteroduplex formation associated with the initiation of meiotic recombination in the yeast *Saccharomyces cerevisiae*. *Genetics*, 165, 47-63.
- MIECZKOWSKI, P. A., DOMINSKA, M., BUCK, M. J., GERTON, J. L., LIEB, J. D. & PETES, T. D. (2006) Global analysis of the relationship between the binding of the Bas1p transcription factor and meiosis-specific double-strand DNA breaks in *Saccharomyces cerevisiae*. *Mol Cell Biol*, 26, 1014-27.
- MIMITOU, E. P. & SYMINGTON, L. S. (2008) Sae2, Exo1 and Sgs1 collaborate in DNA double-strand break processing. *Nature*, 455, 770-774.
- MIMITOU, E. P. & SYMINGTON, L. S. (2010) Ku prevents Exo1 and Sgs1-dependent resection of DNA ends in the absence of a functional MRX complex or Sae2. *Embo J*, advance online publication.
- MITCHEL, K., ZHANG, H., WELZ-VOEGELE, C. & JINKS-ROBERTSON, S. (2010) Molecular structures of crossover and noncrossover intermediates during gap repair in yeast: Implications for recombination. *Mol Cell*, 38, 211-222.

- MOREAU, S., FERGUSON, J. R. & SYMINGTON, L. S. (1999) The nuclease activity of Mre11 Is required for meiosis but not for mating type switching, end joining, or telomere maintenance. *Mol Cell Biol*, 19, 556-566.
- MORIN, I., NGO, H.-P., GREENALL, A., ZUBKO, M. K., MORRICE, N. & LYDALL, D. (2008) Checkpoint-dependent phosphorylation of Exo1 modulates the DNA damage response. *Embo J*, 27, 2400-2410.
- MURAKAMI, H., BORDE, V., SHIBATA, T., LICHTEN, M. & OHTA, K. (2003) Correlation between premeiotic DNA replication and chromatin transition at yeast recombination initiation sites. *Nucl Acids Res*, 31, 4085-4090.
- NAG, D. K. & PETES, T. D. (1993) Physical detection of heteroduplexes during meiotic recombination in the yeast *Saccharomyces cerevisiae*. *Mol Cell Biol*, 13, 2324-31.
- NAG, D. K., WHITE, M. A. & PETES, T. D. (1989) Palindromic sequences in heteroduplex DNA inhibit mismatch repair in yeast. *Nature*, 340, 318-320.
- NAIRZ, K. & KLEIN, F. (1997) *mre11S* - a yeast mutation that blocks double-strand-break processing and permits nonhomologous synapsis in meiosis. *Genes Dev*, 11, 2272-2290.
- NAKAGAWA, T. & KOLODNER, R. D. (2002) *Saccharomyces cerevisiae* Mer3 is a DNA helicase involved in meiotic crossing over. *Mol Cell Biol*, 22, 3281-3291.
- NAKAGAWA, T. & OGAWA, H. (1999) The *Saccharomyces cerevisiae* MER3 gene, encoding a novel helicase-like protein, is required for crossover control in meiosis. *Embo J*, 18, 5714-5723.
- NATARAJAN, K., MEYER, M. R., JACKSON, B. M., SLADE, D., ROBERTS, C., HINNEBUSCH, A. G. & MARTON, M. J. (2001) Transcriptional profiling shows that Gcn4p is a master regulator of gene expression during amino acid starvation in yeast. *Mol Cell Biol*, 21, 4347-68.
- NEALE, M. J., PAN, J. & KEENEY, S. (2005) Endonucleolytic processing of covalent protein-linked DNA double-strand breaks. *Nature*, 436, 1053-1057.
- NEALE, M. J., RAMACHANDRAN, M., TRELLES-STICKEN, E., SCHERTHAN, H. & GOLDMAN, A. S. H. (2002) Wild-type levels of Spo11-induced DSBs are required for normal single-strand resection during meiosis. *Mol Cell*, 9, 835-846.
- NEGRITTO, M. C., QIU, J., RATAY, D. O., SHEN, B. & BAILIS, A. M. (2001) Novel function of Rad27 (FEN-1) in restricting short-sequence recombination. *Mol Cell Biol*, 21, 2349-2358.
- NICOLAS, A. & PETES, T. D. (1994) Polarity of meiotic gene conversion in fungi: Contrasting views. *Cell Mol Life Sci*, 50, 242-252.
- NICOLAS, A., TRECO, D., SCHULTES, N. P. & SZOSTAK, J. W. (1989) An initiation site for meiotic gene conversion in the yeast *Saccharomyces cerevisiae*. *Nature*, 338, 35-9.

- NISHANT, K. T., PLYS, A. J. & ALANI, E. (2008) A mutation in the putative *MLH3* endonuclease domain confers a defect in both mismatch repair and meiosis in *Saccharomyces cerevisiae*. *Genetics*, 179, 747-755.
- NORDLUND, M. E., JOHANSSON, J. O., VON PAWEL-RAMMINGEN, U. & BYSTROM, A. S. (2000) Identification of the *TRM2* gene encoding the tRNA(m5U54)methyltransferase of *Saccharomyces cerevisiae*. *RNA*, 6, 844-860.
- NOVAK, J. E., ROSS-MACDONALD, P. B. & ROEDER, G. S. (2001) The budding yeast Msh4 protein functions in chromosome synapsis and the regulation of crossover distribution. *Genetics*, 158, 1013-1025.
- OH, S. D., LAO, J. P., HWANG, P. Y.-H., TAYLOR, A. F., SMITH, G. R. & HUNTER, N. (2007) BLM ortholog, Sgs1, prevents aberrant crossing-over by suppressing formation of multichromatid joint molecules. *Cell*, 130, 259-272.
- OH, S. D., LAO, J. P., TAYLOR, A. F., SMITH, G. R. & HUNTER, N. (2008) RecQ helicase, Sgs1, and XPF family endonuclease, Mus81-Mms4, resolve aberrant joint molecules during meiotic recombination. *Mol Cell*, 31, 324-336.
- OHTA, K., SHIBATA, T. & NICOLAS, A. (1994) Changes in chromatin structure at recombination initiation sites during yeast meiosis. *Embo J*, 13, 5754-5763.
- OLSON, L. W. E., ULLA; EGEL-MITANI, MICHIKO; EGEL, RICHARD, (1978) Asynaptic meiosis in fission yeast? *Hereditas*, 89, 189-199.
- ORR-WEAVER, T. L. & SZOSTAK, J. W. (1985) Fungal recombination. *Microbiol Rev*, 49, 33-58.
- OSMAN, F., DIXON, J., DOE, C. L. & WHITBY, M. C. (2003) Generating crossovers by resolution of nicked Holliday junctions: a role for Mus81-Eme1 in meiosis. *Mol Cell*, 12, 761-74.
- PADMORE, R., CAO, L. & KLECKNER, N. (1991) Temporal comparison of recombination and synaptonemal complex formation during meiosis in *S. cerevisiae*. *Cell*, 66, 1239-1256.
- PAQUES, F. & HABER, J. E. (1999) Multiple pathways of recombination induced by double-strand breaks in *Saccharomyces cerevisiae*. *Microbiol Mol Biol Rev*, 63, 349-404.
- PAULL, T. T. & GELLERT, M. (1998) The 3' to 5' exonuclease activity of Mre11 facilitates repair of DNA double-strand breaks. *Mol Cell*, 1, 969-979.
- PENKNER, A., PORTIK-DOBOS, Z., TANG, L., SCHNABEL, R., NOVATCHKOVA, M., JANTSCH, V. & LOIDL, J. (2007) A conserved function for a *Caenorhabditis elegans* Com1/Sae2/CtIP protein homolog in meiotic recombination. *Embo J*, 26, 5071-5082.
- PERKINS, D. D. (1949) Biochemical mutants in the smut fungus *Ustilago maydis*. *Genetics*, 34, 607-626.

- PORTER, S. E., WHITE, M. A. & PETES, T. D. (1993) Genetic evidence that the meiotic recombination hotspot at the *HIS4* locus of *Saccharomyces cerevisiae* does not represent a site for a symmetrically processed double-strand break. *Genetics*, 134, 5-19.
- PRINZ, S., AMON, A. & KLEIN, F. (1997) Isolation of *COM1*, a new gene required to complete meiotic double-strand break-induced recombination in *Saccharomyces cerevisiae*. *Genetics*, 146, 781-95.
- REENAN, R. & KOLODNER, R. D. (1992) Characterization of insertion mutations in the *Saccharomyces cerevisiae* *MSH1* and *MSH2* genes: evidence for separate mitochondrial and nuclear functions. *Genetics*, 132, 975-985.
- RICHARDSON, C., STARK, J. M., OMMUNDSEN, M. & JASIN, M. (2004) Rad51 overexpression promotes alternative double-strand break repair pathways and genome instability. *Oncogene*, 23, 546-553.
- ROZEN, S. & SKALETSKY, H. (2000) Primer3 on the WWW for general users and for biologist programmers. IN KRAWETZ, S. & MISENER, S. (Eds.) *Bioinformatics Methods and Protocols: Methods in Molecular Biology*. Totowa, NJ, Humana Press.
- SACHO, E. J., KADYROV, F. A., MODRICH, P., KUNKEL, T. A. & ERIE, D. A. (2008) Direct visualization of asymmetric adenine nucleotide-induced conformational changes in MutL α . *Mol Cell*, 29, 112-121.
- SARTORI, A. A., LUKAS, C., COATES, J., MISTRİK, M., FU, S., BARTEK, J., BAER, R., LUKAS, J. & JACKSON, S. P. (2007) Human CtIP promotes DNA end resection. *Nature*, 450, 509-514.
- SCHERER, S. & DAVIS, R. W. (1979) Replacement of chromosome segments with altered DNA sequences constructed in vitro. *Proc Natl Acad Sci USA*, 76, 4951-4955.
- SCHWACHA, A. & KLECKNER, N. (1995) Identification of double Holliday junctions as intermediates in meiotic recombination. *Cell*, 83, 783-791.
- SHEN, B., NOLAN, J. P., SKLAR, L. A. & PARK, M. S. (1996) Essential amino acids for substrate binding and catalysis of human flap endonuclease 1. *J Biol Chem*, 271, 9173-6.
- SHINOHARA, M., OH, S. D., HUNTER, N. & SHINOHARA, A. (2008) Crossover assurance and crossover interference are distinctly regulated by the ZMM proteins during yeast meiosis. *Nat Genet*, 40, 299-309.
- SMOLKA, M. B., ALBUQUERQUE, C. P., CHEN, S.-H. & ZHOU, H. (2007) Proteome-wide identification of *in vivo* targets of DNA damage checkpoint kinases. *Proc Natl Acad Sci USA*, 104, 10364-10369.
- SNOW, R. (1979) Maximum likelihood estimation of linkage and interference from tetrad data. *Genetics*, 92, 231-245.

- SNOWDEN, T., ACHARYA, S., BUTZ, C., BERARDINI, M. & FISHEL, R. (2004) hMSH4-hMSH5 recognizes Holliday junctions and forms a meiosis-specific sliding clamp that embraces homologous chromosomes. *Mol Cell*, 15, 437-451.
- SOKAL, R. & ROHLF, F. (1969) *Biometry: The principles and practice of statistics in biological research. 1st Edition. W.H. Freeman and Company, NY.*
- SOKOLSKY, T. & ALANI, E. (2000) *EXO1* and *MSH6* are high-copy suppressors of conditional mutations in the *MSH2* mismatch repair gene of *Saccharomyces cerevisiae*. *Genetics*, 155, 589-99.
- STAHL, F. W. (2008) On the "NPD Ratio" as a test for crossover interference. *Genetics*, 179, 701-704.
- STORLAZZI, A., XU, L., CAO, L. & KLECKNER, N. (1995) Crossover and noncrossover recombination during meiosis: timing and pathway relationships. *Proc Natl Acad Sci USA*, 92, 8512-6.
- SUN, H., TRECO, D., SCHULTES, N. P. & SZOSTAK, J. W. (1989) Double-strand breaks at an initiation site for meiotic gene conversion. *Nature*, 338, 87-90.
- SUN, H., TRECO, D. & SZOSTAK, J. W. (1991) Extensive 3'-overhanging, single-stranded DNA associated with the meiosis-specific double-strand breaks at the *ARG4* recombination initiation site. *Cell*, 64, 1155-1161.
- SUN, X., THROWER, D., QIU, J., WU, P., ZHENG, L., ZHOU, M., BACHANT, J., WILSON, D. M., 3RD & SHEN, B. (2003) Complementary functions of the *Saccharomyces cerevisiae* Rad2 family nucleases in Okazaki fragment maturation, mutation avoidance, and chromosome stability. *DNA Repair (Amst)*, 2, 925-40.
- SVETLANOV, A. & COHEN, P. E. (2004) Mismatch repair proteins, meiosis, and mice: understanding the complexities of mammalian meiosis. *Exp Cell Res*, 296, 71-9.
- SZANKASI, P. & SMITH, G. R. (1995) A role for Exonuclease I from *S. pombe* in mutation avoidance and mismatch correction. *Science*, 267, 1166-1169.
- SZOSTAK, J. W., ORR-WEAVER, T. L., ROTHSTEIN, R. J. & STAHL, F. W. (1983) The double-strand-break repair model for recombination. *Cell*, 33, 25-35.
- TERASAWA, M., OGAWA, H., TSUKAMOTO, Y., SHINOHARA, M., SHIRAHIGE, K., KLECKNER, N. & OGAWA, T. (2007) Meiotic recombination-related DNA synthesis and its implications for cross-over and non-cross-over recombinant formation. *Proc Natl Acad Sci USA*, 104, 5965-5970.
- TERASAWA, M., OGAWA, T., TSUKAMOTO, Y. & OGAWA, H. (2008) Sae2p phosphorylation is crucial for cooperation with Mre11p for resection of

DNA double-strand break ends during meiotic recombination in *Saccharomyces cerevisiae*. *Genes Genet Syst*, 83, 209-217.

- TISHKOFF, D. X., AMIN, N. S., VIARS, C. S., ARDEN, K. C. & KOLODNER, R. D. (1998) Identification of a human gene encoding a homologue of *Saccharomyces cerevisiae* EXO1, an exonuclease implicated in mismatch repair and recombination. *Cancer Res*, 58, 5027-5031.
- TISHKOFF, D. X., BOERGER, A. L., BERTRAND, P., FILOSI, N., GAIDA, G. M., KANE, M. F. & KOLODNER, R. D. (1997) Identification and characterization of *Saccharomyces cerevisiae* EXO1, a gene encoding an exonuclease that interacts with MSH2. *Proc Natl Acad Sci USA*, 94, 7487-7492.
- TRAN, P. T., ERDENIZ, N., DUDLEY, S. & LISKAY, R. M. (2002) Characterization of nuclease-dependent functions of Exo1p in *Saccharomyces cerevisiae*. *DNA Repair (Amst)*, 1, 895-912.
- TRAN, P. T., FEY, J. P., ERDENIZ, N., GELLON, L., BOITEUX, S. & LISKAY, R. M. (2007) A mutation in EXO1 defines separable roles in DNA mismatch repair and post-replication repair. *DNA Repair (Amst)*, 6, 1572-1583.
- TRUJILLO, K. M., ROH, D. H., CHEN, L., VAN KOMEN, S., TOMKINSON, A. & SUNG, P. (2003) Yeast Xrs2 binds DNA and helps target Rad50 and Mre11 to DNA ends. *J Biol Chem*, 278, 48957-48964.
- TRUJILLO, K. M. & SUNG, P. (2001) DNA structure-specific nuclease activities in the *Saccharomyces cerevisiae* Rad50-Mre11 Complex. *J Biol Chem*, 276, 35458-35464.
- TSUBOUCHI, H. & OGAWA, H. (1998) A novel Mre11 mutation impairs processing of double-strand breaks of DNA during both mitosis and meiosis. *Mol Cell Biol*, 18, 260-8.
- TSUBOUCHI, H. & OGAWA, H. (2000) Exo1 roles for repair of DNA double-strand breaks and meiotic crossing over in *Saccharomyces cerevisiae*. *Mol Biol Cell*, 11, 2221-2233.
- TUNG, K. S. & ROEDER, G. S. (1998) Meiotic chromosome morphology and behavior in *zip1* mutants of *Saccharomyces cerevisiae*. *Genetics*, 149, 817-32.
- UANSCHOU, C., SIWIEC, T., PEDROSA-HARAND, A., KERZENDORFER, C., SANCHEZ-MORAN, E., NOVATCHKOVA, M., AKIMCHEVA, S., WOGLAR, A., KLEIN, F. & SCHLOGELHOFER, P. (2007) A novel plant gene essential for meiosis is related to the human CtIP and the yeast COM1/SAE2 gene. *Embo J*, 26, 5061-5070.
- USUI, T., OGAWA, H. & PETRINI, J. H. J. (2001) A DNA damage response pathway controlled by Tel1 and the Mre11 complex. *Mol Cell*, 7, 1255-1266.
- VEDEL, M. & NICOLAS, A. (1999) CYS3, a hotspot of meiotic recombination in *Saccharomyces cerevisiae*. Effects of heterozygosity and mismatch repair

- functions on gene conversion and recombination intermediates. *Genetics*, 151, 1245-1259.
- WACH, A., BRACHAT, A., POEHLMANN, R. & PHILIPPSEN, P. (1994) New heterologous modules for classical or PCR-based gene disruptions in *Saccharomyces cerevisiae*. *Yeast*, 10, 1793-1808.
- WANAT, J. J., KIM, K. P., KOSZUL, R., ZANDERS, S., WEINER, B., KLECKNER, N. & ALANI, E. (2008) Csm4, in collaboration with Ndj1, mediates telomere-led chromosome dynamics and recombination during yeast meiosis. *PLoS Genet*, 4, e1000188.
- WANG, T. F., KLECKNER, N. & HUNTER, N. (1999) Functional specificity of MutL homologs in yeast: evidence for three Mlh1-based heterocomplexes with distinct roles during meiosis in recombination and mismatch correction. *Proc Natl Acad Sci USA*, 96, 13914-9.
- WARD, J. F. (1990) The yield of DNA double-strand breaks produced intracellularly by ionizing radiation: A review. *Int J Radiat Biol*, 57, 1141 - 1150.
- WATT, P. M., LOUIS, E. J., BORTS, R. H. & HICKSON, I. D. (1995) Sgs1: A eukaryotic homolog of *E. coli* RecQ that interacts with topoisomerase II *in vivo* and is required for faithful chromosome segregation. *Cell*, 81, 253-260.
- WEI, K., CLARK, A. B., WONG, E., KANE, M. F., MAZUR, D. J., PARRIS, T., KOLAS, N. K., RUSSELL, R., HOU, H., JR., KNEITZ, B., YANG, G., KUNKEL, T. A., KOLODNER, R. D., COHEN, P. E. & EDELMANN, W. (2003) Inactivation of Exonuclease 1 in mice results in DNA mismatch repair defects, increased cancer susceptibility, and male and female sterility. *Genes Dev*, 17, 603-14.
- WHITE, M. A., DETLOFF, P., STRAND, M. & PETES, T. D. (1992) A promoter deletion reduces the rate of mitotic, but not meiotic, recombination at the *HIS4* locus in yeast. *Curr Genet*, 21, 109-16.
- WU, L. & HICKSON, I. D. (2003) The Bloom's syndrome helicase suppresses crossing over during homologous recombination. *Nature*, 426, 870-4.
- WU, T. C. & LICHTEN, M. (1994) Meiosis-induced double-strand break sites determined by yeast chromatin structure. *Science*, 263, 515-8.
- ZALEVSKY, J., MACQUEEN, A. J., DUFFY, J. B., KEMPHUES, K. J. & VILLENEUVE, A. M. (1999) Crossing over during *Caenorhabditis elegans* meiosis requires a conserved MutS-based pathway that is partially dispensable in budding yeast. *Genetics*, 153, 1271-1283.
- ZHU, Z., CHUNG, W.-H., SHIM, E. Y., LEE, S. E. & IRA, G. (2008) Sgs1 helicase and two nucleases Dna2 and Exo1 resect DNA double-strand break ends. *Cell*, 134, 981-994.
- ZOU, L. & ELLEDGE, S. J. (2003) Sensing DNA damage through ATRIP recognition of RPA-ssDNA complexes. *Science*, 300, 1542-1548.